

UNCLASSIFIED

AD NUMBER

ADB013257

LIMITATION CHANGES

TO:

Approved for public release; distribution is unlimited.

FROM:

Distribution authorized to U.S. Gov't. agencies only; Test and Evaluation; AUG 1975. Other requests shall be referred to Air Force Flight Dynamics Laboratory, PTC, Wright-Patterson AFB OH 45433.

AUTHORITY

affdl ltr, 2 may 1979

THIS PAGE IS UNCLASSIFIED

THIS REPORT HAS BEEN DELIMITED
AND CLEARED FOR PUBLIC RELEASE
UNDER DOD DIRECTIVE 5200.20 AND
NO RESTRICTIONS ARE IMPOSED UPON
ITS USE AND DISCLOSURE.

DISTRIBUTION STATEMENT A

APPROVED FOR PUBLIC RELEASE;
DISTRIBUTION UNLIMITED.

↙
AFFDL-TR-76-40

②

ADP013257

DESIGN, FABRICATION, TESTING AND ANALYSIS OF TORSION FREE WING TREND FLUTTER MODELS

GENERAL DYNAMICS
FORT WORTH DIVISION
FORT WORTH, TEXAS 76101

MAY 1976

FINAL REPORT FOR PERIOD APRIL 1975 - MAY 1976

DDC
RECEIVED
SEP 7 1976
C

AD No. _____
DDC FILE COPY

Distribution limited to U.S. Government agencies only; test and evaluation, statement applied August 1975. Other requests for this document must be referred to AF Flight Dynamics Laboratory (PTC), Wright-Patterson Air Force Base, Ohio 45433.

AIR FORCE FLIGHT DYNAMICS LABORATORY
AIR FORCE WRIGHT AERONAUTICAL LABORATORIES
AIR FORCE SYSTEMS COMMAND
WRIGHT-PATTERSON AIR FORCE BASE, OHIO 45433

NOTICE

When Government drawings, specifications, or other data are used for any purpose other than in connection with a definitely related Government procurement operation, the United States Government thereby incurs no responsibility nor any obligation whatsoever; and the fact that the government may have formulated, furnished, or in any way supplied the said drawings, specifications, or other data, is not to be regarded by implication or otherwise as in any manner licensing the holder or any other person or corporation, or conveying any rights or permission to manufacture, use, or sell any patented invention that in any way be related thereto.

This technical report has been reviewed and is approved.



Dr. Squire L. Brown
Project Engineer
Air Force Flight Dynamics Laboratory



E. E. Riccioni, Colonel, USAF
Chief, Aeromechanics Division
Air Force Flight Dynamics Laboratory



Copies of this report should not be returned unless return is required by security considerations, contractual obligations, or notice on a specific document.

UNCLASSIFIED

SECURITY CLASSIFICATION OF THIS PAGE (When Data Entered)

19 REPORT DOCUMENTATION PAGE		READ INSTRUCTIONS BEFORE COMPLETING FORM
1 REPORT NUMBER 18 AFFDL-TR-76-48 ✓	2 GOVT ACCESSION NO.	3 RECIPIENT'S CATALOG NUMBER 9
4 TITLE (and Subtitle) 9 DESIGN, FABRICATION, TESTING AND ANALYSIS OF TORSION FREE WING TREND FLUTTER MODELS.		5 TYPE OF REPORT & PERIOD COVERED Final Report. April 1975 - May 1976.
7 AUTHOR(s) 10 A. C. Murphy, R. P. Peloubet, R. M. Bolding J. J. Hosek		8 CONTRACT OR GRANT NUMBER(s) 15 F33615-75-C-3045 <i>new</i>
9 PERFORMING ORGANIZATION NAME AND ADDRESS General Dynamics Fort Worth Division, P. O. Box 748 Fort Worth, Texas 76101		10 PROGRAM ELEMENT, PROJECT, TASK AREA & WORK UNIT NUMBERS Project 1370
11 CONTROLLING OFFICE NAME AND ADDRESS Air Force Flight Dynamics Laboratory (FXC) Wright-Patterson AFB, Ohio 45433		12 REPORT DATE May 1976
14 MONITORING AGENCY NAME & ADDRESS (if different from Controlling Office) 12 142p.		13 NUMBER OF PAGES
		15 SECURITY CLASS. (of this report) Unclassified
		15a DECLASSIFICATION/DOWNGRADING SCHEDULE
16 DISTRIBUTION STATEMENT (of this Report) Distribution limited to U.S. Government agencies only; test and evaluation, statement applied August 1975. Other requests for this document must be referred to AF Flight Dynamics Laboratory (PTC), Wright-Patterson Air Force Base, Ohio 45433.		
17 DISTRIBUTION STATEMENT (of the abstract entered in Block 20, if different from Report) 16 AF-1370		
18 SUPPLEMENTARY NOTES		
19 KEY WORDS (Continue on reverse side if necessary and identify by block number) Torsion Free Wing Trend Flutter Model Free Floating Wing Torsion Free Wing Trend Flutter Model Flutter Flutter Model		
20. ABSTRACT (Continue on reverse side if necessary and identify by block number) Trend type aluminum plate flutter models of a Torsion Free Wing (or free floating wing) were designed, built and wind tunnel tested. Types of models tested included cantilever, torsion free wing with a forward trim surface and torsion free wing with an aft trim surface. Several flutter points were obtained in the wind tunnel. The models were also vibration tested and static		

UNCLASSIFIED

SECURITY CLASSIFICATION OF THIS PAGE (When Data Entered)

402 709 AB

UNCLASSIFIED

SECURITY CLASSIFICATION OF THIS PAGE(When Data Entered)

deflection tested to measure influence coefficients. These measured data were then used in flutter and divergence analyses. The correlation between analysis results and wind tunnel results is good for some cases and fair or poor for others. Reasons for lack of correlation in some cases are given.

UNCLASSIFIED

SECURITY CLASSIFICATION OF THIS PAGE(When Data Entered)

FOREWORD

This report was prepared by General Dynamics' Fort Worth Division, Fort Worth, Texas under USAF Contract No. F33615-75-C-3045. The contract was administered under the direction of the Air Force Systems Command (AFFDL/FXC) with Dr. Squire L. Brown as Project Engineer.

The program manager was R. P. Peloubet and the principal investigator was A. C. Murphy. Others assisting in the project were J. J. Hosek, R. M. Bolding and J. W. Brickey.

SUMMARY

Torsion Free Wing plate type trend flutter models were designed, built and wind tunnel tested. The purpose of the program was to secure some well documented wind tunnel flutter test points so that flutter analyses of the test configurations could be made and the results correlated with the test data. Divergence analyses were also performed as part of the program.

The test configurations consisted of a cantilever model, cantilever planform restrained at only one point at the root, a torsion free wing with forward trim surface and a torsion free wing with the trim surface aft of the wing at the tip. This program was believed to offer a logical sequence of test and analysis steps from the simplest to the most complex configurations.

Flutter test points were obtained for three configurations. These were the cantilever, the cantilever supported at one point (called the pitch restrained cantilever) and the torsion free wing with trim surface aft. For the torsion free wing with forward trim surface, divergence was experienced before the flutter speed was reached. Therefore, positive correlation of calculated and wind tunnel test flutter speed was impossible for this configuration. However, positive correlation of analytical and experimental divergence speed was possible for this case.

Flutter analyses were conducted using measured vibration modal and measured mass input data utilizing kernel function aerodynamics. Analyses were performed for the cantilever model, pitch restrained cantilever model, two different configurations of the torsion free wing with forward trim surface and one case of the torsion free wing with aft trim surface. For this last case, the flutter analyses were repeated using doublet-lattice aerodynamics. It had been planned to repeat one case using doublet-lattice aerodynamics and originally this was planned for a forward trim surface configuration. However, because no flutter test points were obtained in the wind tunnel with the trim surface forward, it was decided to use doublet-lattice aerodynamics for a trim surface aft case.

Overall correlation of flutter analysis results with wind tunnel test data is not particularly good. Essentially perfect agreement was achieved for the pitch restrained cantilever; however, for the other configurations not nearly so good correlation was achieved. Fairly good correlation was shown for the trim surface aft case using doublet-lattice aerodynamics for one of two flutter cases experienced in the wind tunnel. The flutter speed agreement was within 12 percent of the measured speed and the flutter frequency was within 2 cps of the measured value. The doublet-lattice method of representing the aerodynamic forces included mutual interference effects between surfaces. Perhaps this is one reason for the better correlation achieved using this method.

Divergence analyses were conducted for four configurations. These were: (1) cantilever, (2) pitch restrained cantilever, (3) torsion free wing with forward trim surface and (4) torsion free wing with aft trim surface. Measured deflection influence coefficients were utilized as the model stiffness values in the analyses. A finite element representation of the aerodynamic forces employing aerodynamic influence coefficients computed by the Woodward method was used in the aeroelastic solution.

For both the cantilever and pitch restrained cantilever, very high divergence speeds were calculated. This is consistent with the wind tunnel results since no divergence condition was encountered up to the speed at which flutter occurred. For the trim surface forward case, the calculated divergence speed is considerably above the measured divergence speed. With the trim surface aft the calculated divergence speed is high. This is also consistent with test results wherein flutter was encountered before reaching any divergence condition.

In general, the analyses-test correlation was less satisfactory than was hoped for. There were some cases in the flutter analysis that gave good agreement. A more detail investigation as to the reasons for disagreement, when they occur, may be warranted.

TABLE OF CONTENTS

<u>SECTION</u>	<u>Page</u>
I	INTRODUCTION 1
II	MODEL CHARACTERISTICS 6
III	EXPERIMENTAL PROGRAM 15
	Mass and Geometry 15
	Influence Coefficient Tests 21
	Vibration Testing 29
	Wind Tunnel Testing 30
IV	ANALYSES 35
	Flutter Analyses 35
	Divergence Analyses 47
V	DISCUSSION AND COMPARISON OF EXPERIMENTAL AND ANALYTICAL RESULTS 51
VI	CONCLUSIONS AND RECOMMENDATIONS 55
APPENDIX 56
REFERENCES 124

LIST OF ILLUSTRATIONS

<u>Figure</u>		<u>Page</u>
1	Torsion Free Wing Configuration Flutter Analyzed in 1972	2
2	Torsion Free Wing Configuration Flutter Analyzed in 1974	3
3	Torsion Free Wing Configuration Upon Which Geometry of Trend Flutter Models is Based	6
4	Wing Planform for Scaling Cantilever Model	7
5	Cantilever Model Mounted in Wind Tunnel	9
6	Torsion Free Wing Trend Model Mounted in Wind Tunnel - Symmetric Case	10
7	Torsion Free Wing Trend Model Mounted in Wind Tunnel - Antisymmetric Case	11
8	Mass and Geometry of Cantilever Model	16
9	Mass and Geometry of Pitch Restrained Cantilever Model	16
10	Mass and Geometry of Torsion Free Wing Model with Forward Trim Surface	17
11	Mass and Geometry of Torsion Free Wing Model with Aft Trim Surface	18
12	Mass and Geometry of Fuselage Spar and Mechanism	19
13	Mass and Geometry of Balance Arm	20
14	Deflection Reading Point Location for Cantilever Model	21
15	Deflection Reading Point Location for Pitch Restrained Cantilever Model	23

LIST OF ILLUSTRATIONS (Continued)

<u>Figure</u>		<u>Page</u>
16	Deflection Reading Point Locations for Torsion Free Wing Model with Forward Trim Surface	25
17	Deflection Reading Point Locations for Torsion Free Wing Model with Aft Trim Surface	27
18	Structural Damping Coefficient and Frequency Versus Velocity for Cantilever Model	40
19	Structural Damping Coefficient and Frequency Versus Velocity for Pitch Restrained Cantilever Model	41
20	Structural Damping Coefficient and Frequency Versus Velocity for TFW Trim Surface Forward Model	42
21	Structural Damping Coefficient and Frequency Versus Velocity for TFW Trim Surface Forward Model with Wing Root Stiffener	43
22	Structural Damping Coefficient and Frequency Versus Velocity for TFW Trim Surface Aft Model (Kernel Function)	44
23	Structural Damping Coefficient and Frequency Versus Velocity for TFW Trim Surface Aft Model (Doublet-Lattice)	45
24	Method of Solution of Aeroelastic Problem	48
25	Mode Shape Reading Points for Cantilever and Pitch Restrained Cantilever Models	57
26	Mode Shape Reading Points for Wing of TFW Models	58
27	Mode Shape Reading Points for B Trim Surface (Aft Trim Surface TFW Configuration)	59

LIST OF ILLUSTRATIONS (Continued)

<u>Figure</u>		<u>Page</u>
28	Mode Shape Reading Points for S Trim Surface (Forward Trim Surface TFW Configuration)	60
29	Torsion Free Wing Trend Flutter Models Frequency Survey - Cantilever	61
30	Mode Shape Plot-Cantilever Model, $f=25.2$ cps	62
31	Mode Shape Plot-Cantilever Model, $f=91.2$ cps	63
32	Mode Shape Plot-Cantilever Model, $f=106.2$ cps	64
33	Frequency Survey-Pitch Restrained Cantilever	68
34	Mode Shape Plot-P.R. Cantilever, $f=16.5$ cps	69
35	Mode Shape Plot-P.R. Cantilever, $f=40.1$ cps	70
36	Mode Shape Plot-P.R. Cantilever, $f=92.1$ cps	71
37	Mode Shape Plot-P.R. Cantilever, $f=127.5$ cps	72
38	Frequency Survey-TFW, Aft Trim Surface	77
39	Mode Shape Plot-TFW, Aft Trim Surf, $f=17.3$ cps	78
40	Mode Shape Plot-TFW, Aft Trim Surf, $f=21.3$ cps	79
41	Mode Shape Plot-TFW, Aft Trim Surf, $f=50.2$ cps	80
42	Mode Shape Plot-TFW, Aft Trim Surf, $f=70.0$ cps	81
43	Mode Shape Plot-TFW, Aft Trim Surf, $f=79.5$ cps	82
44	Mode Shape Plot-TFW, Aft Trim Surf, $f=89.6$ cps	83
45	Mode Shape Plot-TFW, Aft Trim Surf, $f=119.2$ cps	84
46	Mode Shape Plot-TFW, Aft Trim Surf, $f=146.7$ cps	85

LIST OF ILLUSTRATIONS (Continued)

<u>Figure</u>		<u>Page</u>
47	Frequency Survey-TFW, Fwd Trim Surface	94
48	Mode Shape Plot-TFW, Fwd Trim Surf, f=18.0 cps	95
49	Mode Shape Plot-TFW, Fwd Trim Surf, f=27.6 cps	96
50	Mode Shape Plot-TFW, Fwd Trim Surf, f=49.6 cps	97
51	Mode Shape Plot-TFW, Fwd Trim Surf, f=87.4 cps	98
52	Mode Shape Plot-TFW, Fwd Trim Surf, f=112.0 cps	99
53	Mode Shape Plot-TFW, Fwd Trim Surf, f=193.5 cps	100
54	Frequency Survey-TFW, Fwd Trim Surface, Stiffened Root	107
55	Mode Shape Plot-TFW, Fwd Trim Surf, Stiffened Root f=18.0 cps	108
56	Mode Shape Plot-TFW, Fwd Trim Surf, Stiffened Root f=30.9 cps	109
57	Mode Shape Plot-TFW, Fwd Trim Surf, Stiffened Root f=77.9 cps	110
58	Mode Shape Plot-TFW, Fwd Trim Surf, Stiffened Root f=84.9 cps	111
59	Mode Shape Plot-TFW, Fwd Trim Surf, Stiffened Root f=94.5 cps	112
60	Mode Shape Plot-TFW, Fwd Trim Surf, Stiffened Root f=108.3 cps	113
61	Mode Shape Plot-TFW, Fwd Trim Surf, Stiffened Root f=120.4 cps	114
62	Mode Shape Plot-TFW, Fwd Trim Surf, Stiffened Root f=129.3 cps	115

LIST OF TABLES

<u>Table</u>		<u>Page</u>
I	FUSELAGE BALANCE WEIGHT DATA	19
II	MEASURED INFLUENCE COEFFICIENTS - CANTILEVER MODEL	22
III	MEASURED INFLUENCE COEFFICIENTS - PITCH RESTRAINED CANTILEVER MODEL	24
IV	MEASURED INFLUENCE COEFFICIENTS - TORSION FREE WING MODEL WITH FORWARD TRIM SURFACE	26
V	MEASURED INFLUENCE COEFFICIENTS - TORSION FREE WING MODEL WITH AFT TRIM SURFACE	28
VI	TORSION FREE WING TREND FLUTTER MODELS WIND TUNNEL TEST DATA	32
VII	COMPARISON OF CALCULATED AND MEASURED FLUTTER SPEEDS	46
VIII	COMPARISON OF MEASURED AND CALCULATED DIVERGENCE SPEEDS	50
IX	MODE SHAPE DATA-CANTILEVER MODEL, $f=25.2$ cps	65
X	MODE SHAPE DATA-CANTILEVER MODEL, $f=91.2$ cps	66
XI	MODE SHAPE DATA-CANTILEVER MODEL, $f=106.2$ cps	67
XII	MODE SHAPE DATA-P.R. CANTILEVER, $f=16.5$ cps	73
XIII	MODE SHAPE DATA-P.R. CANTILEVER, $f=40.1$ cps	74
XIV	MODE SHAPE DATA-P.R. CANTILEVER, $f=92.1$ cps	75
XV	MODE SHAPE DATA-P.R. CANTILEVER, $f=127.5$ cps	76

LIST OF TABLES (Continued)

<u>Table</u>		<u>Page</u>
XXVI	MODE SHAPE DATA-TFW AFT TRIM SURF, f=17.3 cps	86
XXVII	MODE SHAPE DATA-TFW AFT TRIM SURF, f=21.3 cps	87
XXVIII	MODE SHAPE DATA-TFW AFT TRIM SURF, f=50.2 cps	88
XIX	MODE SHAPE DATA-TFW AFT TRIM SURF, f=70.0 cps	89
XX	MODE SHAPE DATA-TFW AFT TRIM SURF, f=79.5 cps	90
XXI	MODE SHAPE DATA-TFW AFT TRIM SURF, f=89.6 cps	91
XXII	MODE SHAPE DATA-TFW AFT TRIM SURF, f=119.2 cps	92
XXIII	MODE SHAPE DATA-TFW AFT TRIM SURF, f=146.7 cps	93
XXIV	MODE SHAPE DATA-TFW FWD TRIM SURF, f=18.0 cps	101
XXV	MODE SHAPE DATA-TFW FWD TRIM SURF, f=27.6 cps	102
XXVI	MODE SHAPE DATA-TFW FWD TRIM SURF, f=49.6 cps	103
XXVII	MODE SHAPE DATA-TFW FWD TRIM SURF, f=87.4 cps	104
XXVIII	MODE SHAPE DATA-TFW FWD TRIM SURF, f=112.0 cps	105
XXIX	MODE SHAPE DATA-TFW FWD TRIM SURF, f=193.5 cps	106
XXX	MODE SHAPE DATA-TFW FWD TRIM SURF, STIFFENED ROOT, f=18.0 cps	116
XXXI	MODE SHAPE DATA-TFW FWD TRIM SURF, STIFFENED ROOT, f=30.9 cps	117
XXXII	MODE SHAPE DATA-TFW FWD TRIM SURF, STIFFENED ROOT, f=77.9 cps	118
XXXIII	MODE SHAPE DATA-TFW FWD TRIM SURF, STIFFENED ROOT, f=84.9 cps	119

LIST OF TABLES (Continued)

<u>Table</u>		<u>Page</u>
XXXIV	MODE SHAPE DATA-TFW FWD TRIM SURF, STIFFENED ROOT, $f=94.5$ cps	120
XXXV	MODE SHAPE DATA-TFW FWD TRIM SURF, STIFFENED ROOT, $f=108.3$ cps	121
XXXVI	MODE SHAPE DATA-TFW FWD TRIM SURF, STIFFENED ROOT, $f=120.4$ cps	122
XXXVII	MODE SHAPE DATA-TFW FWD TRIM SURF, STIFFENED ROOT, $f=129.3$ cps	123

LIST OF SYMBOLS

- L = load
- [S] = stiffness coefficient matrix
- q = dynamic pressure
- [A] = aerodynamic coefficient matrix
- $\Delta\alpha$ = structural angular deflection

S E C T I O N I

INTRODUCTION

The concept of an aircraft with Torsion Free Wings (TFW) is not new. The term Torsion Free Wing as defined herein means a wing which is mounted on the fuselage by means of a spanwise oriented pivot shaft and is mechanically unrestrained in rigid body pitch. Other investigators have used the terms free-wing or free floating wing for similar or identical type configurations.

Early attempts at flying TFW or quasi-TFW aircraft were recorded by the French in the early 1900s. Other attempts to design or build TFW aircraft have been reported over the intervening years. However, these investigations have been few in number and have not received much attention. It was not until 1970 that a serious documented study of a TFW concept was undertaken (Reference 1). This investigation showed the gust alleviation benefits of a TFW airplane and also indicated that longitudinal handling qualities were satisfactory. The study also showed that an artificial roll damper was beneficial to lateral control because of inherently low roll damping and spiral divergence of the TFW configurations under consideration. However, no investigation of the flutter characteristics of a TFW vehicle was undertaken in the investigation.

The study of Reference 2 was an investigation of the effect on the ride quality of a TFW configuration if either an active or passive flutter stability augmentation system were added to increase the flutter speed. A semi span flexible pivoting wing was flutter analyzed as a cantilever, as a TFW configuration and as a TFW with the flutter stability augmentation added. One of the major conclusions of the study was that the inclusion of a flutter stability augmentation system reduced the ride smoothing qualities inherent in a torsion free wing.

¹Porter, R. and Brown, J., "The Gust Alleviation Characteristics and Handling Qualities of a Free-Wing Aircraft," AIAA Paper 70-947, AIAA Guidance, Control and Flight Mechanics Conference, August 17-19, 1970.

²Wattman, W., et al., "Pivoting Wing Ride Smoothing/Flutter SAS Analyses," The Boeing Company, Wichita, Kansas, May 1971.

General Dynamics' Fort Worth Division has studied TFW configurations in some depth over the last several years. This type configuration has received attention because of improved ride quality associated with TFW, better landing and takeoff characteristics, better target tracking, increased maneuverability and more efficient use of structural materials. These studies have been primarily aimed at high performance fighter type aircraft applications. Studies have included aerodynamic, stability and control, stress, weight, gust response and flutter analyses. Included in the work done has been the fabrication and flight testing of a small remotely piloted subsonic model. The model has been successfully flown many times thus demonstrating the feasibility of the TFW concept.

In the studies conducted at General Dynamics' Fort Worth Division, flutter analyses have been conducted for some of the more promising configurations which have been studied for possible future applications. The first of these flutter analyses was completed in 1972 for the wing-trim surface configuration shown in Figure 1. The structural arrangement for this configuration was graphite skins bonded to full depth aluminum honeycomb core. This was idealized to skin panels and ribs and spars for the flutter analysis.

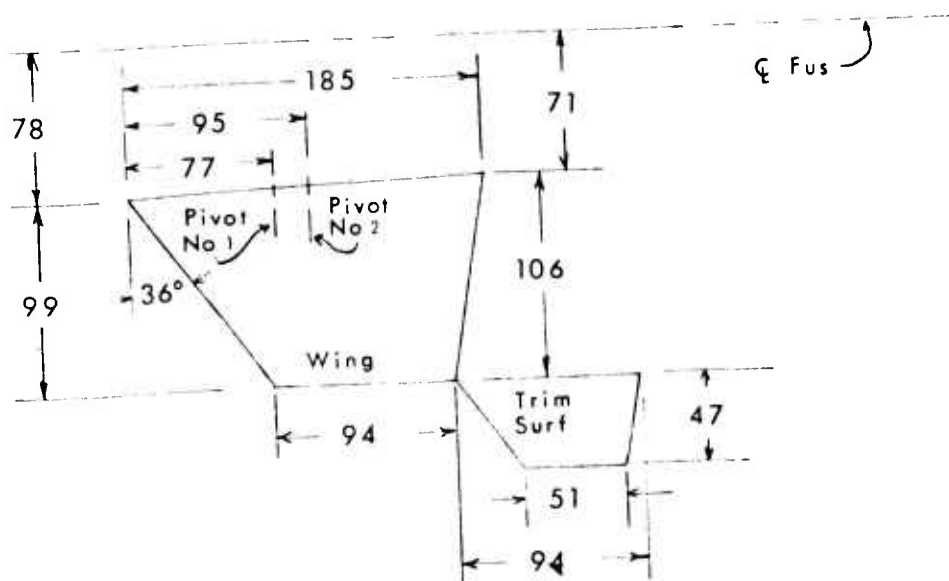


Figure 1 Torsion Free Wing Configuration
Flutter Analyzed in 1972

The required flutter speed at sea level was 1100 knots. This would be unrestrictive for the strength design configuration. Calculated flutter speeds for the alternate wing pivot locations were:

Sta. 77 pivot axis -- flutter speed = 1450 knots

Sta. 95 pivot axis -- flutter speed = 1050 knots

There was no hingeline on the trim surface for this analysis. The trim surface was attached along the root to the structural rib which extended chordwise across the wing tip and the trim surface root. Symmetric analyses only were done. In the modal analysis, the wing was assumed to be clamped at the pivot. For the flutter analysis, however, a rigid body pitch degree of freedom was present.

From the results of this analysis it was concluded that a TFW configuration would not present serious flutter problems in design studies of this concept.

A second configuration was analyzed in 1974. A geometrical sketch of the configuration is shown in Figure 2. This was a larger and heavier vehicle than was analyzed in 1972 but was still a high performance fighter type vehicle. The wing and trim surface structure was aluminum skins with aluminum spars and ribs.

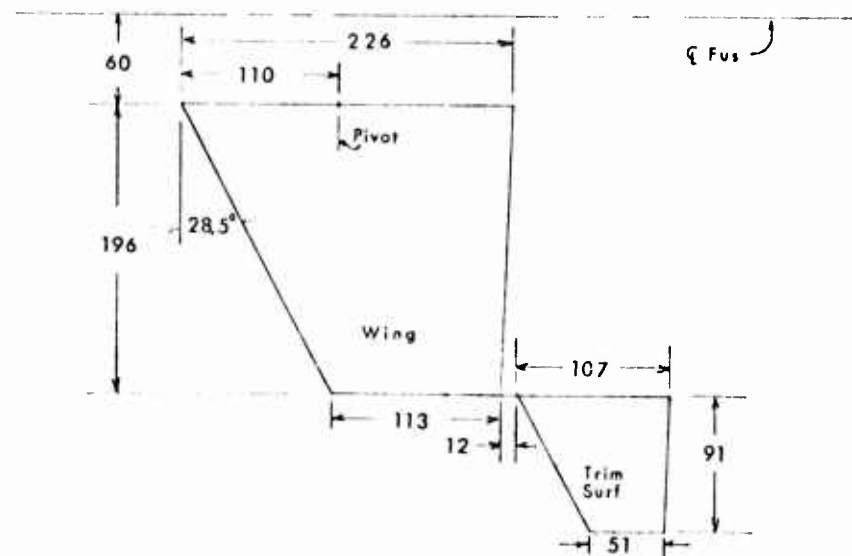


Figure 2 Torsion Free Wing Configuration
Flutter Analyzed in 1974

The flutter speed for the configuration of Figure 2 was computed to be 190 knots. Adding weight to a forward located balance weight boom at the wing tip was not beneficial. For these analyses the vibration modes and frequencies were computed for the wing pivot not clamped. A flutter analysis was also performed using modes calculated by clamping the pivot as was done in the 1972 analysis. This gave a flutter speed of 377 knots.

Because of the low flutter speeds an alternate configuration was analyzed for a smaller planform wing wherein the trim surface was located at the inboard wing root station and forward of the wing leading edge. This arrangement (canard trim surface) raised the flutter speed significantly (to 960 knots for this smaller configuration).

These large differences in flutter speeds were not well understood. All structural sizing for the various configurations was done on the basis of the minimum weight structure to satisfy the strength requirements. Therefore, no extra material was in any of the designs to help raise the flutter speed. On this basis the difference in planform size can be virtually ruled out as a contributor to the difference in flutter speeds. Also, the change in material from one configuration to another should not have any sizable effect. Possible errors in the analyses were searched for and no significant ones found.

However, the flutter analysis (and modal analysis) of a TFW configuration may not be as straightforward and the level of confidence in the results be as high as for more conventional type structures. The presence of the wing pivot may present problems that conventional analyses cannot properly account for. As a result of these possible uncertainties, this program was undertaken in order to provide some wind tunnel test flutter data with which analyses results could be correlated and compared.

In the interest of keeping overall costs low, a program of plate type trend flutter models was proposed as being satisfactory test vehicles which could also be analyzed. They did not need to be dynamically similar to any airplane configuration in order to provide good test data. If flutter points could be obtained and a few parameters varied in an orderly manner, then a quantity of experimental data could be gathered which would form the basis of comparison between analyses and the test configurations.

This program was initiated in April of 1975. The first steps taken were the technical and detail design of the models. Technical design refers to that portion of the design effort which involves establishing planform size; model structural thicknesses, sizes and masses; general design concepts, etc. Detail design refers to that effort required to convert the technical design information into working drawings so that the detail parts can be fabricated and assembled. The detail drawings are not included in this report but copies could be furnished upon the reader's request.

Detail design was followed by fabrication and wind tunnel testing. These phases in turn were followed by vibration testing, influence coefficient testing, flutter analysis and divergence analysis. The significant portions of all test and analysis results are included herein.

SECTION II
MODEL CHARACTERISTICS

The model wing and trim surface planform was established by scaling down the size of an airplane configuration which had been studied in 1974. The full scale wing and trim surfaces are shown in Figure 3.

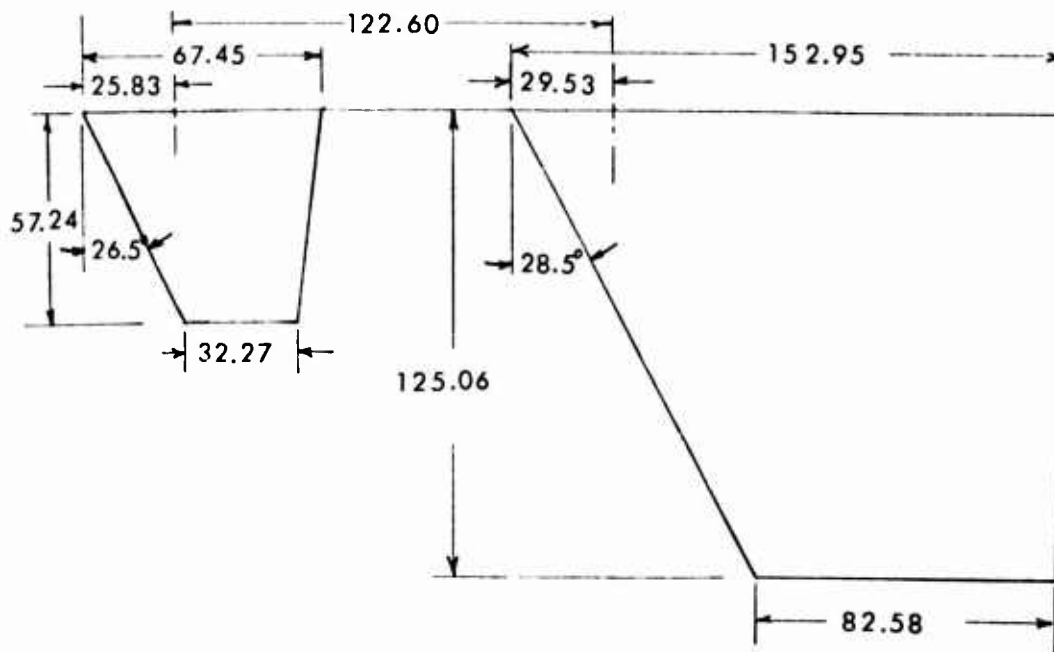


Figure 3 Torsion Free Wing Configuration Upon Which Geometry of Trend Flutter Models is Based

A subsonic wind tunnel with a 14 inch square test section was to be used to test the models. It was decided early that establishing subsonic flutter test points would furnish the best test data base with which to correlate analyses rather than to attempt correlation in the transonic or supersonic speed ranges. With the wind tunnel size fixed, it then became a simple matter to establish the geometric scale of the models. The type models and nature of the test also influenced the model to airplane geometry scale.

It was desired to obtain some fundamental or baseline flutter data from tests of a cantilevered planform configuration as a part of this program. In some of the studies conducted at General Dynamics' Fort Worth Division the TFW configuration had been established by first considering a cantilever wing, then hypothetically slicing the tip off and moving it aft to provide a trim surface and finally providing a pivot axis for the wing itself.

This same thinking helped establish the cantilever model planform and also the geometrical length ratio between model and full scale. The cantilever wing model size to properly fit the wind tunnel was 10 inches root-to-tip. The planform was generated by extending the TFW wing trailing and leading edges a distance such that the wing span was increased an amount equal to the span of the trim surface. This is shown in Figure 4.

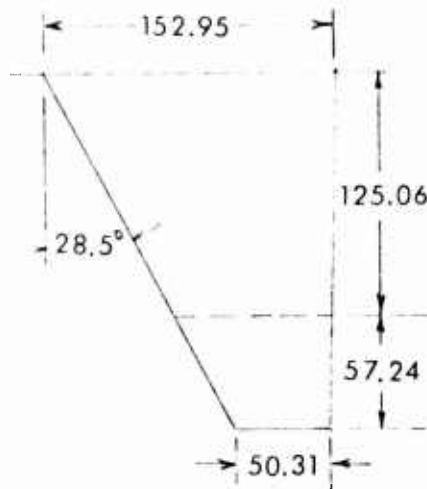


Figure 4 Wing Planform for Scaling Cantilever Model

The length scale then became $10/182.3$ or $1/18.23$. This was used for all models in the program.

Another basic idea that was proposed and followed in the model program was to test four basic types of models. These were: (1) cantilever model (previously discussed), (2) pitch restrained cantilever (cantilever platform mounted on a pivot shaft and tested with the pivot shaft clamped), (3) TFW with the trim surface inboard and forward as in Figure 3 and (4) TFW with the trim surface at the wing tip and aft of the wing. This program was believed to be a logical progression from the simplest model (cantilever) to the most complex (TFW). Provision was made within each type of TFW model to vary important parameters such as wing pivot location, boom stiffness, trim surface size and trim surface pitch stiffness.

The TFW models were conceived and designed to be semi-span type models. It was also required to have the effects of fuselage mass and stiffness in the test results but it was not believed important to include fuselage aerodynamic forces in the tests. Therefore, the models were designed such that the fuselage was supported by a mechanism which could provide symmetric or antisymmetric boundary conditions at the fuselage centerline with the fuselage and support mechanism being placed outside the wind tunnel test airstream. Sketches showing the wind tunnel and the method of supporting the cantilever and TFW models are shown in Figures 5, 6 and 7.

As can be implied in Figure 5, the wind tunnel operates as an injector type which pulls the air through the bell mouth and then through the 14 inch square section leading to an open jet test length. The free jet test length is not substantially different from that of a walled section except for a layer of mixed flow which surrounds the free jet and is probably a little thicker than a normal wall boundary layer. Although no flow studies were made during these tests, it is believed that the root of the TFW models was close to the edge of this layer of mixed flow. For the trim surface forward TFW models, the trim surface and boom extended forward into the walled portion of the 14 inch section as shown in Figures 6 and 7. It is not believed that this had any measurable effect on the test results since these were outside the boundary layer.

The model surfaces were designed as spanwise tapered aluminum plates. It can be shown that this type model structure approximates the spanwise distribution of the full scale stiffness and mass. The structural member representing the fuselage is a standard wall thickness aluminum tube. Weights are clamped

to this tube to provide the correct lumped distribution of fuselage weight and rolling mass moment of inertia. The structural boom tying the trim surface to the wing was designed as a thin walled tube but during the wind tunnel tests, a much stiffer solid aluminum rod was also used to increase the boom stiffness during a portion of the trim surface forward tests.

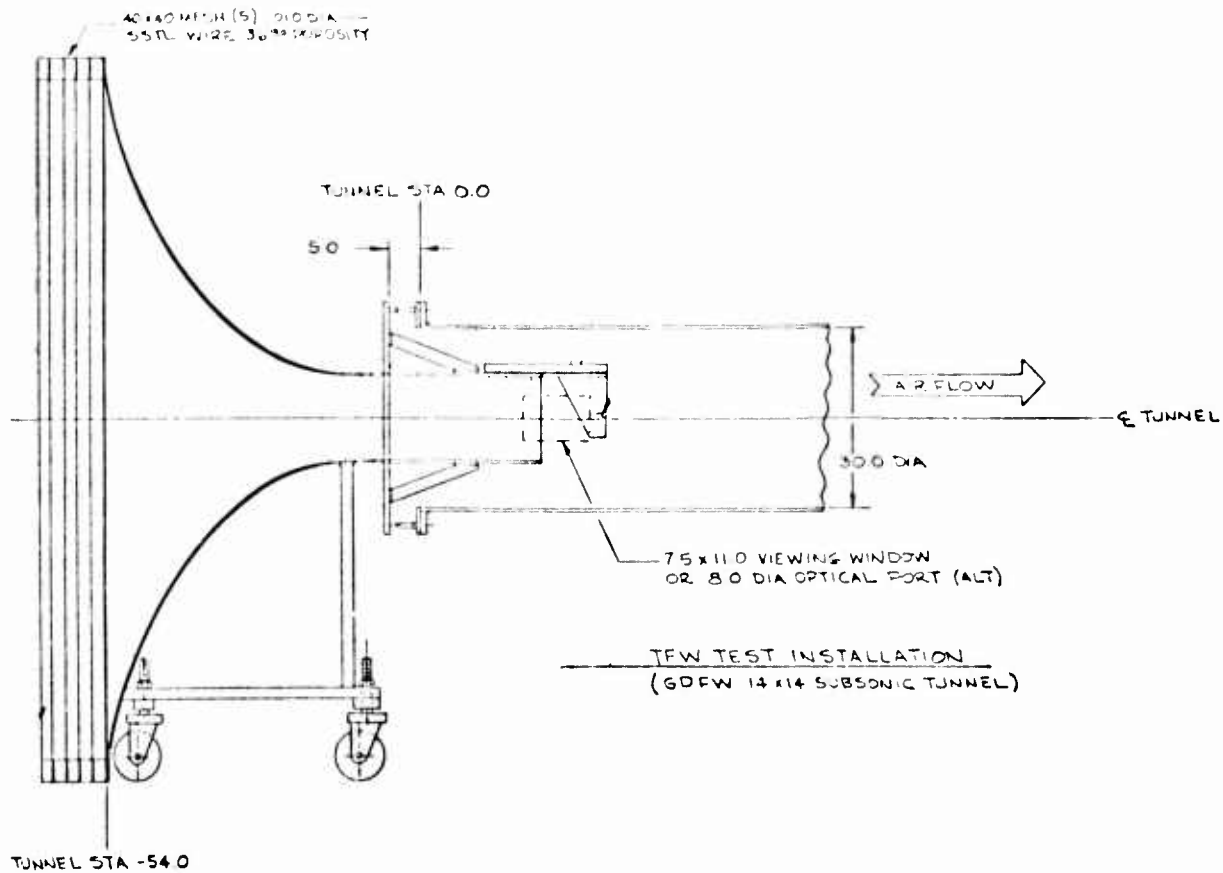


Figure 5 Cantilever Model Mounted in Wind Tunnel

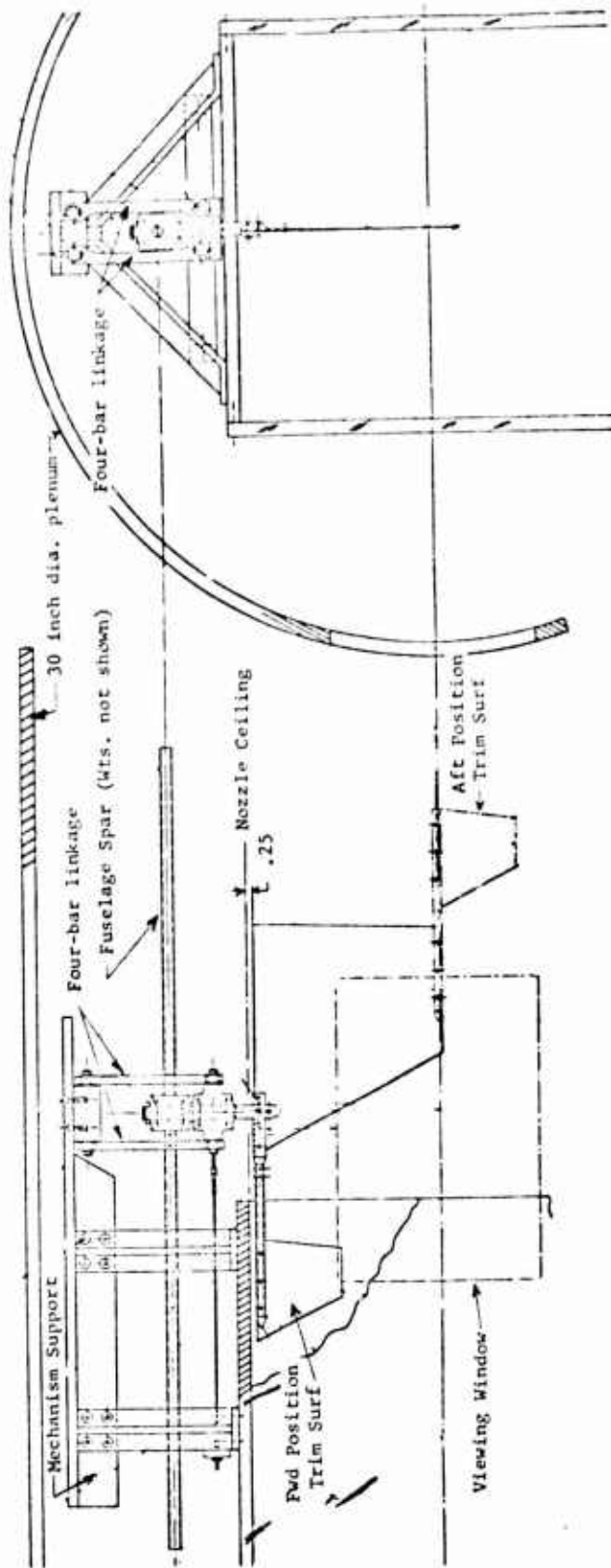


Figure 6 Torsion Free Wing Trend Model Mounted in Wind Tunnel - Symmetric Case

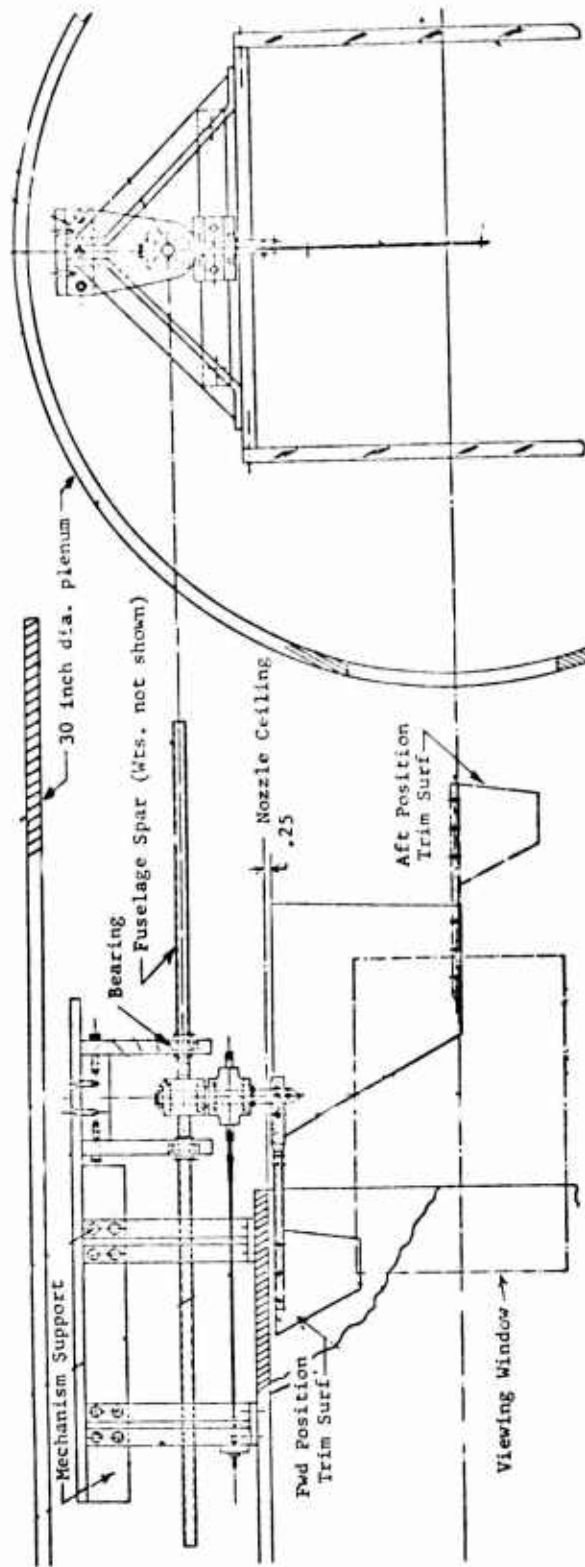


Figure 7 Torsion Free Wing Trend Model Mounted in Wind Tunnel - Antisymmetric Case

The plate thickness was determined such that the cantilever model would flutter near a tunnel speed of 330 feet per second. A model plate stiffness level was established by a Stodola frequency analysis of the cantilever plate model using the assumption that the thickness ratio of the plate, t/c , remained constant along the span. Coupled with this was the assumption, based upon the data of Reference 3 that a value of the flutter parameter

$$\frac{b \omega_{\alpha}}{a} \sqrt{\mu} = .42$$

where b = model semi-chord at $3/4$ span

ω_{α} = uncoupled torsion frequency

a = speed of sound

μ = ratio of model plate mass to mass of cylinder of air surrounding the plate

t = model plate thickness

c = model plate chord

would produce flutter at the desired speed of 330 feet per second. The analysis gave a plate thickness at the root of 0.063 inch to produce the desired flutter speed. To further insure that flutter would be obtained within the speed capability of the tunnel, another model with root thickness equal to 0.052 was also fabricated.

The same planform and thickness were used for the pitch restrained cantilever model, reasoning that the flutter speed for this configuration would be less than that for the cantilever. If this were realized in the wind tunnel tests the flutter speed for this configuration would fall in about the mid range of tunnel speeds.

³Harris, G., "Flutter Criteria for Preliminary Design," Navy, Bureau of Naval Weapons Final Engineering Report 2-53450/3R467, Prepared by LTV Aeronautics and Missile Division, September 1963.

For the TFW models it was believed that the flutter speed for these would be about the same or less than that of the cantilever model. This was based upon intuitive reasoning as much as anything. A flutter analysis of the TFW could not be considered because of cost. Also, there would be, based upon past experience with TFW flutter analyses, less than complete confidence in the results of such an analysis. Therefore, the TFW wing plate root thickness was also made to be 0.063 inch thick. Here again, to help insure getting flutter points within the speed range of the tunnel, a TFW model with root thickness of 0.052 inch and also one with 0.078 root thickness were fabricated. The trim surface thickness was established by assuming that the trim surface root bending stiffness was the same as the wing tip bending stiffness. This relationship existed on the full scale airplane.

The fuselage structural member was sized by selecting a standard wall thickness aluminum tube which had approximately the same ratio of vertical bending stiffness to wing root stiffness as existed on the full scale article near the fuselage mid-length. Fuselage stiffness on the full scale article was nearly constant over about 25 percent of the total fuselage length in the mid-length region where the curvature in the fundamental bending mode is the greatest. Therefore, it was thought to be reasonable for the purposes of these tests to make the model fuselage spar a constant stiffness over the total length.

The boom stiffness on the model was also established by preserving on the model the same ratio of boom bending stiffness at a given boom station to wing root bending stiffness as occurred on the full scale article. This station was near the boom mid-length between the trim surface hingeline and the wing pivot.

In order to provide symmetric boundary conditions at the fuselage centerline, a mechanism was designed consisting primarily of a four-bar linkage which would allow total model vertical translation, wing pitch and fuselage pitch independently of or with each other. Fore and aft body translation was not allowed. As tested the model wings and/or trim surface were oriented in a vertical plane.

For antisymmetric motion the model was allowed a roll degree of freedom about the fuselage centerline by a simple roll bearing support located around the fuselage spar. Wing pitch was also allowed but not total model side translation or yaw. The rudiments of these mechanisms can be seen in Figures 6 and 7.

S E C T I O N I I I

EXPERIMENTAL PROGRAM

The model experimental program consisted primarily of (1) measuring the model mass data, (2) conducting wind tunnel tests, (3) measuring the vibration frequencies and mode shapes and (4) measuring deflection influence coefficients. The information associated with each of these four phases is presented in the tables and figures that follow.

Mass and Geometry

Only the mass or weight data for models which were vibration tested and/or flutter analyzed will be presented. This, along with required geometry for each model or component is presented in the following figures and table.

The weights listed in Figures 8 through 13 and in Table I were determined simply by weighing the items on a gram scale. Mass moments of inertia were not measured because of the lack of need for this data. The balance arm center of gravity was determined by balancing the arm on a knife edge.

The S (small) trim surface is sized to be 15 percent smaller than the scaled or B (big) trim surface. These are shown in Figures 10 and 11. For most of the tunnel runs with TFW model and forward trim surface, the S trim surface was used. This was because the B trim surface forward tended to make the model marginally stable. Similarly, the B trim surface was used for the trim surface aft tests to increase model stability.

In Figures 10 and 11 the pivot axis locations D (design), F (forward) and A (aft) are alternate positions for use with the trim surface forward. Similarly, the positions marked D' (design), F' (forward) and A' (aft) are alternate pivot shaft positions for the trim surface aft.

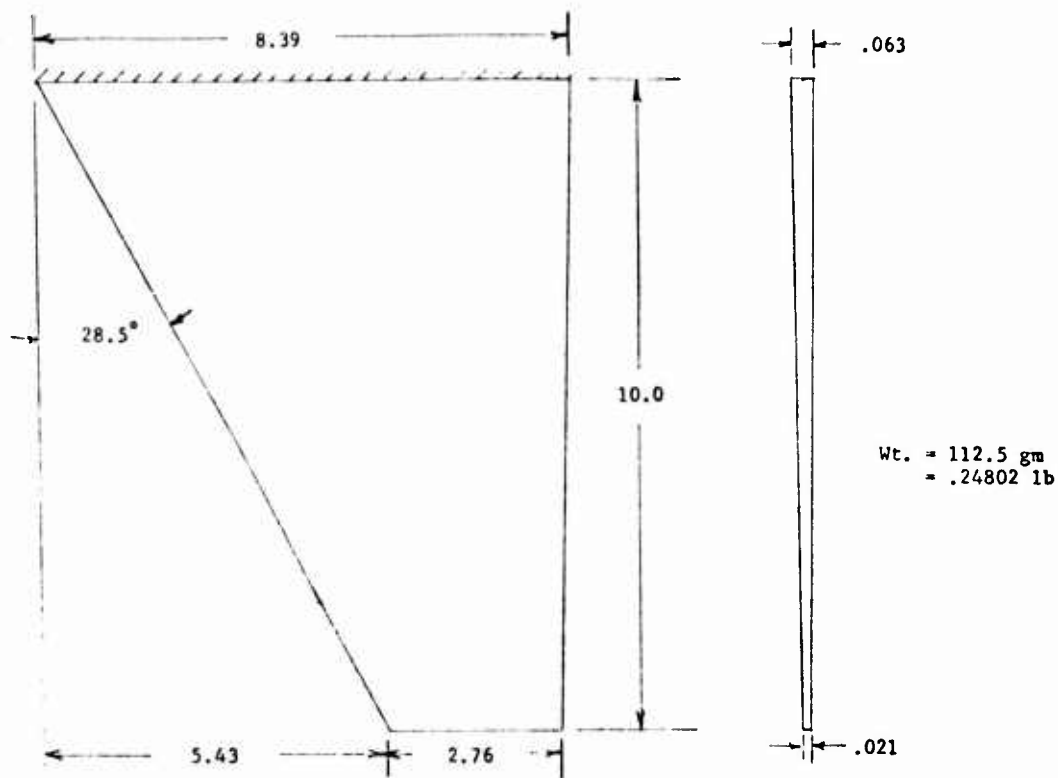


Figure 8 Mass and Geometry of Cantilever Model

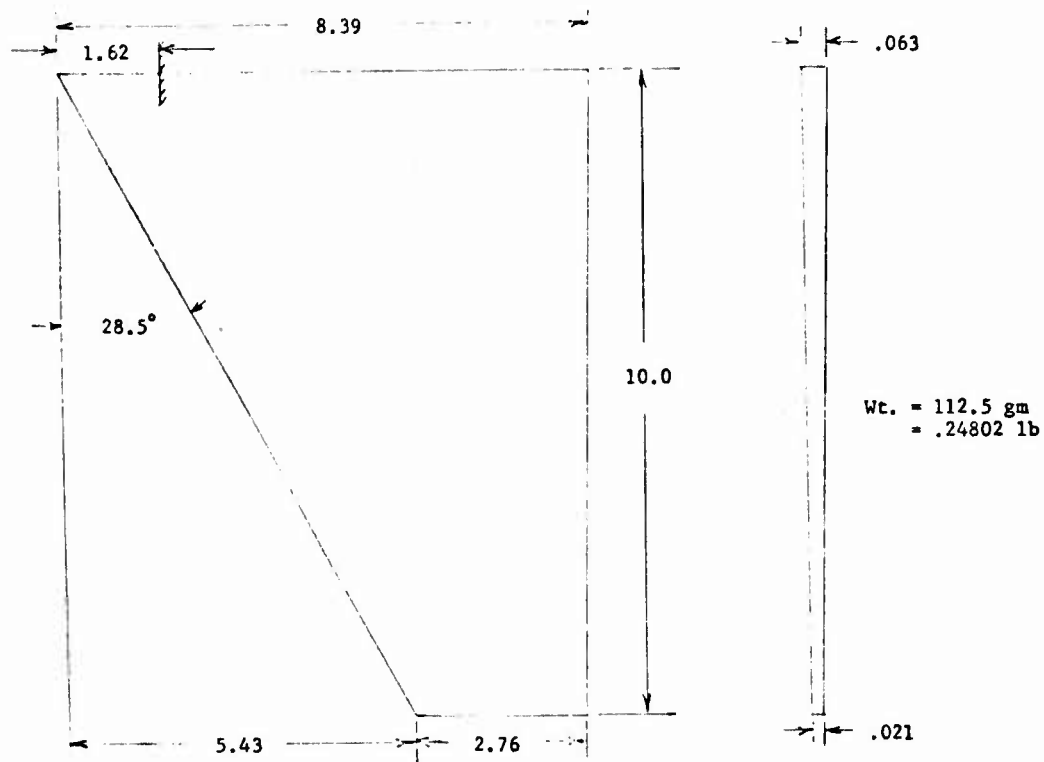


Figure 9 Mass and Geometry of Pitch Restrained Cantilever Model

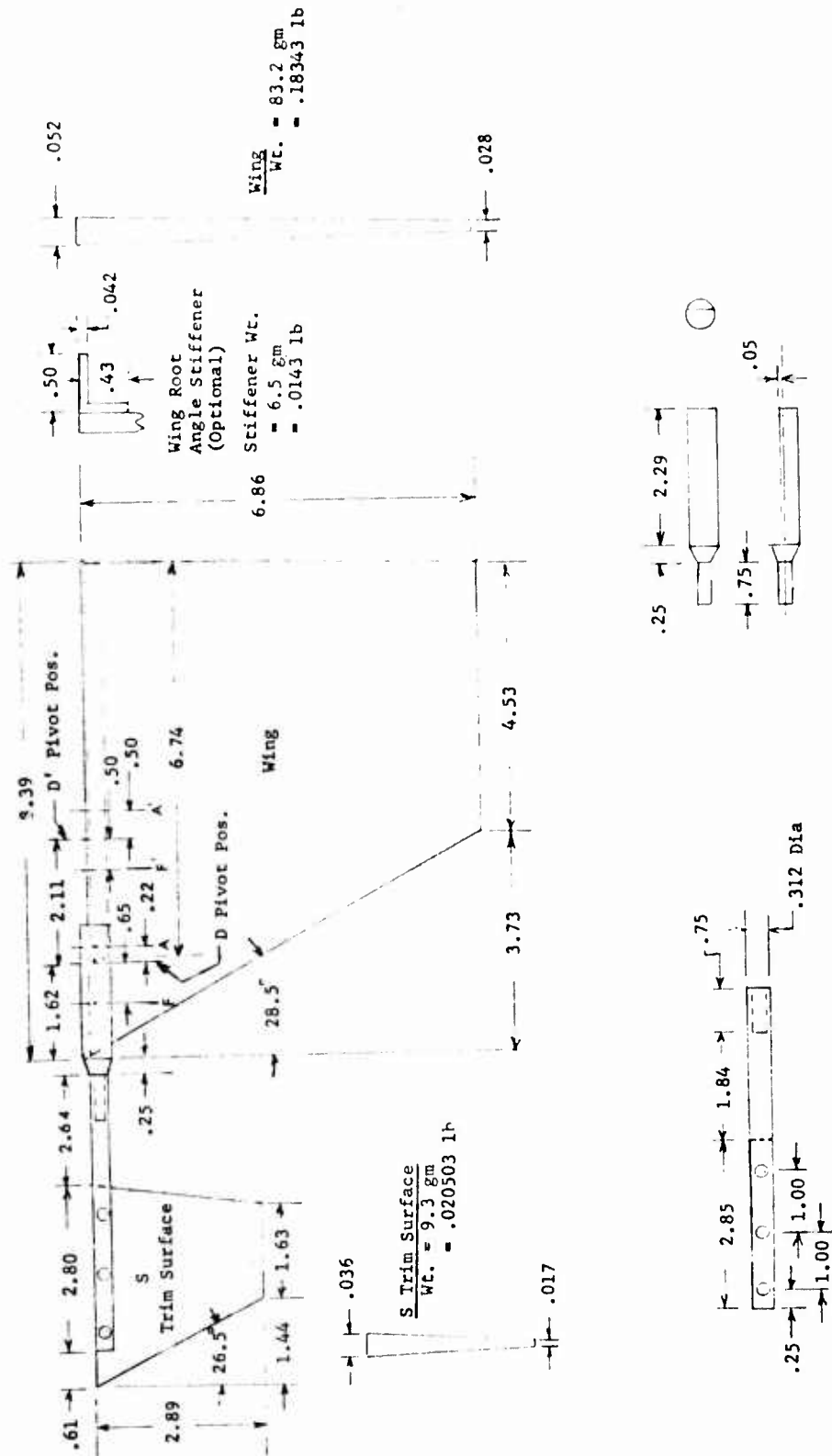


Figure 10 Mass and Geometry of Torsion Free Wing Model with Forward Trim Surface

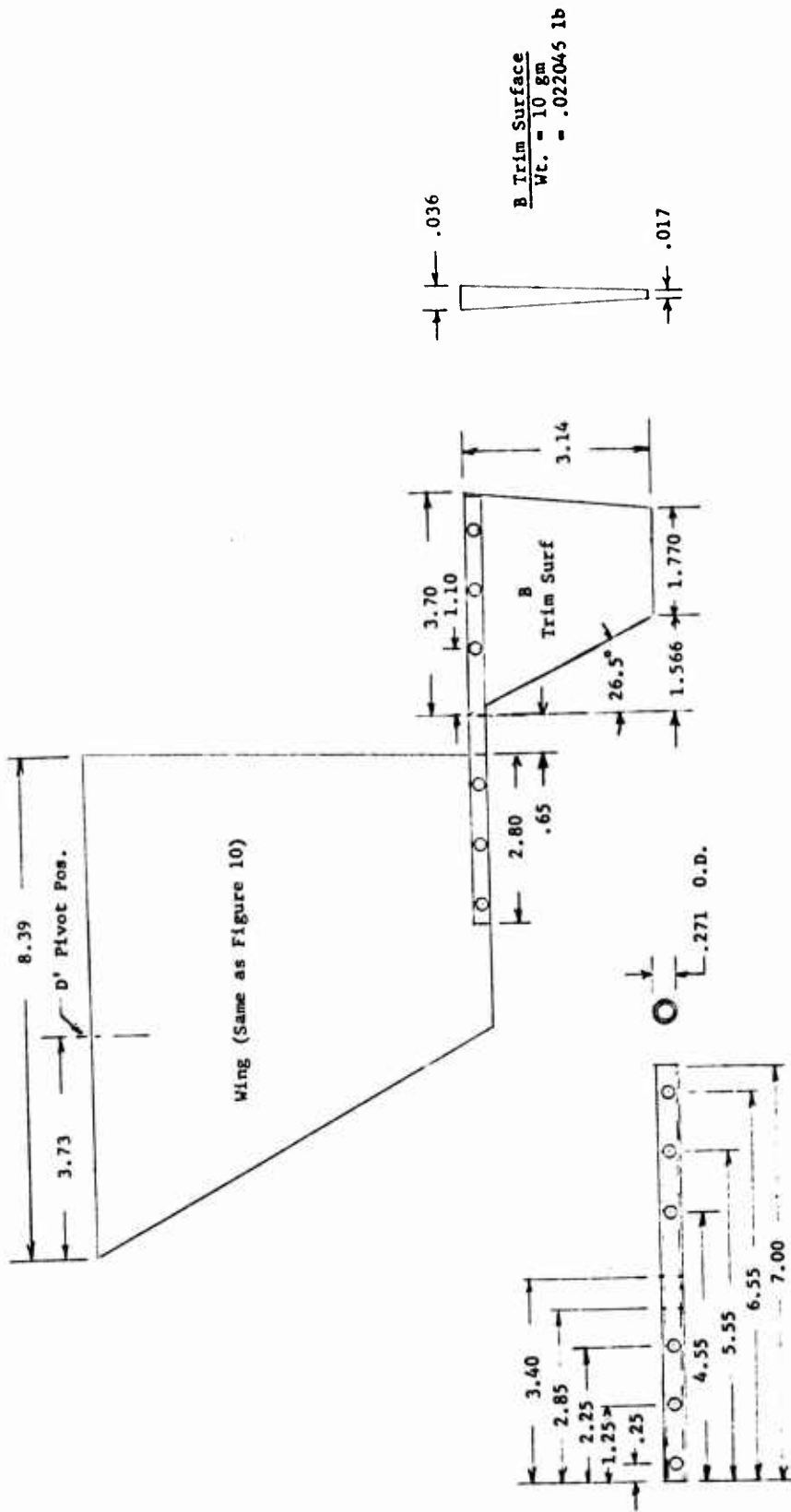


Figure 11 Mass and Geometry of Torsion Free Wing Model with Aft Trim Surface

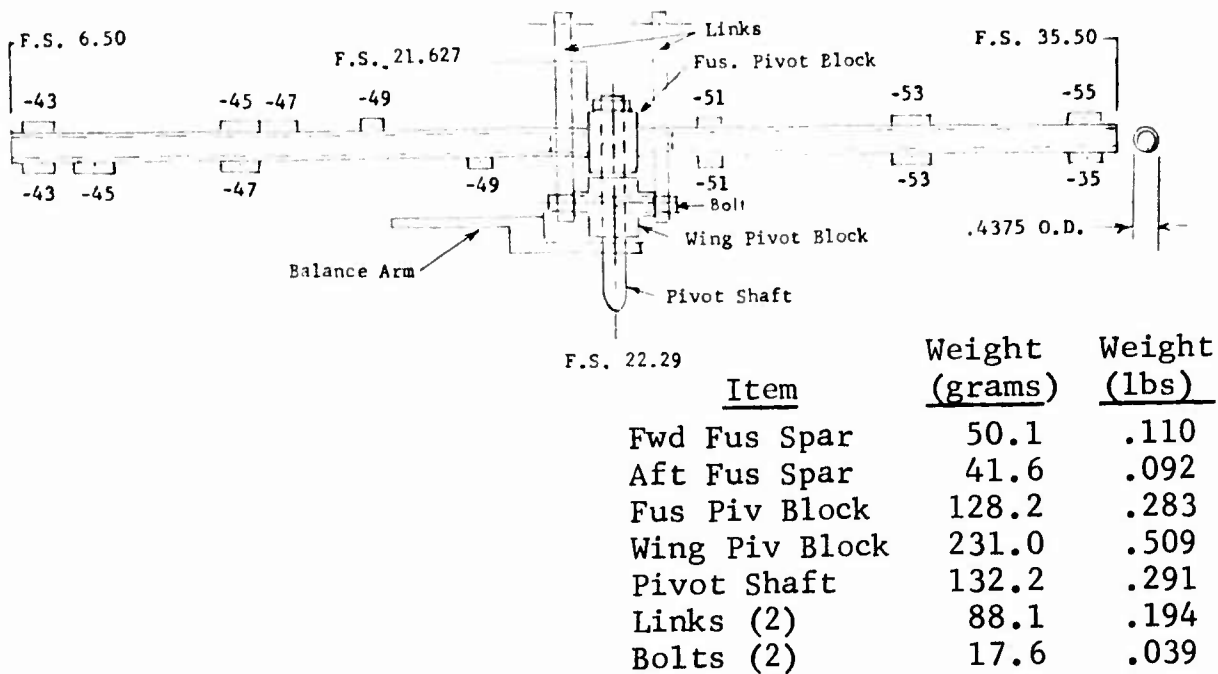
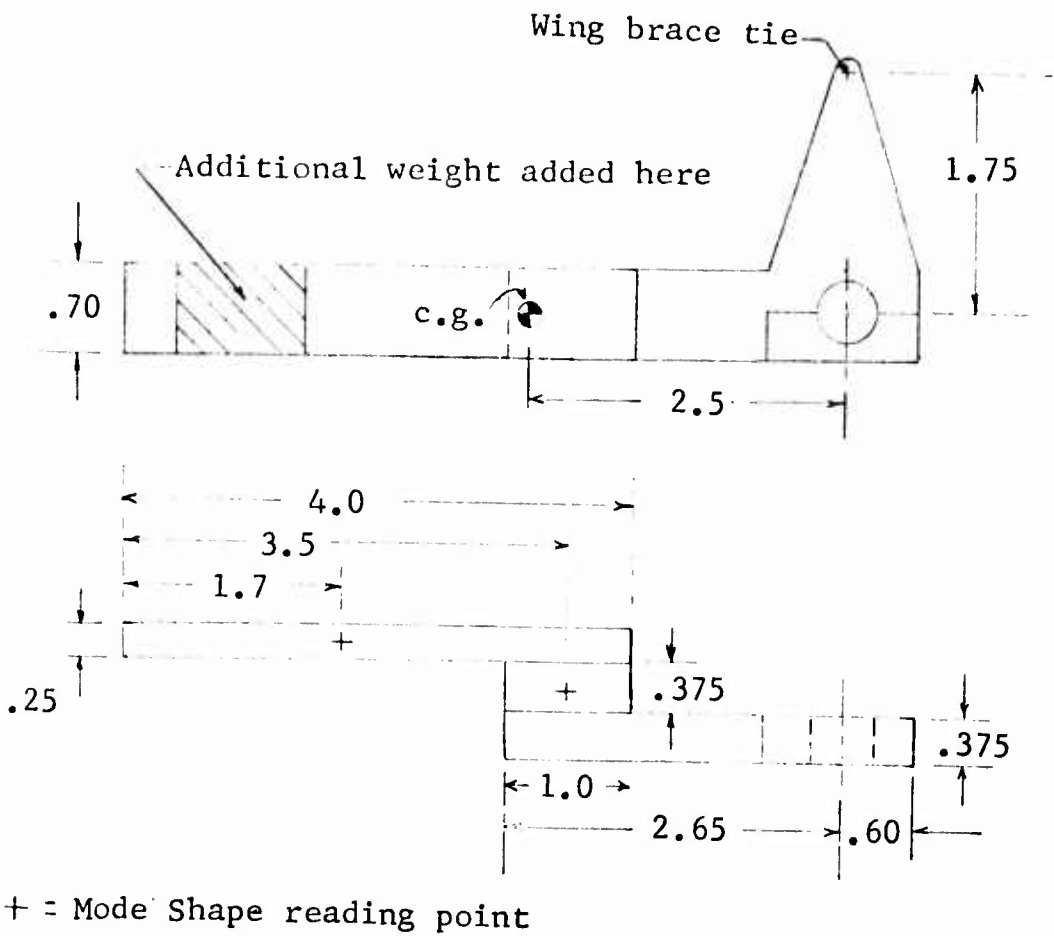


Figure 12 Mass and Geometry of Fuselage Spar and Mechanism

<u>FUS STA</u>	<u>DASH NO.</u>	<u>TOTAL WEIGHT (grams)</u>	<u>TOTAL WEIGHT (pounds)</u>	<u>LENGTH OF WEIGHT (inches)</u>
7.24	-43 (2)	124.0	.273	2.48
8.62	-45 (1)	96.3	.212	2.88
12.43	-45(1), -47(1)	203.4	.448	2.88/3.09
13.48	-47 (1)	113.3	.250	3.09
16.07	-49 (1)	84.0	.185	4.51
18.85	-49 (1)	84.1	.185	4.51
24.79	-51 (2)	93.4	.206	5.46
30.23	-53 (2)	331.6	.731	5.78
34.71	-55 (2)	284.1	.626	5.66

Table I FUSELAGE BALANCE WEIGHT DATA



Wt. (Total) = 123 gm
 = .271 lb

Figure 13 Mass and Geometry of Balance Arm

The pitch restrained cantilever was deflection tested by mounting the model to the pivot shaft located in the design (D) position. This is 1.62 inches aft of the apex of the wing. The pivot shaft was clamped for these measurements. Deflection reading point locations are shown in Figure 15 and the influence coefficients are in Table III.

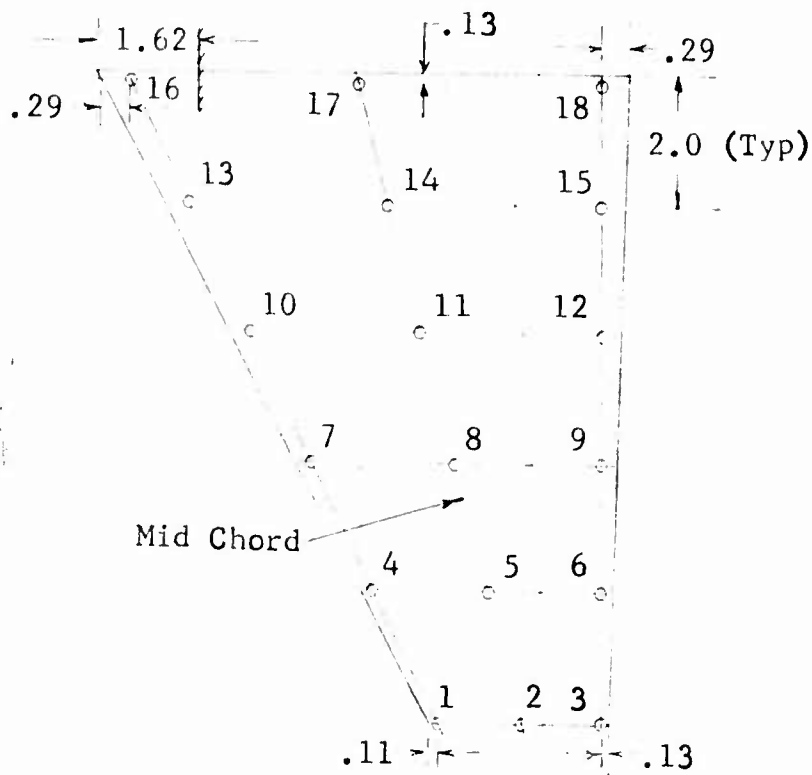


Figure 15 Deflection Reading Point Locations for Pitch Restrained Cantilever Model

	1	2	3	4	5	6	7	8	9	10	11	12	13	14	15	16	17	18
1	.730	.761	.784	.469	.534	.574	.243	.326	.382	.089	.175	.239	.008	.068	.123	-.004	-.001	.047
2		.836	.906	.485	.579	.663	.251	.369	.452	.090	.197	.296	.006	.082	.175	-.004	.009	.088
3			1.042	.495	.628	.768	.254	.394	.527	.089	.222	.360	.006	.100	.225	-.003	.017	.125
4				.344	.365	.381	.190	.236	.263	.072	.129	.166	.007	.050	.086	-.003	-.002	.028
5					.435	.495	.197	.283	.358	.071	.162	.244	.005	.070	.151	-.003	.010	.082
6						.626	.200	.328	.459	.070	.192	.327	.003	.093	.217	-.004	.022	.136
7							.127	.137	.142	.053	.079	.090	.006	.030	.043	-.003	-.003	.007
8								.201	.256	.051	.123	.188	.003	.057	.125	-.003	.013	.077
9									.382	.049	.162	.296	0	.086	.214	-.003	.029	.152
10										.030	.031	.029	.005	.011	.010	-.001	-.004	-.005
11											.085	.132	.001	.045	.098	-.002	.014	.071
12												.260	-.002	.079	.210	-.002	.035	.169
13													.003	-.001	-.005	0	-.002	-.007
14														.031	.069	-.001	.016	.061
15															.199	-.002	.041	.185
16																.004	0	-.001
17																	.017	.045
18																		.201

Table III MEASURED INFLUENCE COEFFICIENTS - PITCH
RESTRAINED CANTILEVER MODEL

Influence coefficients for the TFW with the forward trim surface were measured with the pivot shaft clamped and located in the forward (F) location. This is 0.97 inch aft of the wing apex. The very stiff (HH) boom was used and the small (S) trim surface size was also used. Deflection reading point locations for this configuration are shown in Figure 16 and the influence coefficients are presented in Table IV.

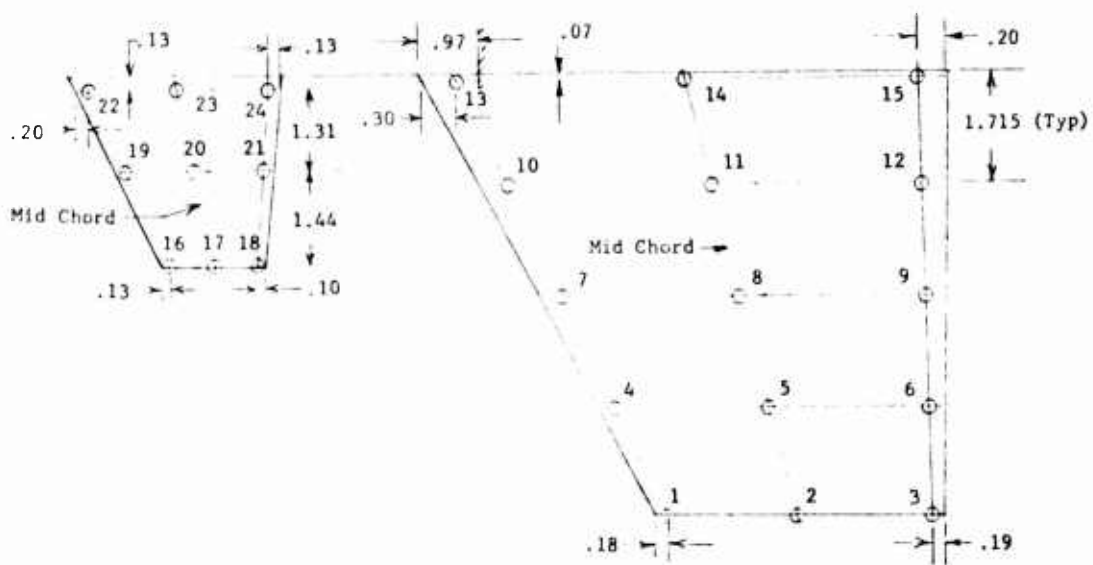


Figure 16 Deflection Reading Point Locations for Torsion Free Wing Model with Forward Trim Surface

	1	2	3	4	5	6	7	8	9	10	11	12	13	14	15	16	17	18	19	20	21	22	23	24
1	.371	-.383	.405	.218	.269	.304	.0954	.160	.209	.0133	.0724	.127	-.0000409	.00360	.0529	.000496	.000286	.000735	-.00176	-.00174	-.00116	-.00363	-.00340	-.00269
2	.310	-.586	.222	.222	.360	.437	.0915	.222	.334	.00629	.114	.235	-.000717	.0228	.144	-.00307	-.00107	-.00237	-.00459	-.00405	-.00472	-.00860	-.00829	-.00628
3		.782	.231	.410	.617	.617	.0891	.269	.470	.00832	.147	.350	-.00195	.311	.244	-.00087	-.00047	-.00467	-.0139	-.0122	-.00958	-.0178	-.0153	-.0119
4			.169	.176	.161	.337	.0701	.0991	.120	.0105	.0945	.0703	0	.00154	.245	.00070	.000407	.000933	.000979	.000795	.000420	.00234	.00210	.00163
5				.270	.270	.337	.0665	.175	.264	.00629	.0940	.195	-.000297	.0236	.130	.00102	-.00174	-.00264	-.00740	.00042	-.00472	-.00944	-.00508	-.00456
6					.533	.533	.0421	.0421	.429	.00489	.134	.340	-.00228	.0699	.256	-.0103	-.00133	-.00256	-.0168	.00128	.0102	.0183	.0155	.0120
7							.0421	.0421	.429	.00756	.0179	.0204	-.0006476	.00201	.0035	.000234	.000933	.000233	.000540	.000513	-.000373	-.00307	-.00108	-.00044
8								.122	.382	.00373	.0720	.132	-.000466	.0267	.112	-.00565	-.00509	-.00420	-.00733	.000486	-.00351	.0101	.00852	.00640
9										.00281	.0507	.328	-.00247	.0561	-.271	-.0129	-.0117	-.00981	-.0169	-.0147	-.0117	.0201	.0164	.0131
10											.000934	.109	-.000143	-.00135	-.00444	-.00014	-.000374	-.00028	-.000375	-.000465	-.000422	.000562	.000952	.000513
11											.0507	.317	-.000855	.0257	.0933	-.00719	-.00630	-.00551	-.00900	-.00756	-.00626	-.0106	-.00870	-.00689
12													-.00299	.0625	.292	-.0156	-.0144	-.0123	-.0192	-.0168	-.0136	-.0221	-.0186	-.0145
13													.000280	.000702	.0630	-.00775	-.00714	-.00607	-.00904	.000887	.000795	.000840	.000885	.000599
14														.0257	.3060	-.01780	-.01630	-.01400	-.02100	-.01820	-.01490	-.02310	-.00860	-.006350
15																.1260	.1080	.0979	.0576	.0524	.0441	.0399	.02380	.01550
16																	.1180	.1180	.0472	.0504	.0517	.0253	.0230	.0132
17																		.1440	.0677	.0677	.0592	.01980	.0260	.0132
18																			.0391	.0363	.0254	.01980	.0269	.0175
19																			.0492	.0341	.0278	.0278	.0214	.0175
20																					.0394	.0197	.0157	.0111
21																						.0417	.0228	.0149
22																								
23																								
24																								

Table IV MEASURED INFLUENCE COEFFICIENTS - TORSION FREE WING MODEL WITH FORWARD TRIM SURFACE

Influence coefficients for the TFW model with trim surface aft were measured with the pivot shaft in the aft design (D') position. The pivot shaft was clamped for these measurements. A high stiffness (H) boom was used and the big (B) trim surface was installed for these measurements. The aft design (D') position of the pivot shaft was used and is 3.73 inches aft of the wing apex. Deflection reading point locations are shown in Figure 17 and the measured influence coefficients are presented in Table V.

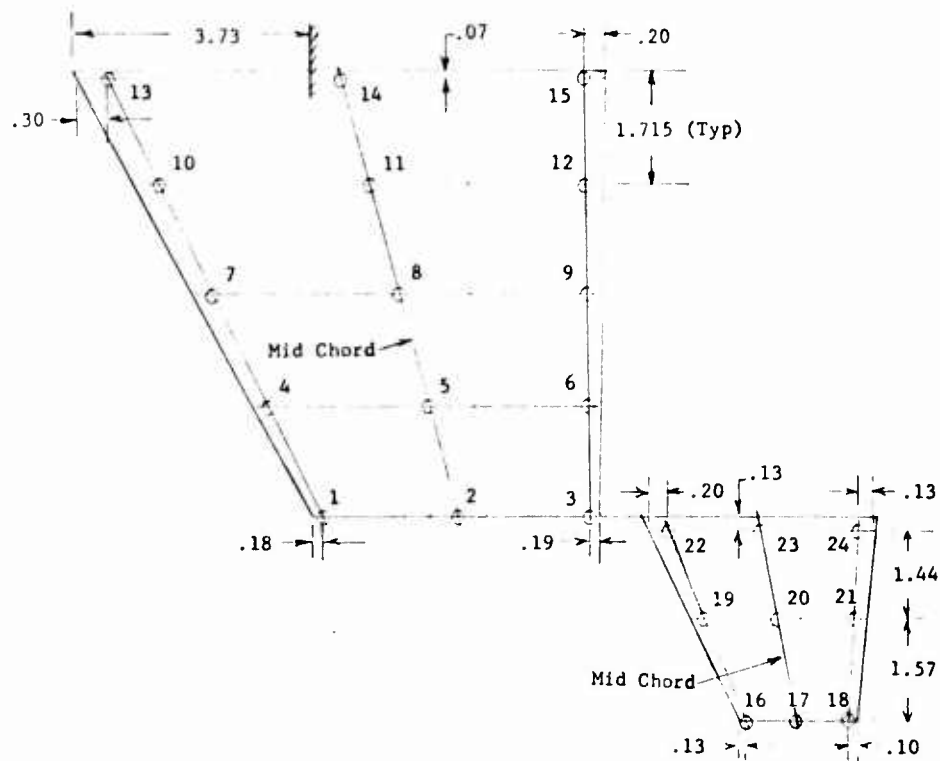


Figure 17 Deflection Reading Point Locations for Torsion Free Wing Model with Aft Trim Surface

	1	2	3	4	5	6	7	8	9	10	11	12	13	14	15	16	17	18	19	20	21	22	23	24
1	.147	.130	.110	.0849	.0829	.0673	.0306	.00306	.00942	-.000439	-.0147	-.00114	-.0329	.298	.276	.287	.230	.213	.194	.176	.154	.130		
2	.159	.179	.256	.0663	.101	.123	.0189	-.00707	.0137	.0314	-.0215	-.000351	-.00244	.482	.517	.589	.413	.428	.444	.329	.349	.359		
3				.0476	.112	.187	.00480	-.0177	.0170	.0641	-.0280	-.000349	.0311	.737	.774	.816	.812	.666	.731	.500	.570	.646		
4				.0630	.0457	.0267	.0315	.00654	.00550	-.00925	-.00716	-.000698	-.0218	.121	.103	.0948	.6907	.0758	.0607	.0691	.0501	.0284		
5					.0707	.0822	.0135	.0360	.0507	.0243	-.0161	.000175	.00375	.290	.294	.301	.242	.250	.260	.202	.213	.219		
6						.154	-.00209	.0437	.0861	.0661	-.0230	.000087	.0397	.496	.525	.556	.425	.471	.524	.363	.420	.481		
7							.0251	-.00698	-.00899	.00122	-.00271	-.000697	-.0181	.0122	-.00271	-.00542	.00542	-.00542	-.0176	.00135	-.0122	-.0284		
8								.0218	.0303	.00716	-.00978	.000262	.0611	.145	.148	.152	.123	.131	.137	.106	.114	.121		
9								.0912	-.0157	.0118	-.0175	.000349	.0318	.295	.317	.341	.261	.295	.334	.230	.272	.321		
10									-.00175	-.0140	-.00646	-.0000875	-.00550	.0393	-.0474	-.0528	-.0379	-.0447	-.0315	.0325	-.0433	-.0528		
11									-.00366	.00864	-.00646	.000785	.0632	.171	.185	.204	.154	.181	.211	.142	.172	.213		
12									-.00175	-.0140	-.00646	.000785	.0632	.171	.185	.204	.154	.181	.211	.142	.172	.213		
13									-.00175	-.0140	-.00646	.000785	.0632	.171	.185	.204	.154	.181	.211	.142	.172	.213		
14									-.00175	-.0140	-.00646	.000785	.0632	.171	.185	.204	.154	.181	.211	.142	.172	.213		
15									-.00175	-.0140	-.00646	.000785	.0632	.171	.185	.204	.154	.181	.211	.142	.172	.213		
16									-.00175	-.0140	-.00646	.000785	.0632	.171	.185	.204	.154	.181	.211	.142	.172	.213		
17									-.00175	-.0140	-.00646	.000785	.0632	.171	.185	.204	.154	.181	.211	.142	.172	.213		
18									-.00175	-.0140	-.00646	.000785	.0632	.171	.185	.204	.154	.181	.211	.142	.172	.213		
19									-.00175	-.0140	-.00646	.000785	.0632	.171	.185	.204	.154	.181	.211	.142	.172	.213		
20									-.00175	-.0140	-.00646	.000785	.0632	.171	.185	.204	.154	.181	.211	.142	.172	.213		
21									-.00175	-.0140	-.00646	.000785	.0632	.171	.185	.204	.154	.181	.211	.142	.172	.213		
22									-.00175	-.0140	-.00646	.000785	.0632	.171	.185	.204	.154	.181	.211	.142	.172	.213		
23									-.00175	-.0140	-.00646	.000785	.0632	.171	.185	.204	.154	.181	.211	.142	.172	.213		
24									-.00175	-.0140	-.00646	.000785	.0632	.171	.185	.204	.154	.181	.211	.142	.172	.213		

Table V MEASURED INFLUENCE COEFFICIENTS - TORSION FREE WING MODEL WITH AFT TRIM SURFACE

Vibration Testing

Vibration modes were measured for five model configurations. These are (1) cantilever, (2) pitch restrained cantilever, (3) TFW with forward trim surface-no root rib stiffener, (4) TFW with forward trim surface-with root rib stiffener and (5) TFW with aft trim surface.

The vibration test was conducted with the models mounted in the same section of the wind tunnel (this section was removed from the wind tunnel) as they were for the wind tunnel tests. Excitation was provided by an acoustic speaker fitted with an open ended cone to direct the oscillating volume of air to a small area. The amplitude of motion was measured by a non-contacting (no mass added to the models) proximity transformer.

Frequencies of interest were located by plotting relative response (amplitude of motion) versus frequency on an x-y plotter. The x axis motion (frequency) was driven by an oscillator output signal whose dc amplitude is proportional to frequency. The y axis motion (amplitude of motion) was driven by the output of a narrow band pass tracking filter. The dc output of the filter was proportional to amplitude of motion as measured by the non-contacting transducer. Frequency surveys are presented in the Appendix.

Once the response frequencies of interest were located, each one was excited in turn by locating the acoustic speaker at a point of significant motion. This was sensed with a lightly held pencil. Only one vibrator was used. The mode shape was then measured by moving the non-contacting transducer to a pre-selected series of reading point locations in turn and reading the relative amplitude of motion by means of an electrical meter. Phasing was determined by comparing the waveform of the output of the transducer to a fixed sine wave of the same frequency. Plotted mode shapes and the tabulated mode shape amplitude and phasing data are in the Appendix. It should be noted in reviewing the modes and frequencies that only symmetric modes were measured for the TFW models.

Wind Tunnel Testing

Wind tunnel tests were conducted in a 14 inch square free jet injection tunnel at General Dynamics' Fort Worth Division in September 1975. The tunnel was calibrated prior to testing. Smooth air flow was provided by placing fine screens over the bell mouth inlet. Access to the model was achieved by moving, with hydraulic actuators, the bell mouth and inlet sections to which the models were attached out of the 30 inch diameter plenum. Model access could also be gained through the viewing windows in the plenum section.

It was planned to test the cantilever model, the pitch restrained cantilever model, TFW model symmetric and anti-symmetric with trim surface forward and TFW model symmetric and antisymmetric with trim surface aft. Several parameter variations were planned for each TFW configuration. However, circumstances which developed during the test prevented many of the planned tunnel runs from being completed.

No antisymmetric tests were accomplished due to a very low speed (about 30 ft per second) instability involving rigid wing pitch and total configuration roll. Several different ways were tried to eliminate the instability or increase the speed at which it occurred. Only one was moderately successful. This consisted of moving the trim surface aft of the wing at the wing root and simultaneously placing a large forward balance weight on a boom at the wing tip. Speeds up to 130 ft per second were achieved for this configuration without the roll instability occurring. However, this so distorted the model configuration that testing was not attempted because of the lack of a reasonable model configuration.

Difficulties were also experienced in the symmetric tests with the trim surface forward. These consisted of two types. The first was a low speed instability involving rigid wing pitch and total configuration translation normal to the plane of the wing. This was easily solved by adding a forward balance weight to the pivot shaft inboard of the wing root. No aerodynamic forces were on the balance weight arm during test because of its inboard location.

The second problem which manifested itself during the symmetric tests, particularly with the trim surface forward, was wing static divergence. Items which were tried to increase the divergence speed above the flutter speed were testing only

in the forward pivot shaft position, using a much stiffer boom to support the forward trim surface, using a 15 percent smaller area trim surface, adding a balsa fairing at the wing root to make the airflow more symmetrical about the wing chord plane, blocking out the translation degree of freedom, and finally testing a thinner wing surface with an aluminum angle stiffener attached to the wing root aft of the pivot. None of these things enabled flutter speeds to be lower than the divergence speed. Therefore, no flutter speeds were obtained with the forward trim surface.

Several flutter points were obtained with the trim surface at the wing tip and aft. However, with the pivot shaft in the aft position (A') wing divergence was again experienced rather than flutter. However, for the trim surface aft the flutter speeds for the forward (F') and design (D') positions of the pivot shaft were about the same. Similarly, boom stiffness and trim surface pitch stiffness changes seemed to have only small effect on the flutter speed. Two cases of flutter were inherent in the trim surface aft tests. One was particularly mild and occurred at a low frequency with a definite flutter speed sometimes difficult to determine. The other case was a higher speed, higher frequency flutter instability that was present every time it was searched for. However, for some runs this instability was avoided.

The cantilever and pitch restrained cantilever both had definite but not explosive flutter speeds and frequencies. It was possible, not only on these two models but also on the TFW models, to probe into the flutter regime a long way, speed-wise, with no dangerous amplitude buildup.

Major wind tunnel tests results were:

1. The pitch restrained cantilever flutter speed was less than the cantilever.
2. No flutter was experienced with the trim surface forward. Static divergence occurred at a speed lower than the flutter speed.
3. For wings of the same root thickness, the flutter speed with the trim surface aft was slightly higher than the cantilever flutter speed.

A summary of the wind tunnel test data and variables tested is given in Table VI.

Table VI TORSION FREE WING TREND FLUTTER MODELS
WIND TUNNEL TEST DATA

Run No.	Model Configuration	Root Thickness (in.)	Pivot Shaft Pos.	Trim Surf Pos.	Trim Surf Pitch Stiff.	Boom Stiff.	Fus. Stiff.	Trim Surf Size	Flutter Speed (ft/sec)	Flutter Freq. (cps)	Remarks
1	Cantilever	.063	-	-	-	-	-	-	240	87	
1A	Pitch Restrained Cant.	.063	D	-	-	-	-	-	215	37	Pivot shaft clamped.
2	TFW (Trim Surf Fwd)	.063	D,F,A	F	H	H	H	B	-	-	Low speed run to check model stability. Fwd pivot pos. stable; design pivot pos. less stable; aft pivot pos. marginally stable.
2(rpt)	TFW (Trim Surf Fwd)	.063	F	F	K	H	H	B	-	-	Model not stable enough.
2(rpt)	TFW (Trim Surf Fwd)	.063	F	F	H	H	H	S	40	2.7	Flutter involving rigid body trans. and wing pitch. Made balance wt. arm and attached to pivot shaft-stopped flutter.
3	TFW (Trim Surf Fwd)	.063	F	F	H	H	H	S	-	-	No flutter to 240 fps. Had model trim/divergence problems.
3a	TFW (Trim Surf Fwd)	.063	F	F	H	HH	H	S	-	-	No flutter. Trim/divergence problems. Blocked out fus. transl. and went to 300 fps before divergence occurred.
3b	TFW (Trim Surf Fwd)	.063	F	F	H	HH	H	S	-	-	No flutter. Trimmed canard trailing edge by bending and added balsa fairing at wing root. With fus. transl. blocked out went to 350 fps before divergence.
3c	TFW (Trim Surf Fwd)	.063	F	F	H	HH	H	S	-	-	No flutter. Took balsa fairing off wing root and freed up fus. transl. Went to 310 fps before trim/divergence occurred.
3d	TFW (Trim Surf Fwd)	.052	F	F	H	HH	H	S	-	-	No flutter. Went to 250 fps with fus. transl. freed up before divergence occurred. Model wing bent during divergence. Straightened wing.

Legend:
D or D' = Design
F or F' = Forward
A or A' = Aft
H = High
L = Low
M = Medium
HH = Very High
B = Big
S = Small

Table VI (CONTINUED)

Run No.	Model Configuration	Root Thickness (in.)	Pivot Shaft Pos.	Trim Surf Pos.	Trim Surf Pitch Stiff.	Boom Stiff.	Fus. Stiff.	Trim Surf Size	Flutter Speed (ft/sec)	Flutter Freq. (cps)	Remarks
3e	TFW (Trim Surf Fwd)	.052	F	F	H	HH	H	S	-	-	No flutter. Added metal angle stiffener to wing along root chord to try to get flutter before divergence. Model diverged and bent wing at 325 fps. Straightened wing.
3f	TFW (Trim Surf Fwd)	.052	F	F	H	HH	H	S	-	-	No flutter. With metal angle stiffener on wing root and fus. transi. blocked out went to 410 fps before wing diverged.
7	TFW (Trim Surf Aft)	.063	D'	A	H	H	H	B	330	54	Not definite flutter up to 310 fps although looked close to flutter. Continued up to 350 fps with high freq. flutter at 330 fps.
7a	TFW (Trim Surf Aft)	.052	D'	A	H	H	H	B	210	9.2	Low speed, low frequency flutter - speed not real definite.
8	TFW (Trim Surf Aft)	.063	F'	A	H	H	H	B	260	43.8	High speed, high frequency flutter.
8a	TFW (Trim Surf Aft)	.052	F'	A	H	H	H	B	260	11.0	Low speed, low frequency flutter - speed not real definite.
8b	TFW (Trim Surf Aft)	.052	F'	A	H	H	H	B	330	52.5	High speed, high frequency flutter.
9	TFW (Trim Surf Aft)	.063	A'	A	H	H	H	B	200	10.0	Fus. transi. blocked out - low speed, low frequency flutter. Did not try for high speed, high frequency flutter.
9a	TFW (Trim Surf Aft)	.052	A'	A	H	H	H	B	210	10.9	Fus. transi. freed up - low speed, low frequency flutter. Did not try for high speed, high frequency flutter.
											No flutter. Wing divergence at 290 fps.
											No flutter. Wing divergence at 240 fps.

Legend:

D or D' = Design
 F or F' = Forward
 A or A' = Aft
 H = High
 L = Low
 M = Medium
 HH = Very High
 B = Big
 S = Small

Table VI (CONTINUED)

Run No.	Model Configuration	Root Thickness (in.)	Pivot Shaft Pos.	Trim Surf Pos.	Trim Surf Pitch Stiff.	Boom Stiff.	Fus. Stiff.	Trim Surf Size	Flutter Speed (ft/sec)	Flutter Freq. (cps)	Remarks
10	TFW (Trim Surf Aft)	.052	D'	A	H	L	H	E	210 240	9.7 10	Low speed flutter - speed not real definite.
11	TFW (Trim Surf Aft)	.052	F'	A	H	L	H	B	200	10.8	High speed flutter. Low speed, low frequency flutter. Did not try for high speed.
13	TFW (Trim Surf Aft)	.052	D'	A	M	H	H	B	200 270	9.2 39	Low speed, low frequency flutter. High speed, high frequency flutter.
14	TFW (Trim Surf Aft)	.052	F'	A	M	H	H	B	210	11.5	Low speed, low frequency flutter. Did not try for high speed.
15	TFW (Trim Surf Aft)	.052	D'	A	M	L	H	B	220	9.7	Low speed, low frequency flutter - speed not real definite.
17	TFW (Trim Surf Aft)	.052	F'	A	M	L	H	B	270	44.4	High speed, high frequency flutter.
25	TFW (Trim Surf Aft)	.052	D'	A	L	H	H	B	200 260	10.7 45.7	Low speed, low frequency flutter. High speed, high frequency flutter.
26	TFW (Trim Surf Aft)	.052	F'	A	L	H	H	B	270 250	9.1 43.3	Low speed, low frequency flutter. High speed, high frequency flutter.
28	TFW (Trim Surf Aft)	.052	D'	A	L	L	H	B	210 245	11.1 46	Low speed, low frequency flutter. High speed, high frequency flutter.
28'	TFW (Trim Surf Aft)	.052	F'	A	L	L	H	B	220 250	9.3 45	Low speed, low frequency flutter. High speed, high frequency flutter.
31	TFW (Trim Surf Aft)	.052	F'	A	H	H	H	B	210 240 340	11 46.7 57.5	Low speed, low frequency flutter. High speed, high frequency flutter. Only flutter condition. Wing brace added for this run.

Legend:

D or D' = Design
 F or F' = Forward
 A or A' = Aft
 H = High
 L = Low
 M = Medium
 HH = Very High
 B = Big
 S = Small

S E C T I O N I V

ANALYSES

Both flutter and static aeroelastic analyses were performed during this program. Flutter analyses were conducted upon five different configurations using measured mass and vibration mode data as input to the analysis. Kernel function aerodynamics were utilized for all analyses and one configuration with trim surface aft was reanalyzed using doublet-lattice aerodynamics. The doublet-lattice method includes mutual aerodynamic interference effects between surfaces whereas the kernel function method does not.

Static aeroelastic analyses were performed upon four configurations using measured structural influence coefficients to describe the stiffness characteristics of each model. Aerodynamic influence coefficients were computed using the method of F. A. Woodward. The static aeroelastic analyses were used to determine divergence speeds described later.

Flutter Analyses

Conventional V-g flutter analyses and the number of modes used in the analyses were conducted upon the following five configurations:

1. Cantilever (3 modes used)
2. Pitch restrained cantilever (4 modes used)
3. TFW with trim surface forward (7 modes used)
4. TFW with trim surface forward and stiffened wing root chord (6 modes used)
5. TFW with trim surface aft (7 modes used)

Kernel function aerodynamics were utilized in the analyses of all configurations and in addition the last one (number 5) was also analyzed using doublet-lattice aerodynamic theory.

The kernel function method used for application to the torsion free wing flutter models was mechanized by R. P. Peloubet and P. G. Waner (Reference 4) and follows the approach described by P. T. Hsu (Reference 5). The present method uses an integral equation obtained from linearized compressible subsonic flow which relates the downwash to the pressure difference over a finite span surface, i.e.,

$$\bar{W}(x,y) = \frac{1}{4\pi\rho V} \iint_{S_w} \Delta p(\xi,\eta) K(x-\xi, y-\eta, k, M) d\xi d\eta$$

where

\bar{W} = downwash at coordinate x,y

ρ = air density

V = free stream velocity

Δp = difference in pressure between upper and lower surface of wing

K = kernel function

k = reduced frequency

M = Mach number

S_w = Wing area

x, y, ξ, η = coordinates in the plane of the wing

⁴Peloubet, R. P., "Finite Span Subsonic Flutter Analysis Method Utilizing M.I.T. Series Method for Computing Pressure Distributions," General Dynamics Memorandum Report SDGM-80, August 1958.

⁵Hsu, P. T., "Flutter of Low Aspect Ratio Wings, Part I, Calculation of Pressure Distributions for Oscillating Wings of Arbitrary Planform in Subsonic Flow by the Kernel-Function Method," Aeroelastic and Structures Research Lab. TR 64-1, MIT, Cambridge, Mass., October 1957.

The solution to the previous equation is accomplished by the use of an assumed pressure distribution with unknown coefficients. The assumed pressure functions are weighted simple polynomials where the weighting function satisfies the necessary edge boundary conditions. The equation is then satisfied at as many collocation points as there are unknown coefficients in the assumed pressure distributions. The integration of this equation is accomplished via Chebyshev-Gaussian quadrature for each term in the assumed polynomial at each collocation point reducing the problem to solving a set of simultaneous algebraic equations. Given the modal displacement the downwash is determined and the unknown coefficients of the pressure distributions determined. The integrated product of the pressure distribution and the modal displacement over the surface gives the generalized aerodynamic forces.

In all applications of the kernel function method to TFW models, five spanwise rows of five collocation points each were used on each aerodynamic surface. Furthermore, 11 chordwise rows of 10 integration points were used in computing the generalized aerodynamic terms. The edge of the free jet in the wind tunnel was assumed to act as a reflecting plane. Therefore, symmetric aerodynamics were used for all aerodynamic surfaces except for the aft trim surface for which antisymmetric aerodynamics best satisfies the pressure distribution at the root. It should be noted that this method as applied here does not provide for aerodynamic interaction between surfaces on multiple surface configurations.

The doublet-lattice method used for the analysis of the "trim-surface-aft" configuration provides an approximate solution to the linearized formulation of the oscillatory subsonic lifting surface theory. The method, developed by E. Albano and W. P. Rodden (References 6 and 7), is an extension of the

⁶Albano, E., Rodden, W. P., "A Doublet Lattice Method for Calculating Lift Distribution on Oscillating Surfaces in Subsonic Flows," AIAA Paper No. 68-73, AIAA 6th Aerospace Sciences Meeting, January 1968.

⁷Albano, E., "Planar Doublet-Lattice Method for Aerodynamic Forces," Northrop Corporation, Norair Division Report NOR 68-147, October 1968.

one developed by Hedman for steady flow (Reference 8). One important feature of the method is that it provides for aerodynamic interaction between surfaces.

As applied to the trim-surface-aft model, the wing was divided into 42 boxes (6 spanwise x 7 chordwise) with smaller boxes near the leading edge to compensate for the steep pressure gradient. In addition, the wing planform was extended slightly to compensate for the "end cap effect" of the trim surface boom. The aft trim surface was extended inboard for the same reason and divided into 25 constant span, constant percent chord boxes (5 spanwise x 5 chordwise). Again, symmetric aerodynamics were used.

Conventional V-g flutter analyses using the modal method were performed for the TFW models using flutter subroutines coded into the respective aerodynamic codes. The generalized mass was computed from lumped mass models of various TFW configurations and the experimentally measured modes. Orthogonality of the experimental modes was checked and non-orthogonal modes deleted from the analysis. This resulted in not deleting any modes for the cantilever, pitch restrained cantilever, and TFW forward trim surface models (no wing root stiffener). Three modes were eliminated on the TFW forward trim surface model (with wing root stiffener) and one mode was eliminated on the TFW trim aft model. The general criterion for eliminating a mode was based on the calculation of the product of the mass coupling terms for a pair of modes divided by the product of the diagonal generalized mass terms for the same pair of modes. If this ratio exceeded 0.15, one of the two modes was eliminated. To avoid the non-orthogonal effects of the remaining modes, off diagonal terms of the generalized mass matrices were set equal to zero.

⁸Hedman, S. G., "Vortex Lattice Method for Calculation of Quasi-Steady-State Loading on Thin Elastic Wings," Aeronautical Research Institute of Sweden Report 105, October 1965.

Where applicable, analyses included rigid body modes, i.e., fuselage pitch and wing pitch. Due to the model suspension the vertical translation mode appeared as a pendulum mode with a frequency of approximately 1.6 Hz. This mode was also included in the analyses.

The results of the flutter analyses are presented in the form of structural damping and frequency versus velocity curves in Figures 18 through 23. A comparison of measured and calculated flutter speeds is shown in Table VII. Also, the experimentally measured modes are plotted in Figures 30 through 62 in the Appendix.

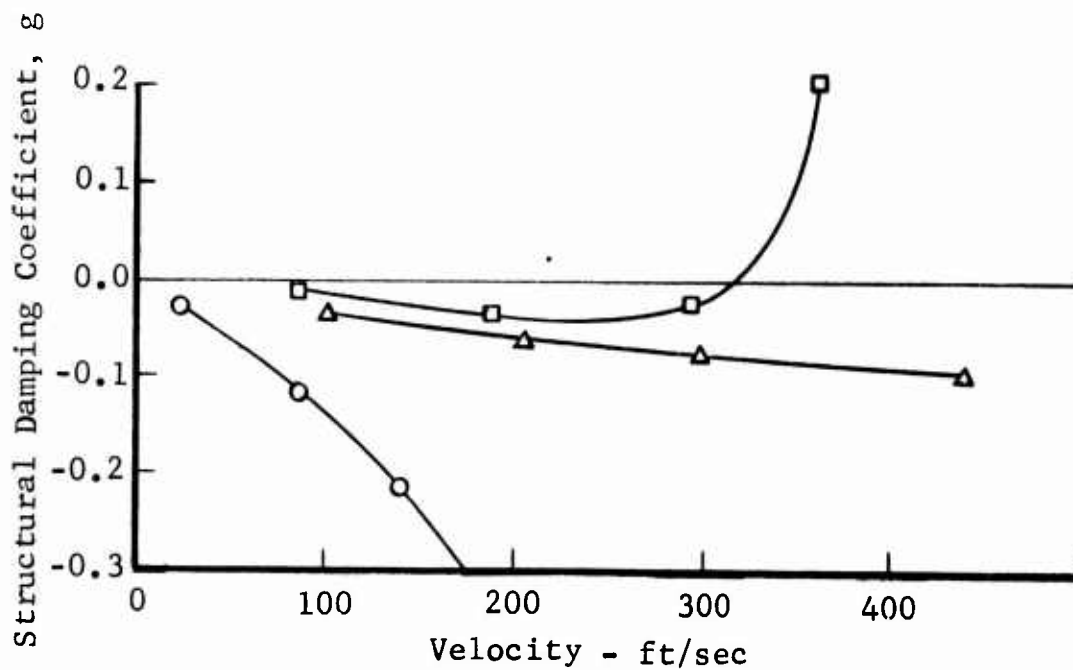
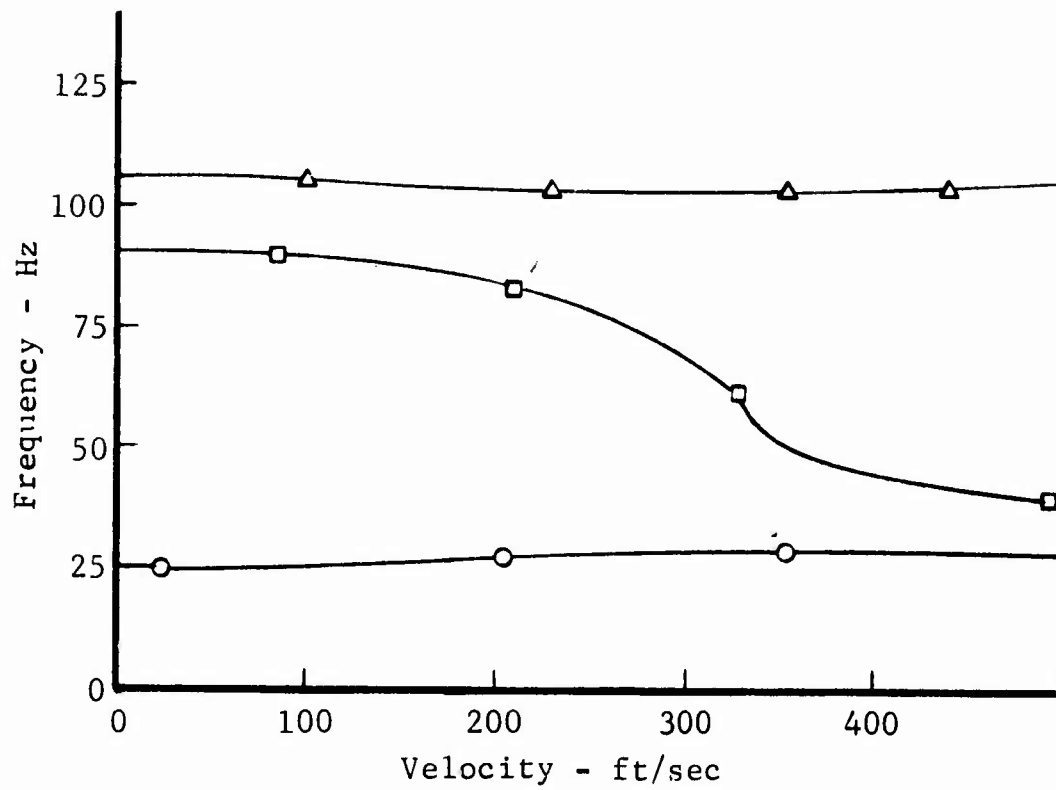


Figure 18 Structural Damping Coefficient and Frequency Versus Velocity for Cantilever Model

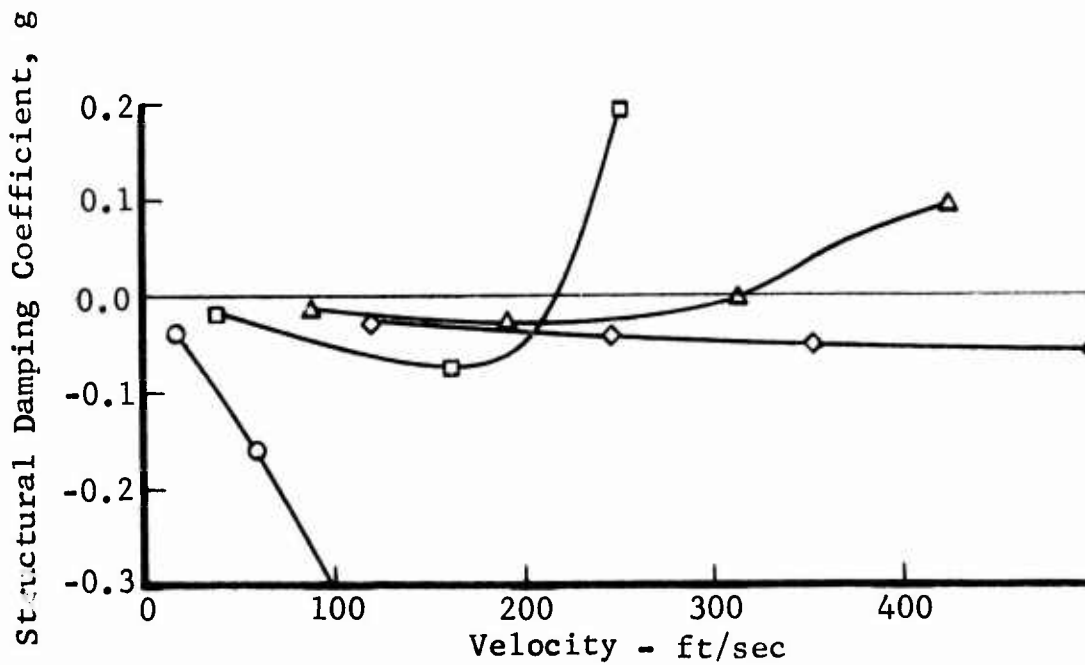
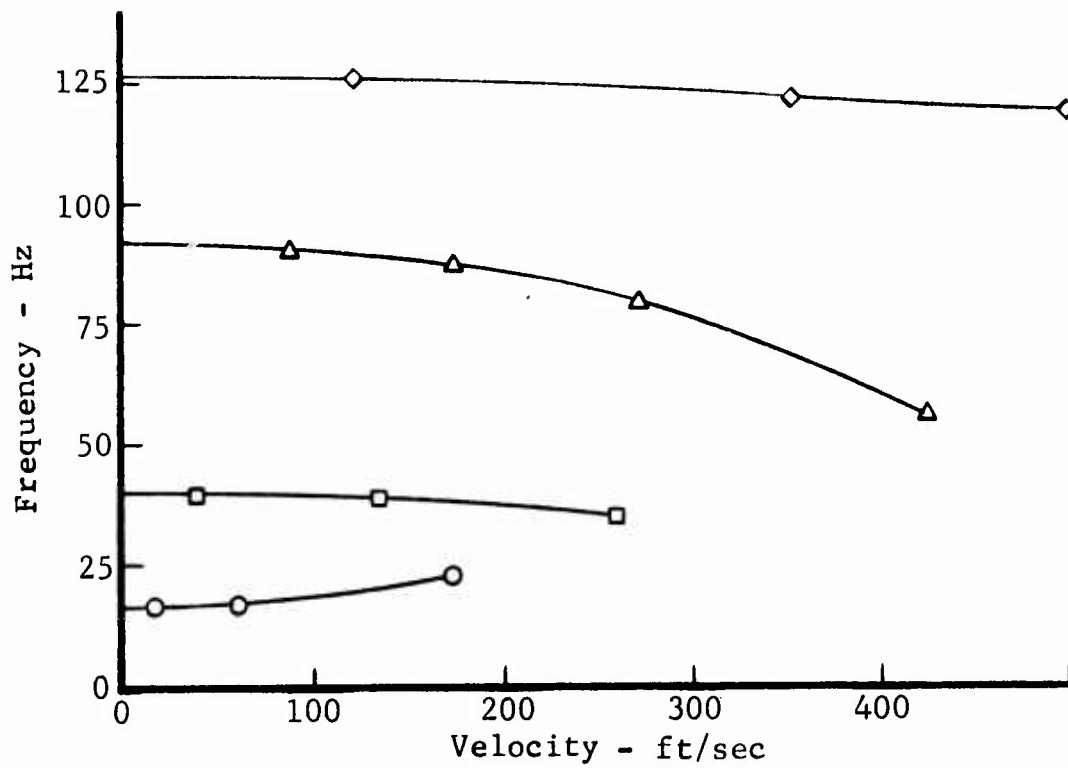


Figure 19 Structural Damping Coefficient and Frequency Versus Velocity for Pitch Restrainted Cantilever Model

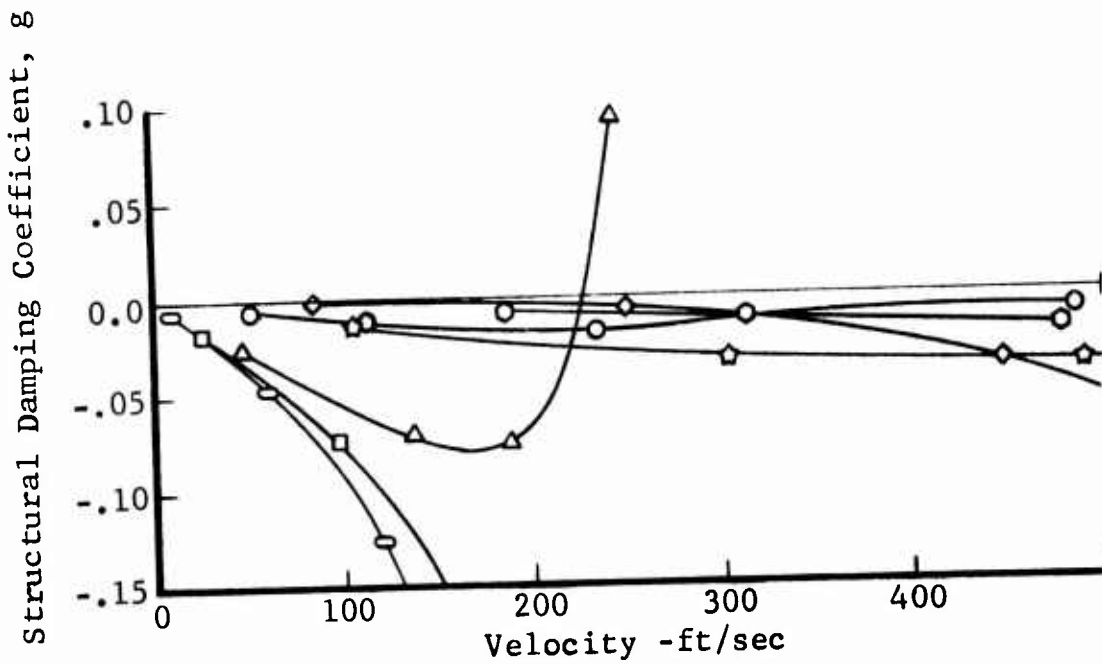
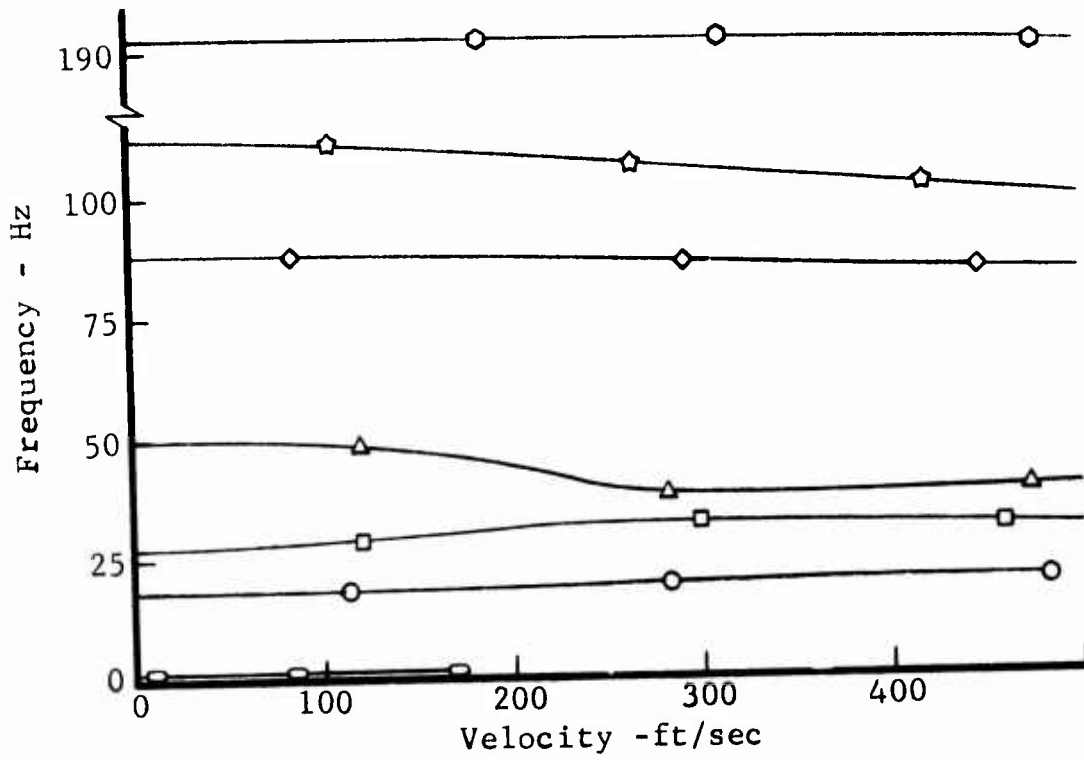


Figure 20 Structural Damping Coefficient and Frequency Versus Velocity for TFW Trim Surface Forward Model

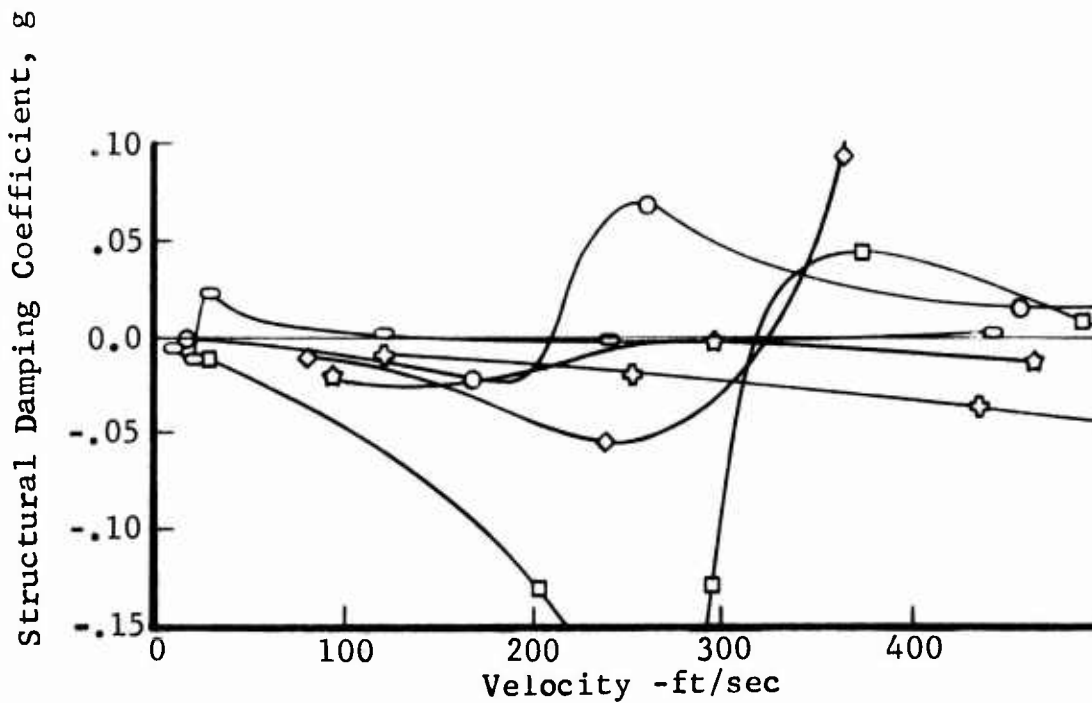
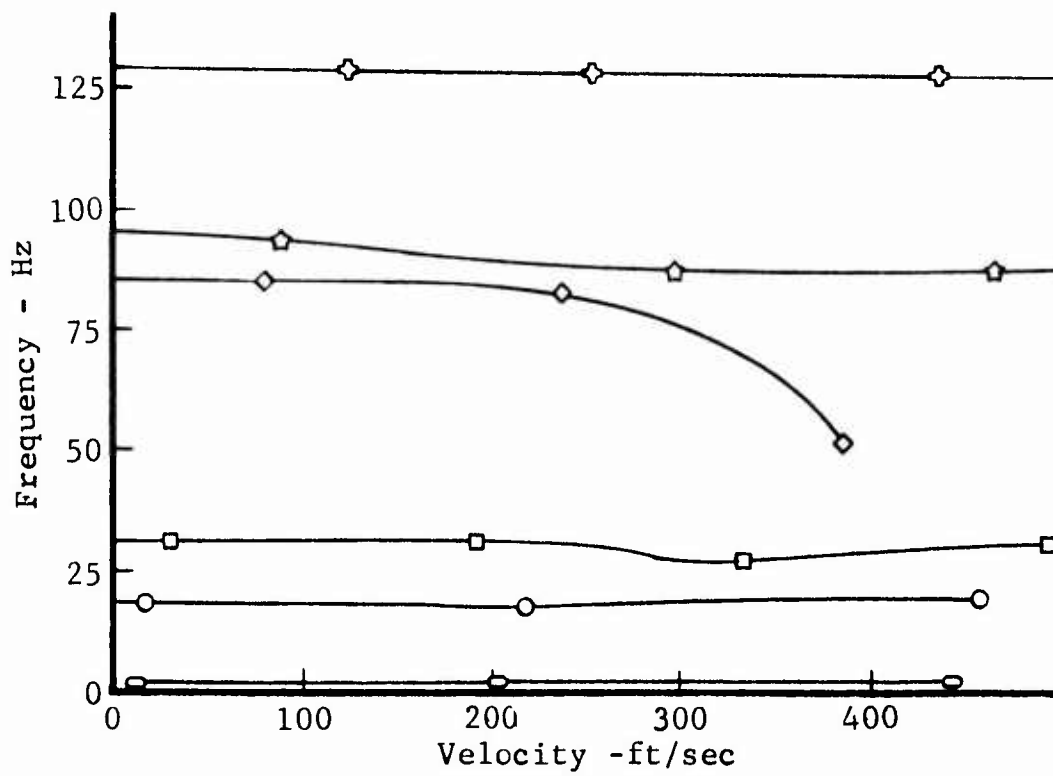


Figure 21 Structural Damping Coefficient and Frequency Versus Velocity for TFW Trim Surface Forward Model With Wing Root Stiffener

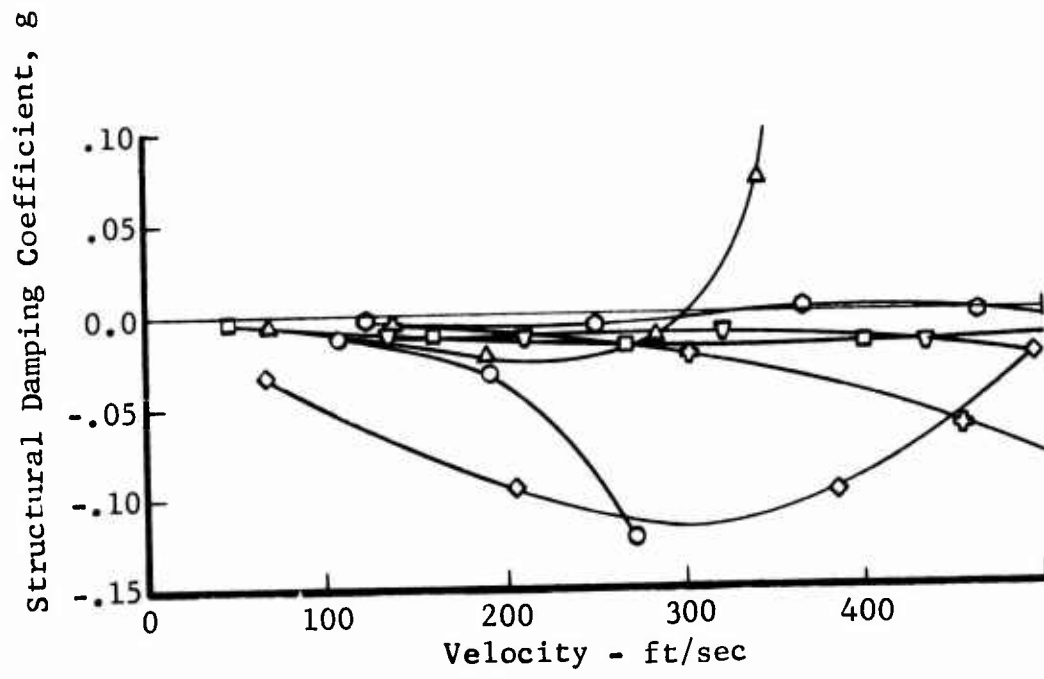
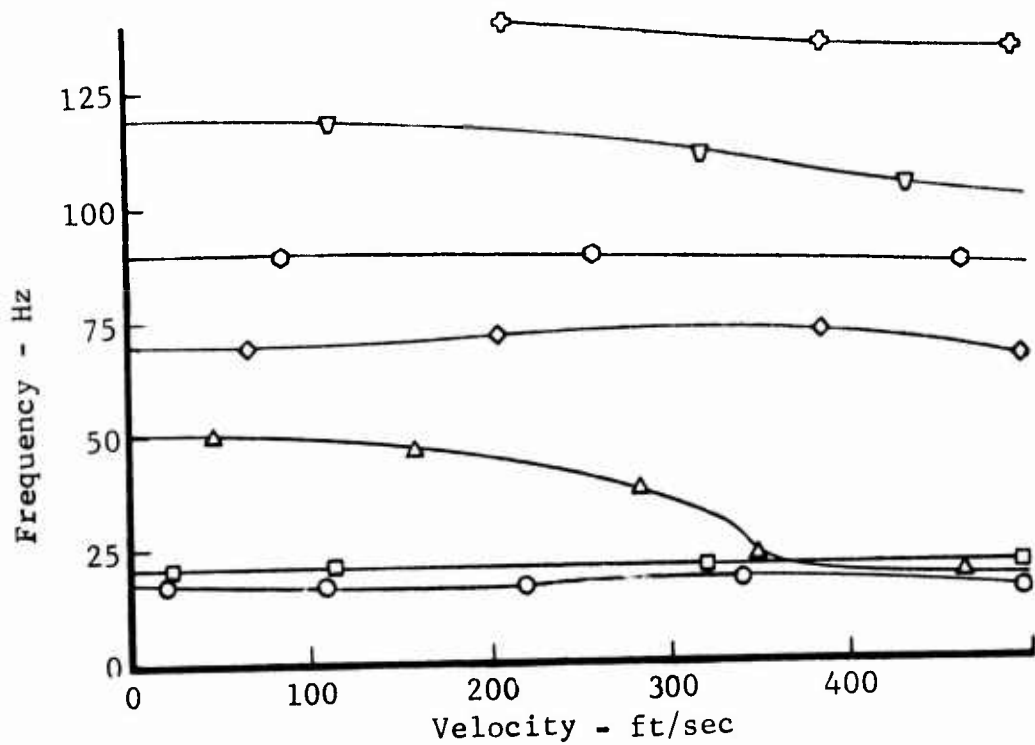


Figure 22 Structural Damping Coefficient and Frequency Versus Velocity for TFW Trim Surface Aft Model (Kernel Function)

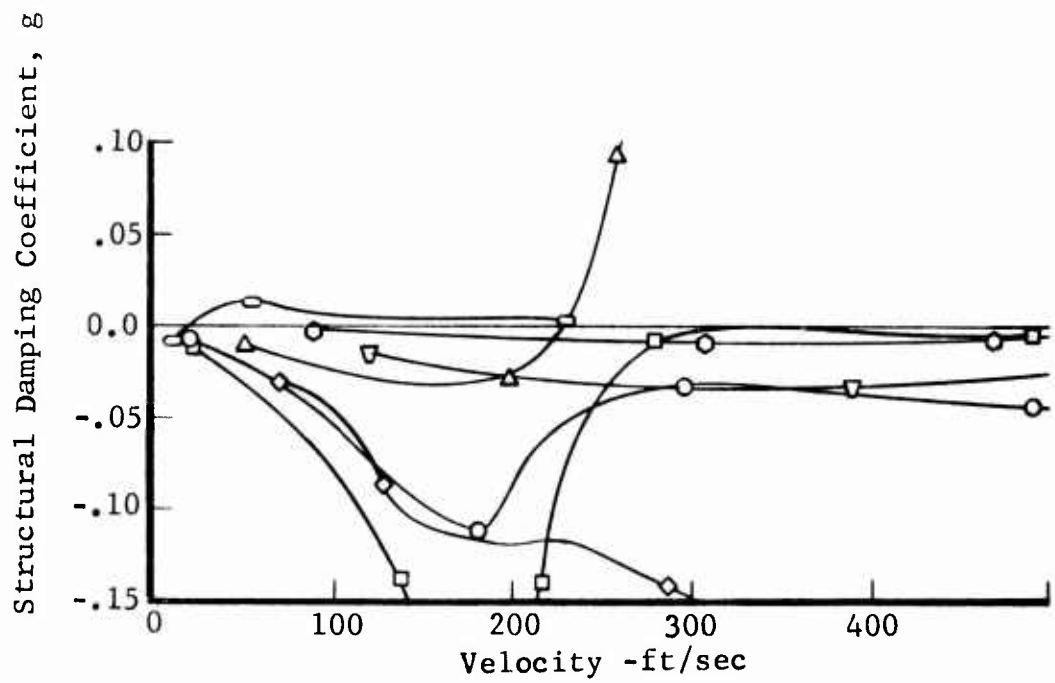
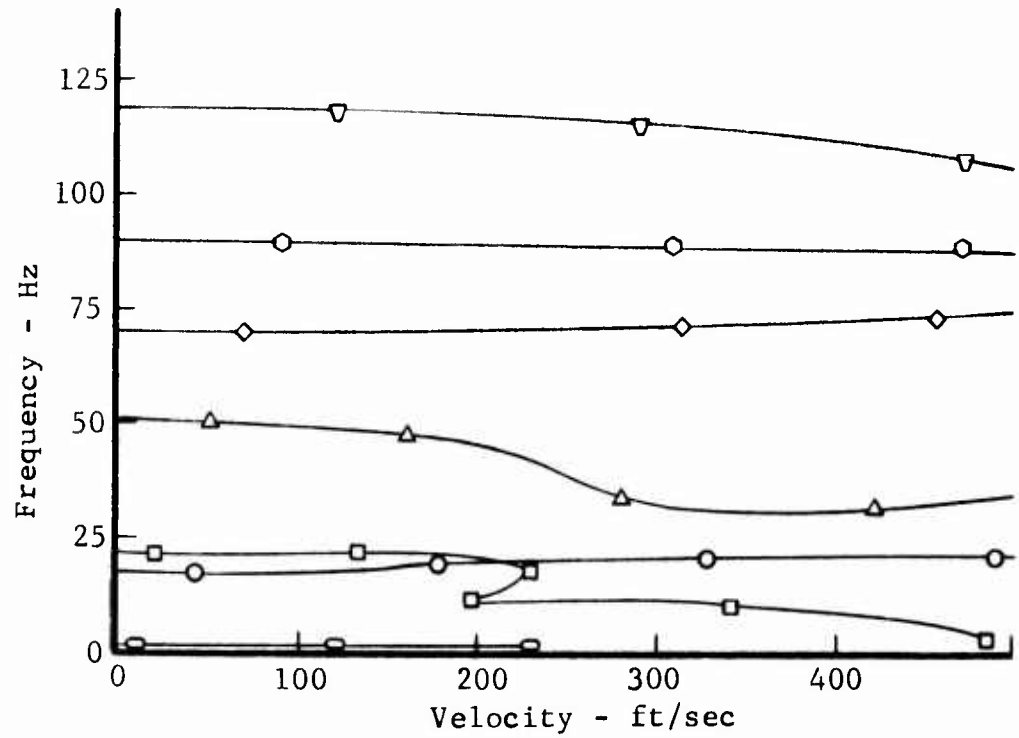


Figure 23 Structural Damping Coefficient and Frequency Versus Velocity for TFW Trim Surface Aft Model (Doublet-Lattice)

Table VII COMPARISON OF CALCULATED AND MEASURED FLUTTER SPEEDS

<u>Configuration</u>	<u>Calculated</u>		<u>Measured</u>	
	<u>Flutter Speed</u>	<u>Frequency</u>	<u>Flutter Speed</u>	<u>Frequency</u>
Cantilever	315 fps (a)	65 cps	240 fps	87 cps
P.R. Cant.	218 fps (a)	37 cps	215 fps	37 cps
TFW (Fwd Trim Surf)	228 fps ¹ (a) 21 fps ¹ (a) 208 fps ² (a)	31 cps ¹ 1.6 cps ¹ 17 cps ²	None*	None*
TFW (Aft Trim Surf)	305 fps ³ (a) 20 fps ³ 229 fps ⁴	35 cps ³ 1.59 cps ³ 42 cps ⁴	210 fps 260 fps	9.2 cps 43.8 cps

(a) Kernel function aerodynamics used

- 1 Stiffened wing root-rigid body translation
 - 2 Stiffened wing root-lowest speed involving flexible mode
 - 3 Rigid body translation-doublet lattice
 - 4 Lowest speed involving flexible mode-doublet lattice
- * Did not get flutter - experienced divergence instead

Divergence Analyses

The divergence speeds for the Torsion Free Wing (TFW) were computed for the four configurations which are:

1. Fully cantilevered (Figure 8)
2. Pitch restrained cantilever (Figure 9)
3. Wing supported at a single point plus a forward trim surface (Figure 10)
4. Wing supported at a single point plus a wing tip aft trim surface (Figure 11)

Thus, in order to calculate the divergence speeds for the above configurations, the following tasks were required:

1. The experimental test determination of the structural influence coefficients. The grid points where the influence coefficients were measured are shown in Figures 14 through 17, respectively. Tables II through V summarize the results of the measured influence coefficients for each respective configuration. The method used in the determination of these influence coefficients is discussed in the Experimental Program section of this report.
2. The theoretical calculation of the aerodynamic influence coefficients utilizing the method presented in Reference 9.

The two items above were then combined in the same manner as shown in Figure 24, equation (6).

⁹Woodward, F. A., Hague, D. S., "A Computer Program for the Aerodynamic Analysis and Design of Wing-Body-Tail Combinations at Subsonic and Supersonic Speeds, Volume I: Theory and Program Utilization," General Dynamics' Fort Worth Division ERR-FW-867, February 1969.

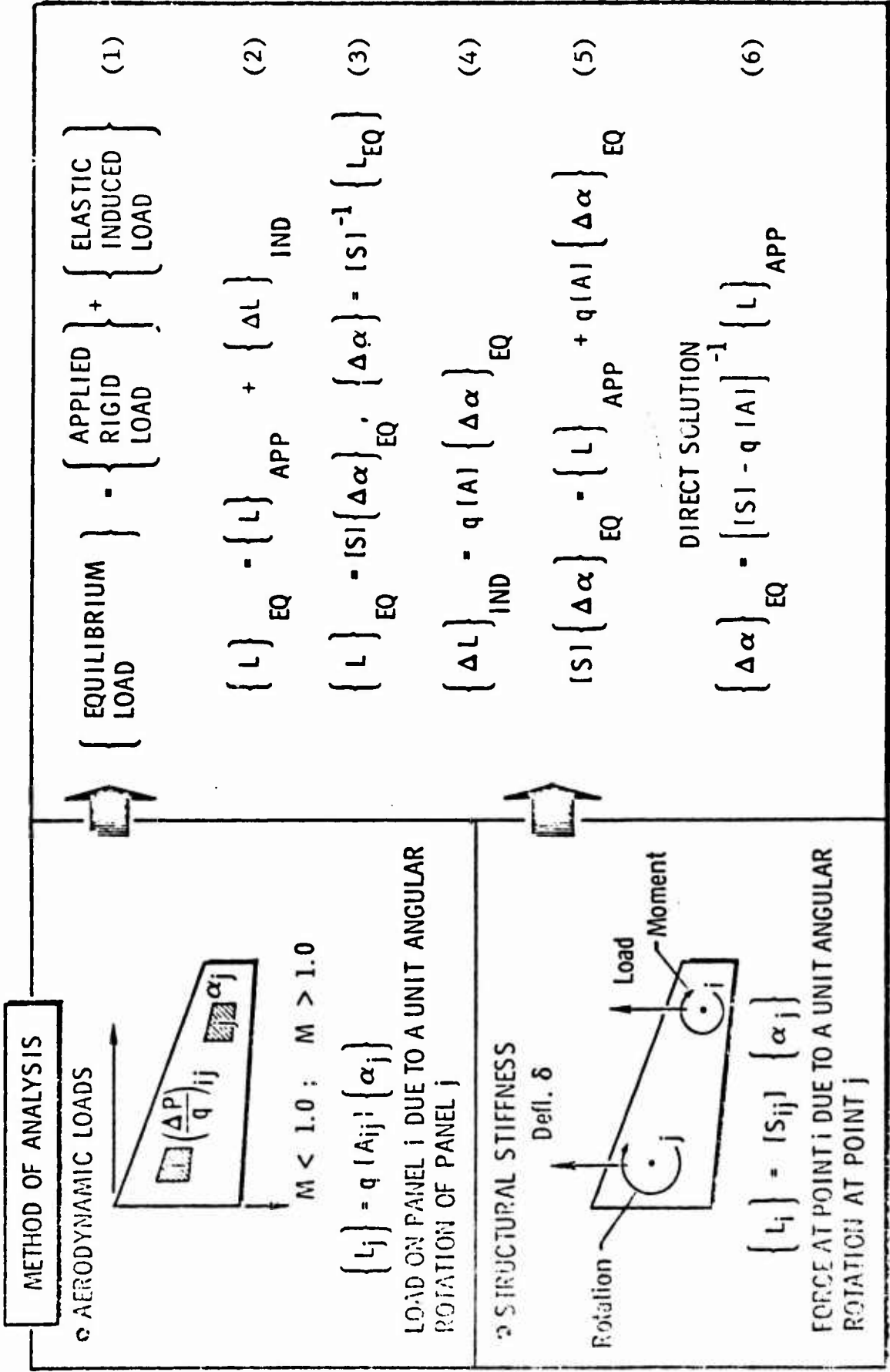


Figure 24 Method of Solution of Aeroelastic Problem

Figure 24 shows a schematic representation of the aeroelastic equations solved to obtain the divergence speeds. All details pertinent to the development of the aeroelastic theoretical and computer programs are given in Reference 10 and Reference 11.

Prior to combining the structural and aerodynamic matrices, the matrix of structural influence coefficients was inverted in order to yield a structural stiffness matrix, [S]. Also, the structural control points (i.e., the grid points where measurements were made in obtaining the structural influence coefficients) did not coincide with the aerodynamic control points. Thus, in order to properly combine the operations required by equation (6), Figure 24, the aerodynamic influence coefficients matrix was transformed to yield loads at the structural control points. The details of this transformation are presented in Reference 1. Finally, the final form of equation (6) for the calculation of the surface divergence speed is

$$[S] - q[A] = 0.$$

The above equation was then solved for the divergence speed by maintaining the structural restraint against plunging and pitching as was done during the measurement of the experimental structural influence coefficients matrices for the last two (TFW) configurations.

Since the torsion free wing is free to rotate about the pitch axis in normal operation, it might seem to be inconsistent to conduct divergence analyses based on structural influence coefficients that were measured with the model clamped at the pitch axis. However, similar apparent inconsistencies exist in the divergence analysis of fixed wing aircraft. That is, divergence analyses are often conducted for cantilever boundary conditions. The wing loads are reacted at the support. However,

¹⁰Hosek, J. J., Peloubet, R. P., Lyons, P. F.,
"Development of Airframe Structural Design Loads for Flexible Military Aircraft, Volume I: Theoretical Development," AFFDL-TR-75-79, July 1975.

¹¹Hosek, J. J., Peloubet, R. P., Lyons, P. F.,
"Development of Airframe Structural Design Loads for Flexible Military Aircraft, Volume II: Computer Program," AFFDL-TR-75-79, July 1975.

in flight, the summation of aerodynamic moments about the airplane c.g. must be zero for straight and level flight. Hence, as speed increases the airplane must be retrimmed to balance the loads.

Divergence speeds are seldom encountered in flight since the trim capabilities of the control surfaces prevent flight to the divergence speed. Similarly, as the speed of the torsion free wing is increased, aeroelastic effects cause a redistribution of loads which requires the wing to be retrimmed. The only difference in comparison with the fixed wing is that the torsion free wing must also be balanced in pitch about the wing pivot axis. Hence, the divergence speed computed with the pitch axis clamped represents only an upper limit of flight speeds at which it would be impossible to trim the airplane even with unlimited trim capabilities. Since the trim capabilities are finite the airplane is limited to some speed less than the divergence speed. The trend flutter models were even more limited in speed since they had no trim capabilities.

A comparison of calculated and measured divergence speeds for the four cases analyzed is shown in Table VIII.

Table VIII

COMPARISON OF MEASURED AND CALCULATED DIVERGENCE SPEEDS

<u>Model</u>	<u>Calc Divergence Speed</u>	<u>Meas Divergence Speed</u>
Cantilever	5670 fps	None*
P.R. Cant	3675 fps	None*
TFW(Fwd Trim Surf)	532 fps	250 fps
TFW(Aft Trim Surf)	520 fps	None*

* Did not get divergence in tunnel tests - experienced flutter instead.

The computer program (Reference 11) used to analyze the TFW for wing divergence speeds was developed under a AFFDL contract. The program has the capability for predicting both the structural design loads and aerodynamic characteristics for flexible military aircraft.

The major results in the development of the program has been the unification of the structural and aerodynamic technologies through the use of efficient interface matrices in the overall plan for computing the elastic airplane loads and aerodynamic characteristics utilizing a direct solution to the aeroelastic problem.

S E C T I O N V

DISCUSSION AND COMPARISON OF EXPERIMENTAL AND ANALYTICAL RESULTS

The wind tunnel test flutter speeds and frequencies were, in general, quite definite and accurately determined. This is particularly true of the cantilever, pitch restrained cantilever and the higher speed flutter case of the TFW model with trim surface aft. The lower speed mild case of flutter (flutter frequency around 10 cps) was not as clearly defined, however, and is subject to some interpretation. It appeared to be the type of flutter which may occur in a flutter analysis as a shallow "hump" type crossing or a V-g plot. With the trim surface forward no case of flutter occurred in the test but instead, divergence was encountered.

Actual determination of divergence speed for the tests conducted is perhaps not an accurate, well determined quantity. It might be argued that divergence testing should proceed with the model always trimmed out at zero lift. Then at some speed, a small increment of lift produces simultaneously a large change in angle of attack and large lift forces such that structural failure would occur. The divergence speeds reported herein were not determined in this manner and may therefore be too low.

During the wind tunnel tests it was not possible to trim the model to zero lift during testing. Instead, the model would assume whatever angle of attack it wanted to as speed was increased. This occurred primarily for the trim surface forward configuration since divergence was the only instability encountered for this configuration. The only kind of trimming tried was to bend (camber) the trim surface trailing edge before the start of a run in an attempt to reach higher speeds with the model at zero angle of attack. This was done on a succeeding trial-and-error run basis.

Other tasks undertaken in the experimental portion of the program proceeded in a straightforward manner with no particular problems appearing. The one area where some improvement might have been desired was in the vibration testing of the models. Only one acoustic type speaker was used to excite the modes. However, experience has shown that a better job of excitation can be realized if more than one exciter is used. This improvement usually manifests itself in the computed orthogonality of the modes. It is believed that perhaps some improvement in the vibration modes, particularly in the higher frequencies, might have been realized had additional shakers been used. This was

considered but not followed primarily because of the type exciters used and the possible phase shift between vibrators in the pulsating volume of air involved at the high frequencies under consideration. Also, with multiple shakers proper "mode tuning" must be followed which involves measurement of the excitation force. This was impossible for the type shakers used.

Most of the vibration modes as measured were very close to being orthogonal. However, for a few isolated cases a higher frequency mode was eliminated from the analysis because of poor orthogonality with the other modes. This was done only a very few times thus indicating that the modes as measured were excited and measured properly.

The comparison between calculated and measured flutter speeds for the cantilever configuration is not as good as was hoped for. The calculated flutter speed is 31 percent higher than the measured speed and the frequency difference is 22 cps out of 87. There is no known reason why this case should not compare better. One possible, although doubtful, reason may be that if higher frequency modes had been measured and included in the analysis better agreement might have been realized.

There is essentially perfect agreement between calculated and measured flutter speeds and frequencies for the pitch restrained cantilever. Little else need be said about this case.

For the TFW model with trim surface forward (no root stiffener) the analysis shows a definite and quite likely rapidly divergent flutter instability at 228 fps and 31 cps (Figure 20). Of course, the wind tunnel tests did not indicate any kind of flutter condition at this speed but the model did diverge statically at 250 fps (Table VI, Run 3d). Whether impending divergence with its probable accompanying large angle of attack at 228 fps could mask or eliminate a flutter condition is not known.

For the TFW trim surface forward model and stiffened wing root, several instabilities are shown in the analysis. Again, no flutter condition was encountered in the wind tunnel. The analysis shows a very low speed instability (Figure 21) involving rigid body translation (a pendulum mode the way the model was mounted in the wind tunnel). This was not encountered during the wind tunnel tests nor was the instability which is shown analytically at 208 fps and 17 cps. Here again, the model

experienced static divergence at 325 fps (Table VI, Run 3e) which may or may not have affected an impending flutter condition at some lower speed.

Based on the results of a TFW trim surface aft case, discussed later, wherein doublet-lattice aerodynamics were used, it would be interesting to see if a similar analysis of the trim surface forward cases might yield results which are in better agreement with test data. Use of this method, which accounts for mutual aerodynamic interference effects, resulted in better agreement for the trim surface aft case and may show similar improvement in the trim surface forward configuration. There is little doubt that a strong aerodynamic interference field exists for the trim surface forward case.

For the TFW trim surface aft model, the analysis utilized separately both kernel function and doublet-lattice aerodynamics. The lowest speed instability (Figure 22) shown for the kernel function analysis was 305 fps at a frequency of 35 cps. The doublet-lattice analysis (Figure 23) shows both a very low speed, low frequency instability and the higher speed instability at 229 fps and 42 cps. This latter case compares reasonably well with the measured flutter speed of 260 fps at a frequency of 43.8 cps (Table VI, Run 7a). It is interesting to note that neither type analysis shows the instability measured at 210 fps and 9.2 cps. This was a very mild case of flutter whose speed was sometimes difficult to determine very accurately in the wind tunnel. However, this particular case of flutter occurred at about the same speed and frequency for several different trim surface aft configurations.

The calculated divergence speeds for the TFW configurations are considerably higher than that which was measured. For the two different types of cantilever models, the analytical divergence speeds are very high and of course no indication of divergence occurred during the wind tunnel tests. For the TFW cases, the measured divergence speed may be too low due to the inability to trim the models as discussed earlier. However, it seems unlikely that a speed as high as the calculated value could have been realized during the tests even with the ability to trim the model.

Perhaps one of the key elements missing from this investigation is the comparison between computed and measured vibration modes for the configurations which were flutter analyzed in this program. From inception it was not planned to calculate any vibration modes for comparison with measured modes. However, it may be in this area that a major reason for the large change in calculated flutter speeds for the airplane studies of 1972 and 1974 exist.

S E C T I O N V I

CONCLUSIONS AND RECOMMENDATIONS

One of the significant conclusions of this program is that the flutter speed of these particular torsion free wing models, with trim surface either forward of the wing at the root or aft of the wing at the tip, is higher than that of the cantilever model. This was shown to be true in the wind tunnel tests and is presented in Table VI runs 1, 3c, 7 and 8. A similar conclusion cannot be substantiated by the analysis, however.

It can also be concluded from the test results of these models that the flutter speed of the TFW models with the trim surface forward is higher than that for the TFW models with trim surface aft. This can be seen by a comparison of runs 3c and 8, 3d and 8b in Table VI. In these runs, speeds as high or higher were reached with the trim surface forward with no flutter occurring (divergence occurred at a higher speed) than were reached with the trim surface aft when flutter occurred. The analysis did not verify this conclusion, however.

The generally high test flutter speeds for the TFW models relative to the cantilever model may be an indication that excessively low flutter speeds do not necessarily accompany a torsion free wing design. This may lead to questioning the results of the flutter analysis results performed in 1974 on the TFW configuration with the trim surface at the wing tip and aft wherein a very low flutter speed was calculated.

It is recommended that further work be done to pinpoint the reasons for some of the larger disparities between calculated and measured flutter and divergence speeds. This may take the form of different analytical procedures or of more sophisticated test procedures used in measuring vibration mode shapes and deflection influence coefficients.

It is also recommended that an effort be made to calculate the mode shapes and frequencies and influence coefficients. Gaining confidence in the analytical procedures to do this for the types of configurations tested in this program would be very valuable.

APPENDIX

The mode shape reading point locations for the configurations which were vibration tested and flutter analyzed are shown in Figures 25 through 28. Mode shape data including frequency surveys, plotted modes and tabulated amplitude data are included in the figures and tables of this appendix.

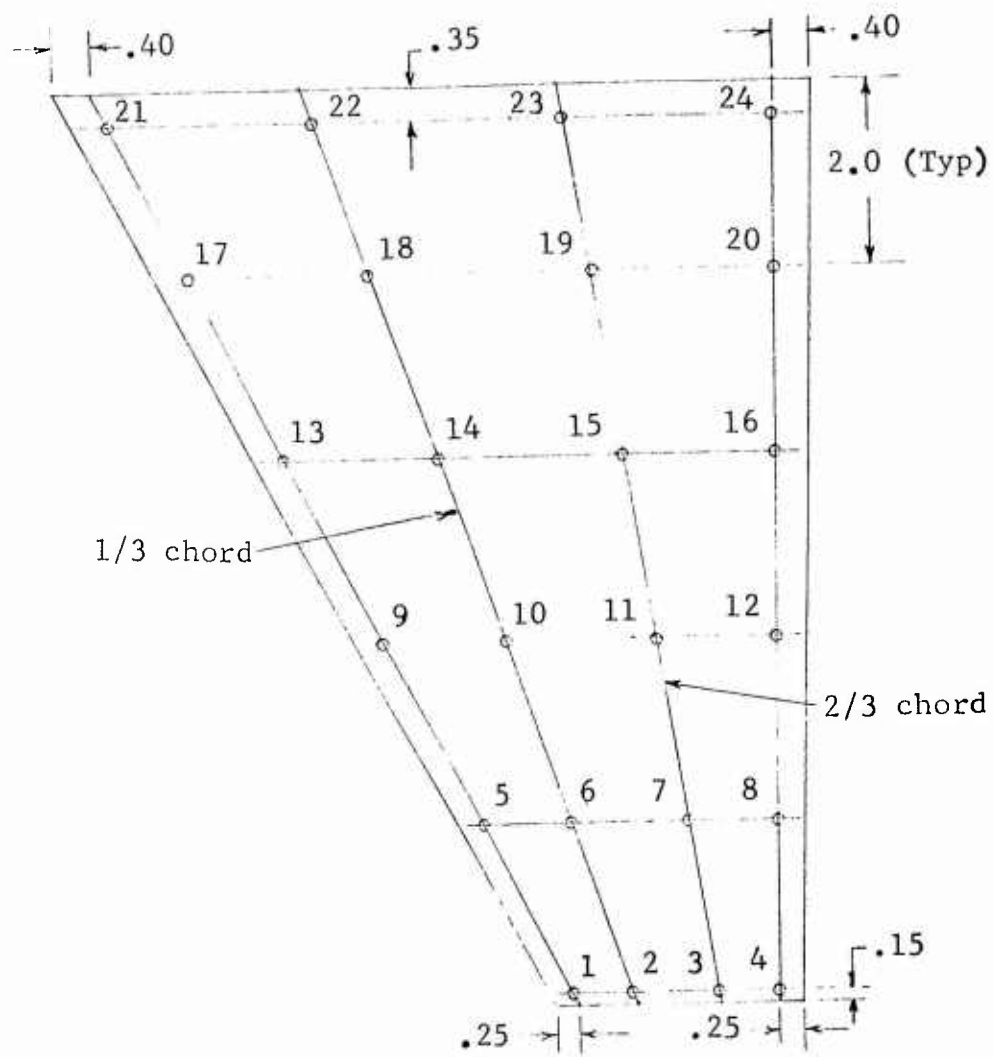


Figure 25 Mode Shape Reading Points for Cantilever
And Pitch Restrained Cantilever Models

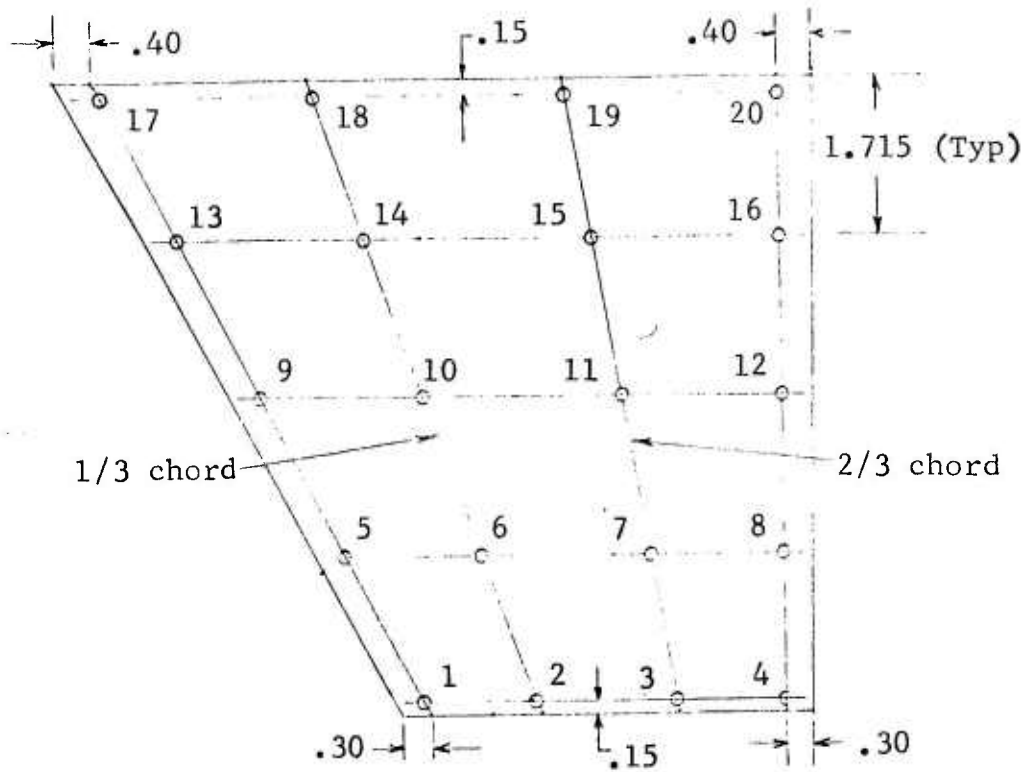


Figure 26 Mode Shape Reading Points for Wing of TFW Models

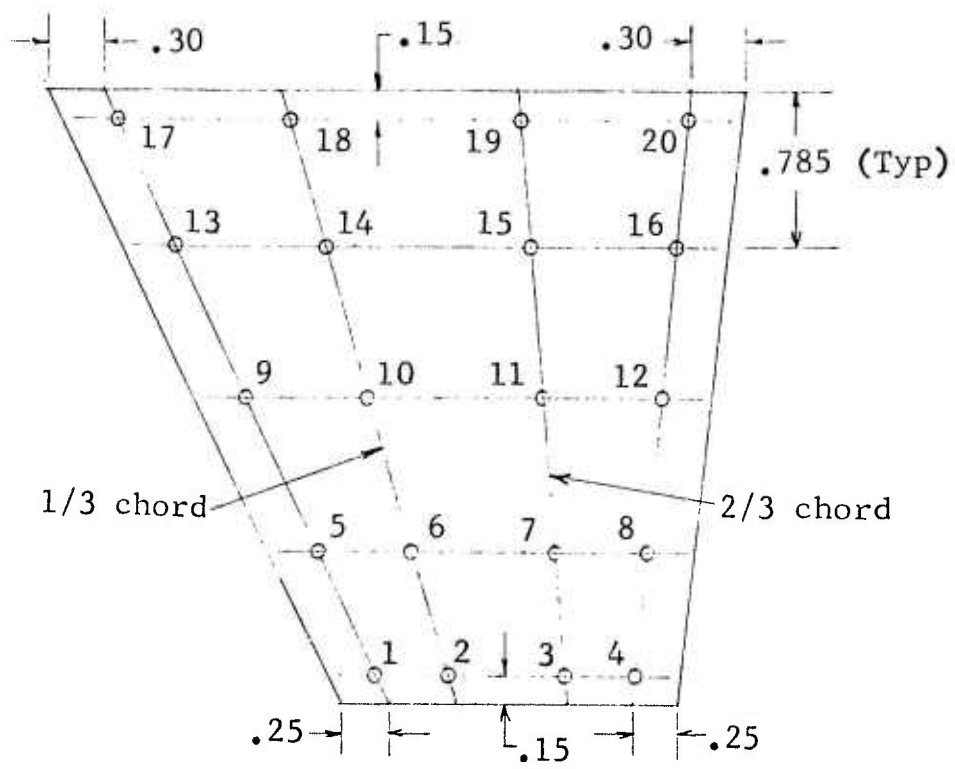


Figure 27 Mode Shape Reading Points for B Trim Surface (Aft Trim Surface TFW Config.)

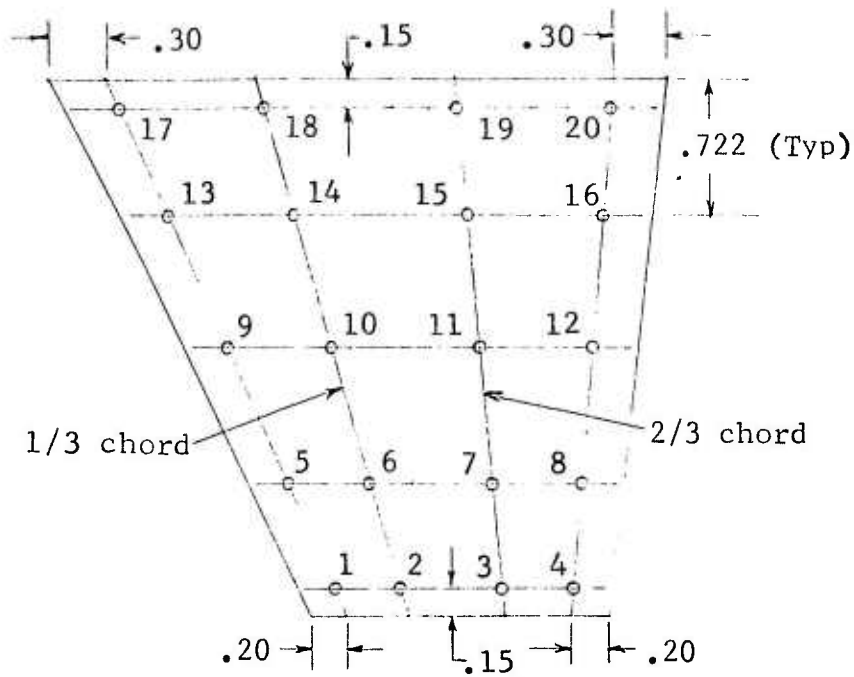
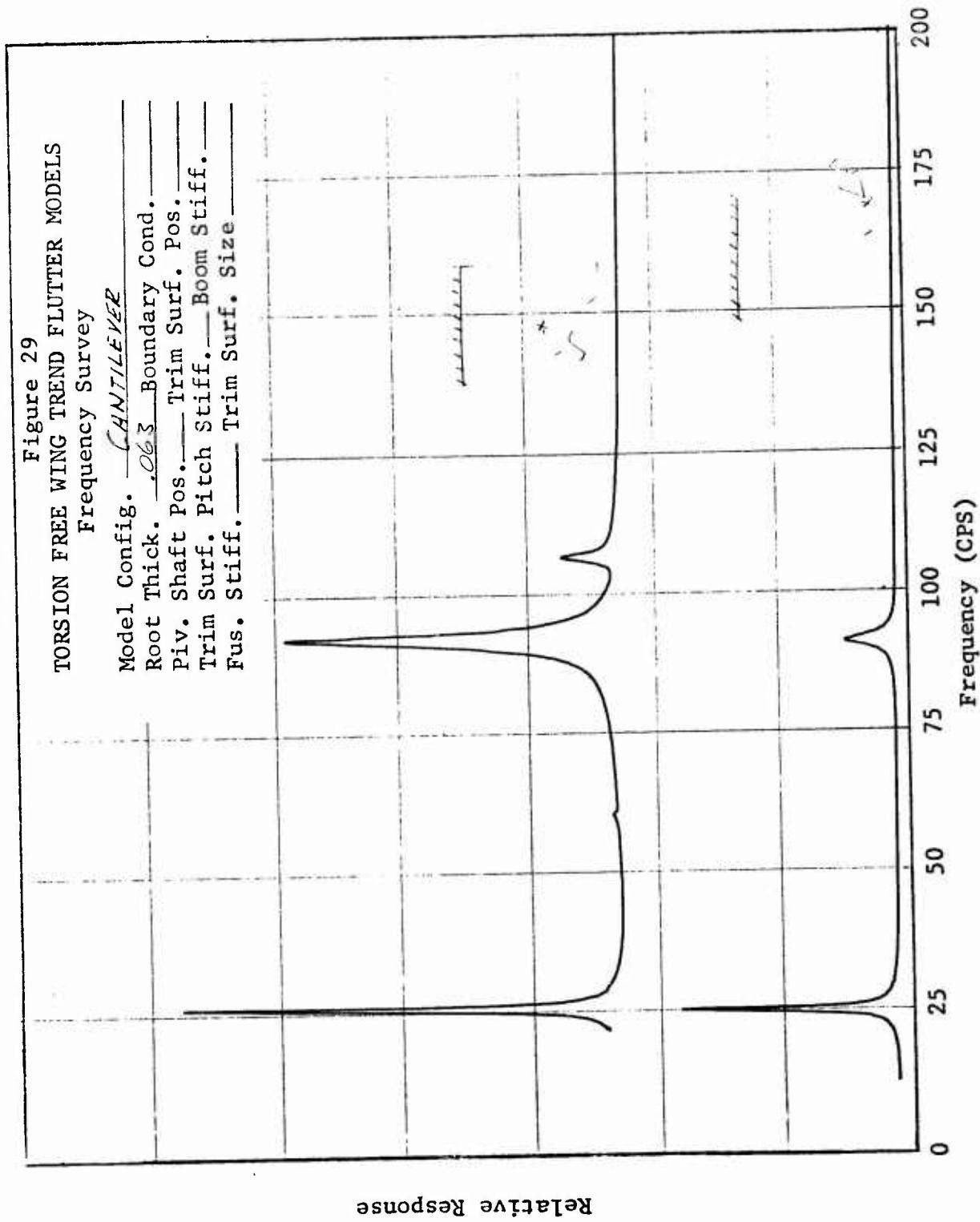


Figure 28 Mode Shape Reading Points for S Trim Surface (Forward Trim Surface TFW Config.)

Figure 29
 TORSION FREE WING TREND FLUTTER MODELS
 Frequency Survey

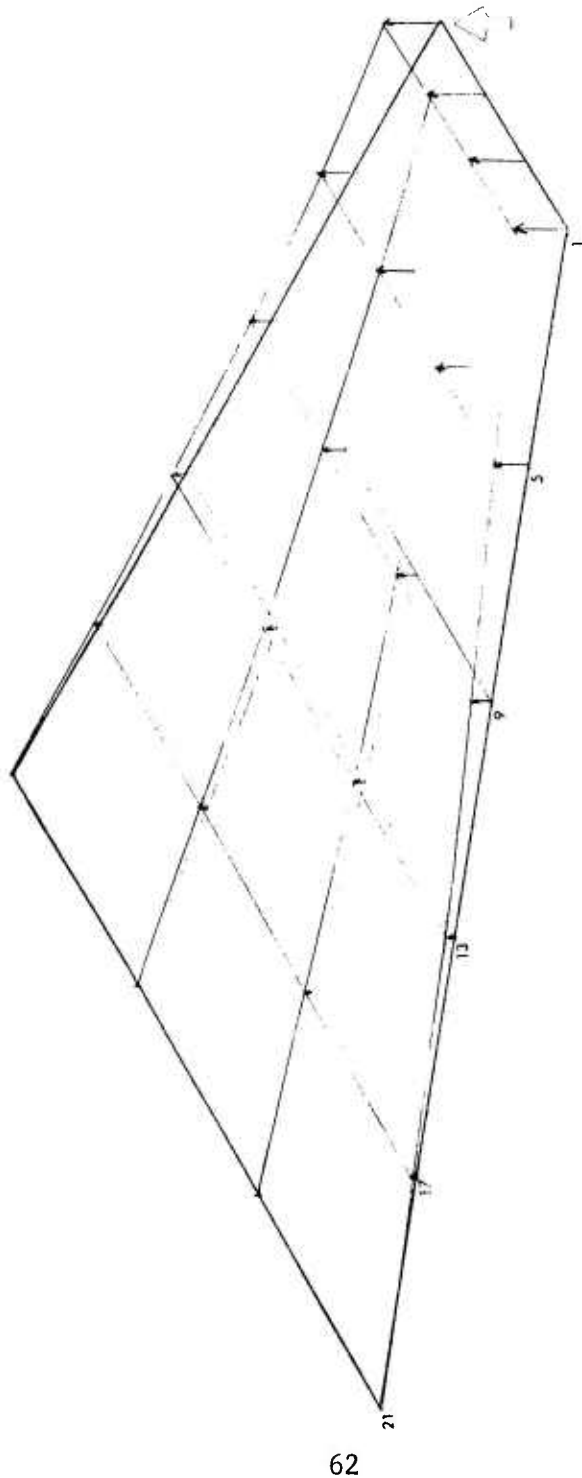
Model Config. CHANTELIER
 Root Thick. .063 Boundary Cond. _____
 Piv. Shaft Pos. _____ Trim Surf. Pos. _____
 Trim Surf. Pitch Stiff. _____ Boom Stiff. _____
 Fus. Stiff. _____ Trim Surf. Size _____



Relative Response

Figure 30
 TORSION FREE WING TREND FLUTTER MODELS
 MODE SHAPE PLOT
 CANTILEVER MODEL

Root Thick. .063



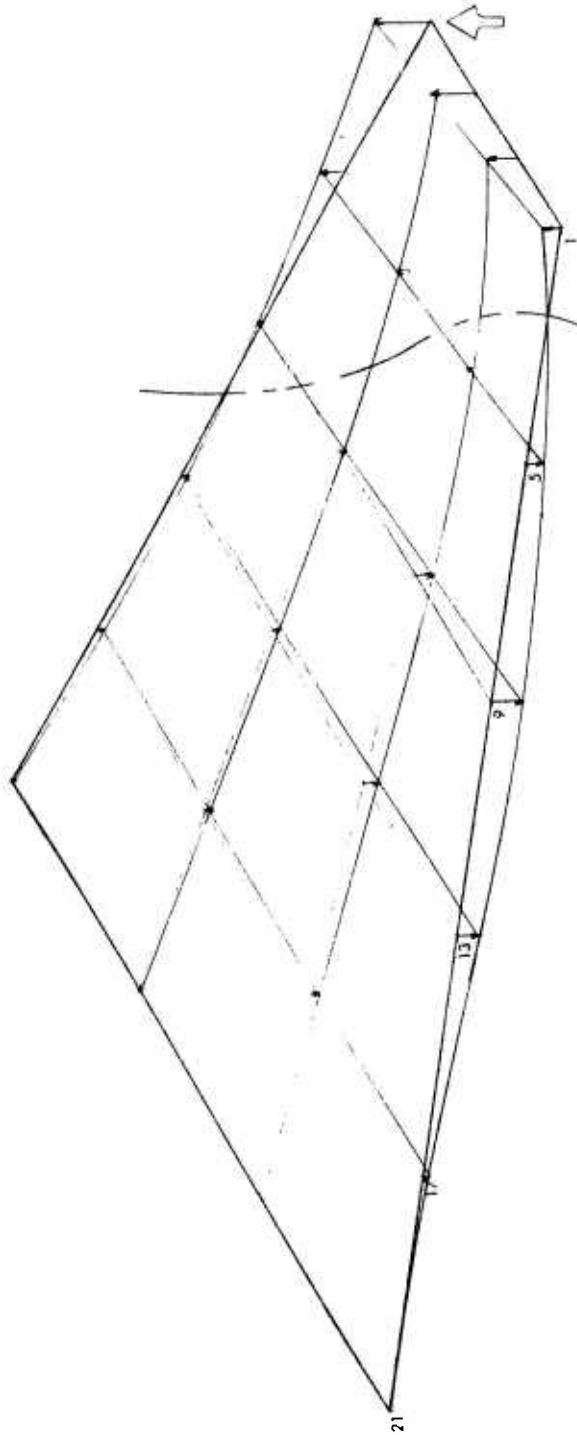
Frequency 25.2 cps
 Damping Coeff .0081 (g)

↑
 In Phase

↑
 Shaker Location

Figure 31
 TORSION FREE WING TREND FLUTTER MODELS
 MODE SHAPE PLOT
 CANTILEVER MODEL

Root Thick. .063



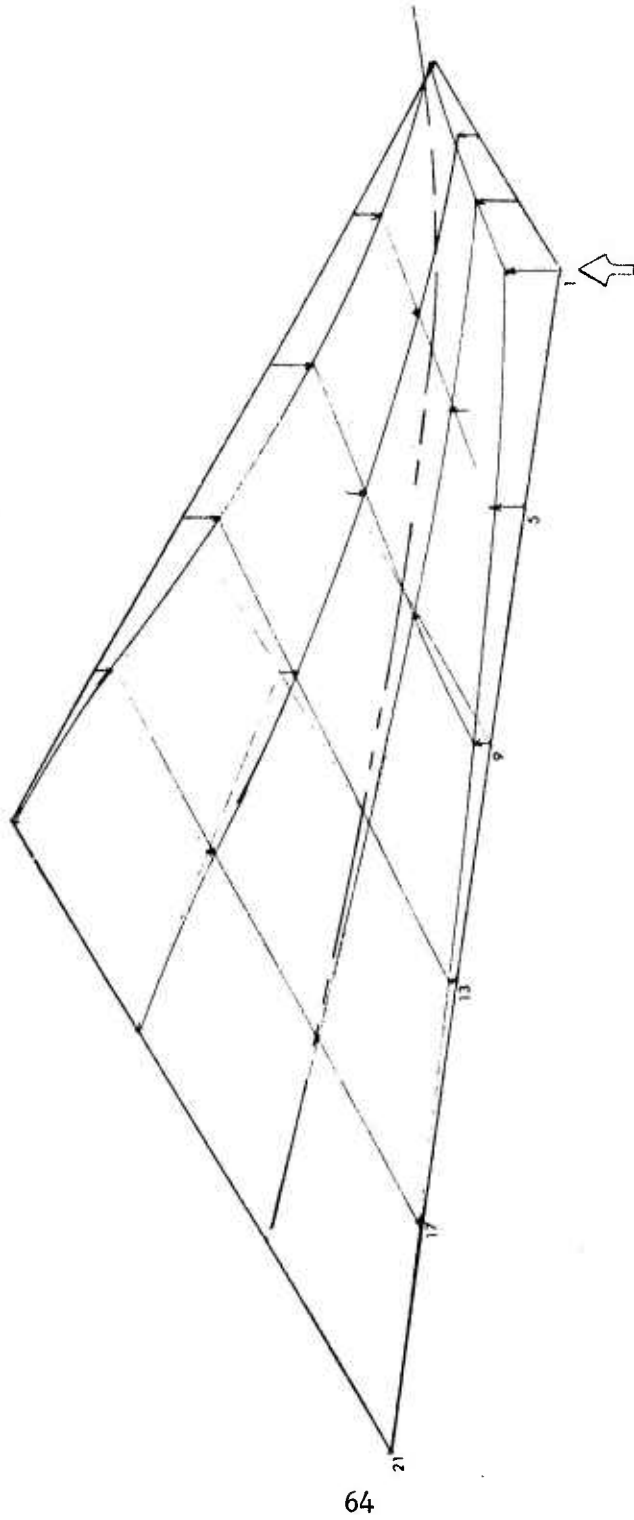
Frequency 91.2 cps
 Damping Coeff. .0018 (g)

↑ Shaker Location

↑ In Phase

Figure 32
 TORSION FREE WING TREND FLUTTER MODELS
 MODE SHAPE PLOT
 CANTILEVER MODEL

Root Thick. .063



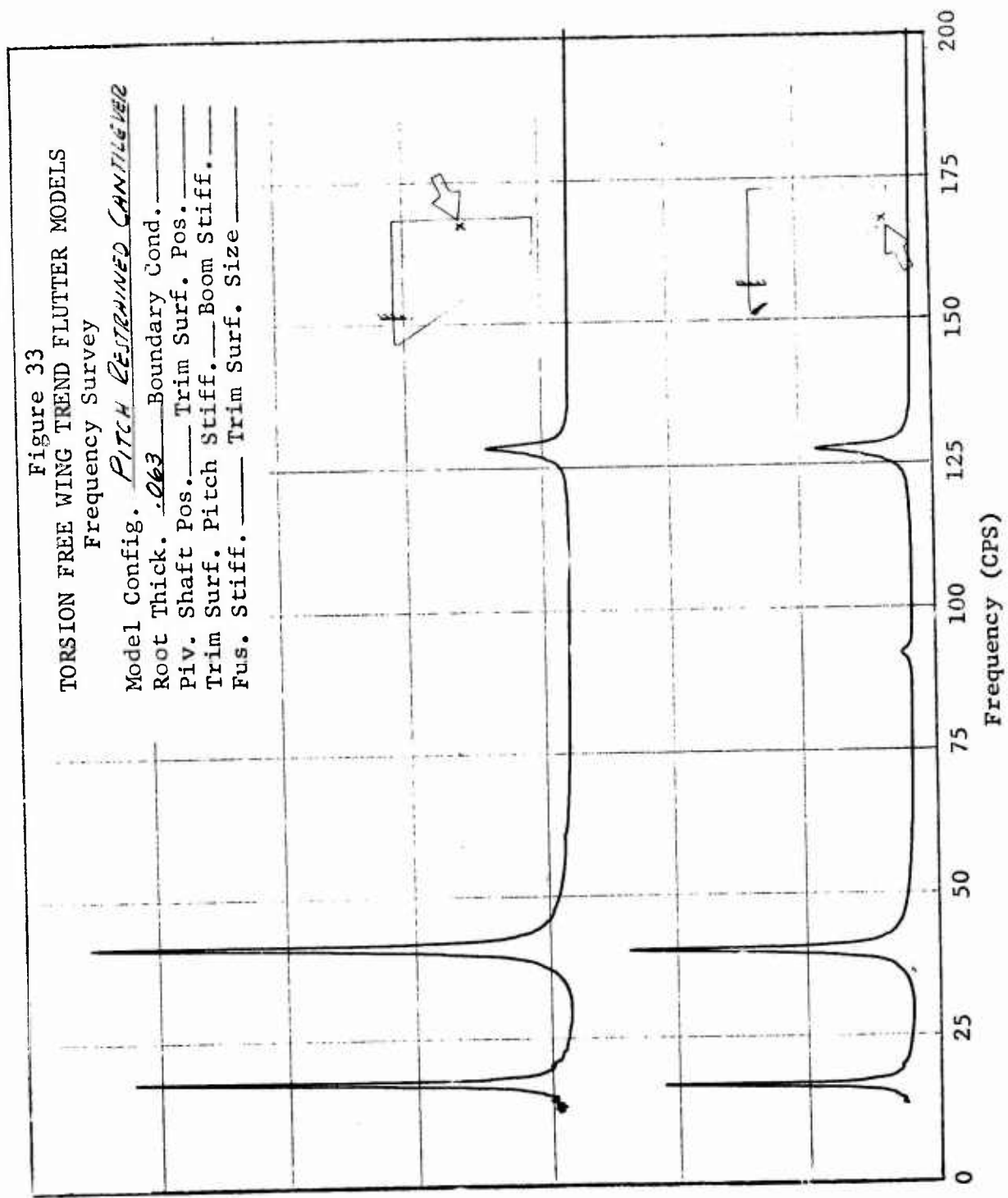
Frequency 106.2 cps
 Damping Coeff .0026 (g)

↑ Shaker Location

↑ In Phase

Figure 33
 TORSION FREE WING TREND FLUTTER MODELS
 Frequency Survey

Model Config. *PITCH RESTRAINED CANTILEVER*
 Root Thick. *.063* Boundary Cond. _____
 Piv. Shaft Pos. _____ Trim Surf. Pos. _____
 Trim Surf. Pitch Stiff. _____ Boom Stiff. _____
 Fus. Stiff. _____ Trim Surf. Size _____

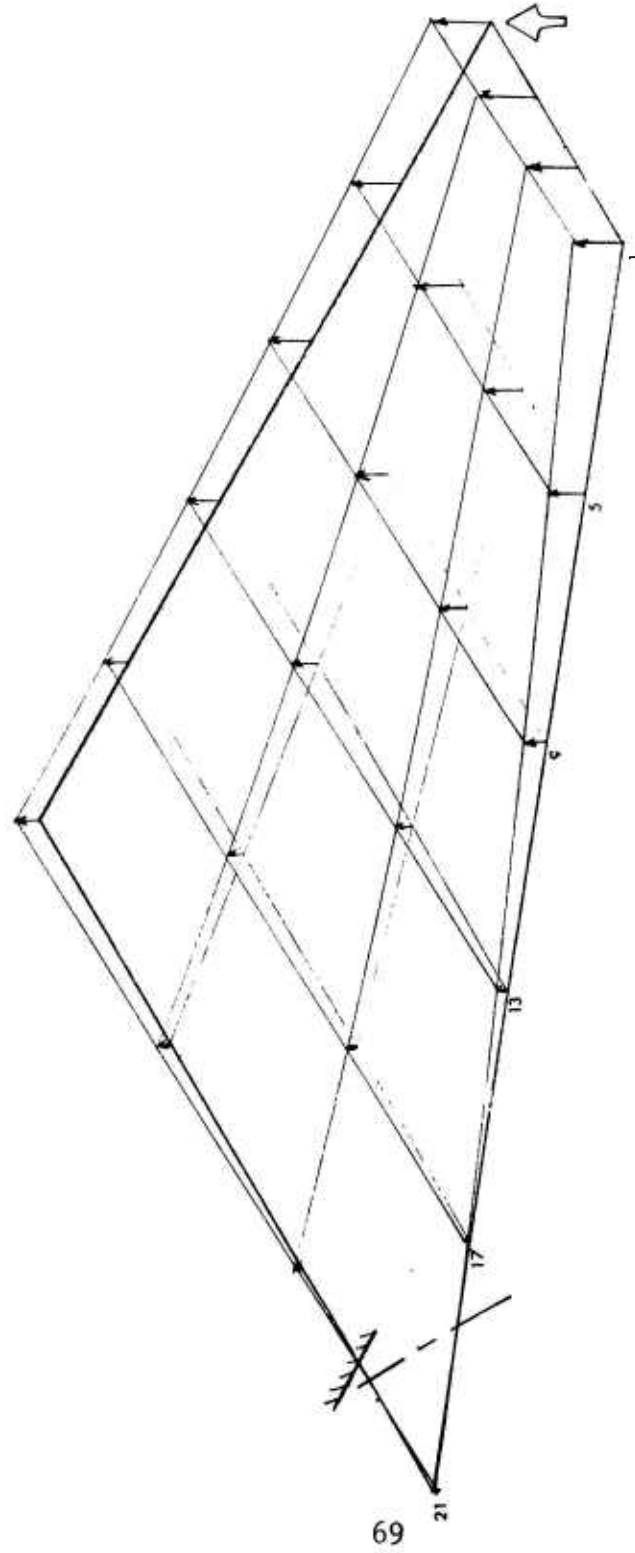


Relative Response

Frequency (CPS)

Figure 34
 TORSION FREE WING TREND FLUTTER MODEL
 MODE SHAPE PLOT
 PITCH RESTRAINED CANTILEVER MODEL

Root Thick. .063



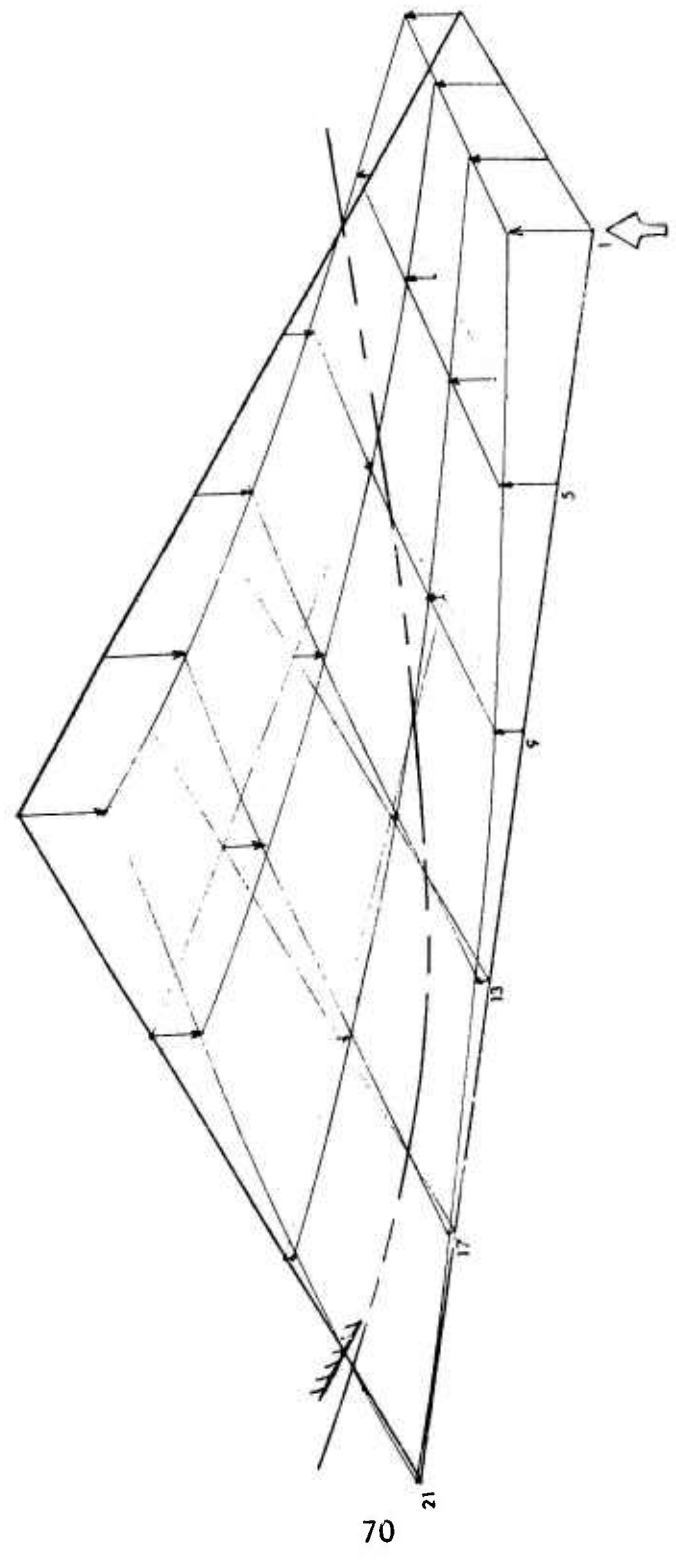
Frequency 16.5 cps
 Damping Coeff .0096 (g)

↑
 In Phase

↑
 Shaker Location

Figure 35
 TORSION FREE WING TREND FLUTTER MODEL
 MODE SHAPE PLOT
 PITCH RESTRAINED CANTILEVER MODEL

Root Thick. .063



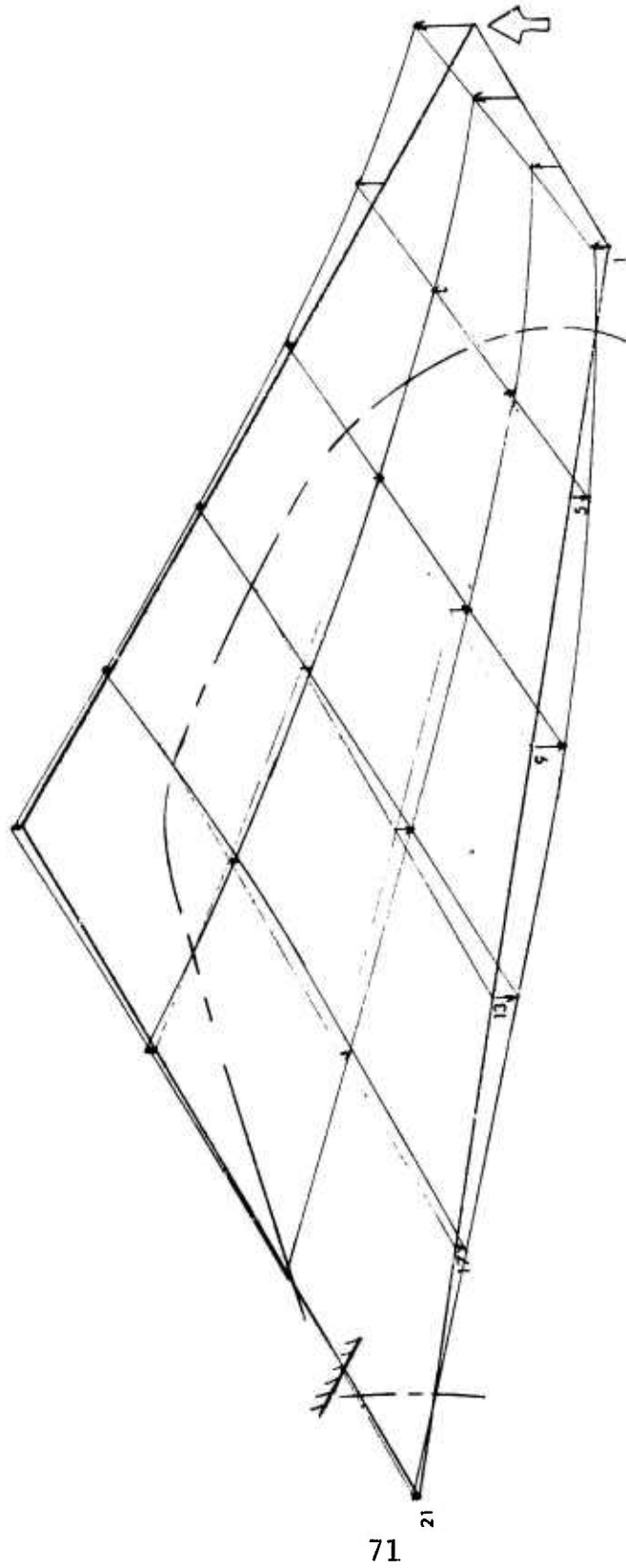
Frequency 40.1 cps
 Damping Coeff .0065 (g)

↑ In Phase

↑ Shaker Location

Figure 36
 TORSION FREE WING TREND FLUTTER MODEL
 MODE SHAPE PLOT
 PITCH RESTRAINED CANTILEVER MODEL

Root Thick. .063



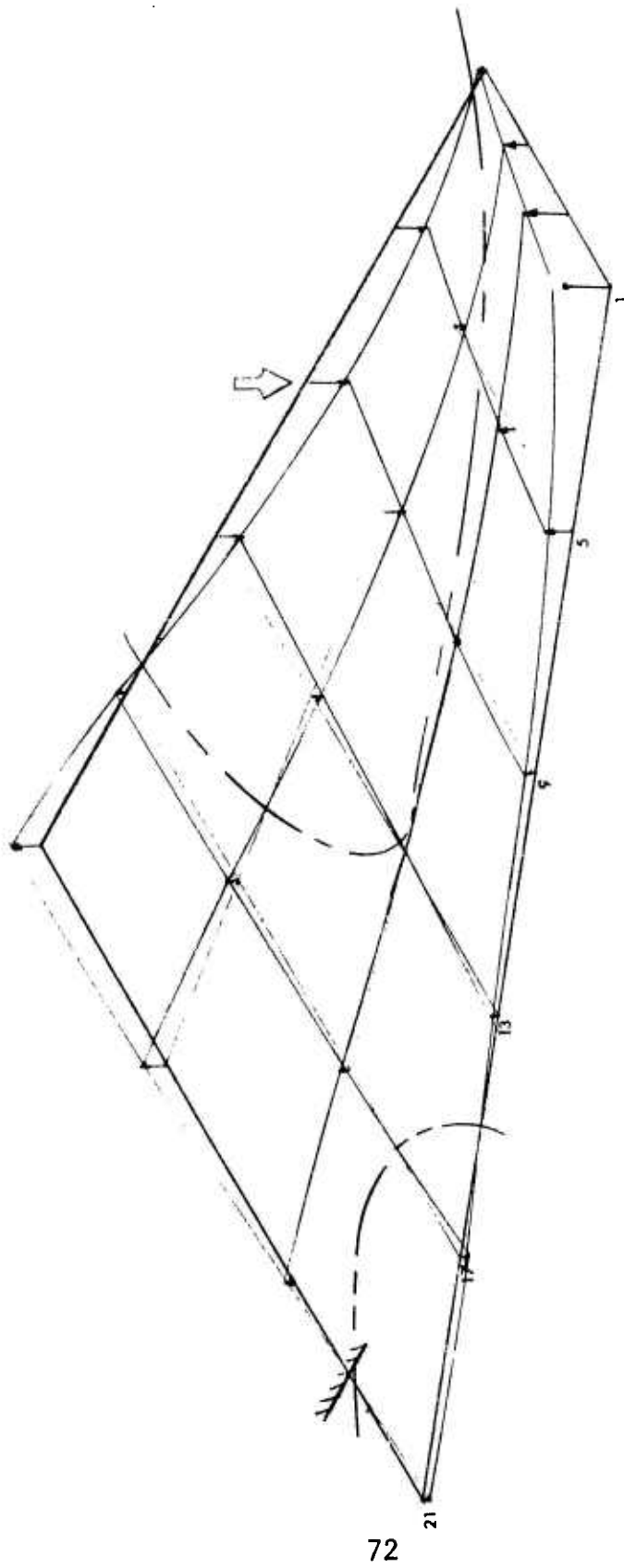
Frequency 92.1 cps
 Damping Coeff 0.0065 (g)

↑ Shaker Location

↑ In Phase

Figure 37
 TORSION FREE WING TREND FLUTTER MODEL
 MODE SHAPE PLOT
 PITCH RESTRAINED CANTILEVER MODEL

Root Thick. .063



72

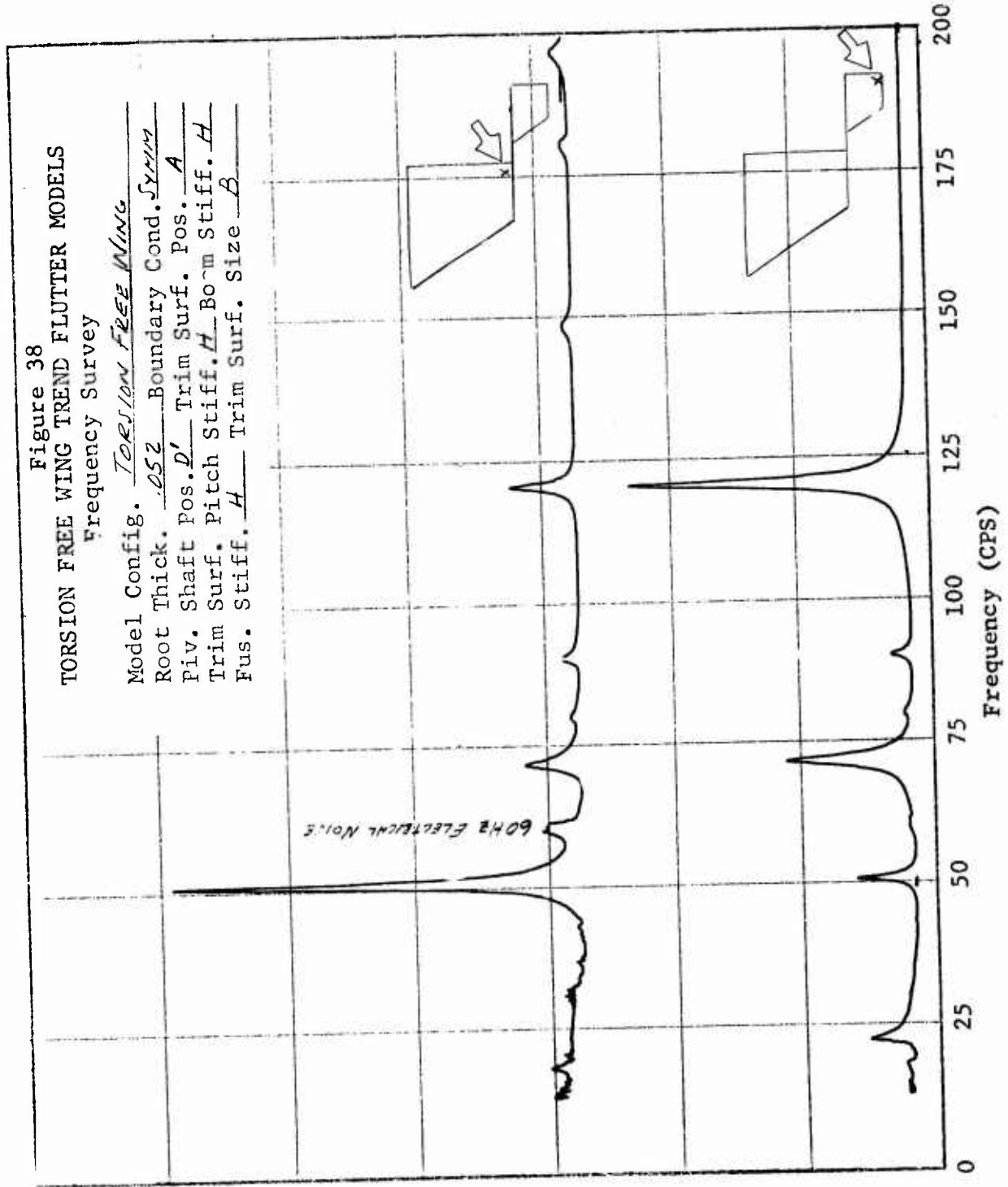
Frequency 127.5 cps
 Damping Coeff .0020 (g)

↑ In Phase

↑ Shaker Location

Figure 38
 TORSION FREE WING TREND FLUTTER MODELS
 Frequency Survey

Model Config. TORSION FREE WING
 Root Thick. .052 Boundary Cond. SYMM
 Piv. Shaft Pos. D' Trim Surf. Pos. A
 Trim Surf. Pitch Stiff. H Born Stiff. H
 Fus. Stiff. H Trim Surf. Size B



Relative Response

Figure 39
 TORSION FREE WING TREND FLUTTER MODEL
 MODE SHAPE PLOT
 SYMMETRIC BOUNDARY CONDITION

Root Thick
 Trim Surf. Pos.
 Trim Surf. Pitch Stiff.
 Boom Stiff.
 Fus. Stiff.
 Trim Surf. Size

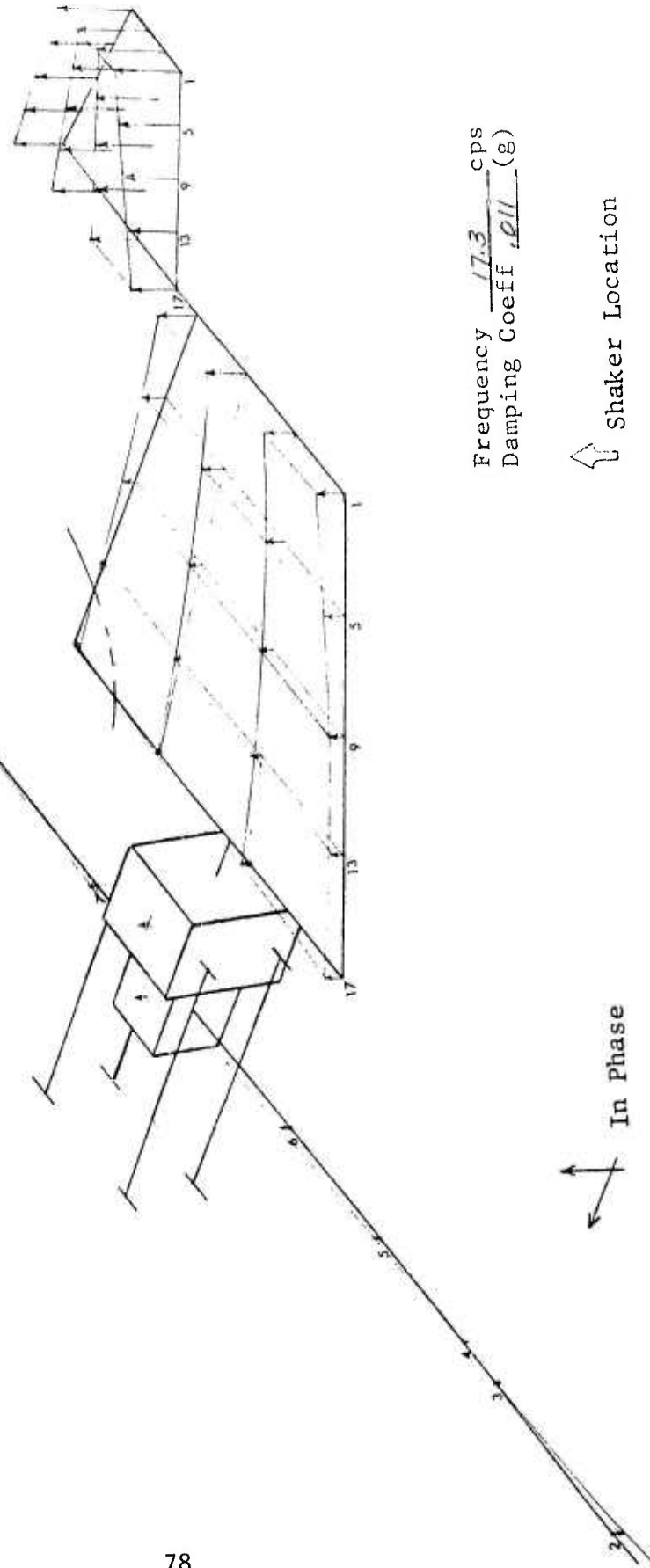
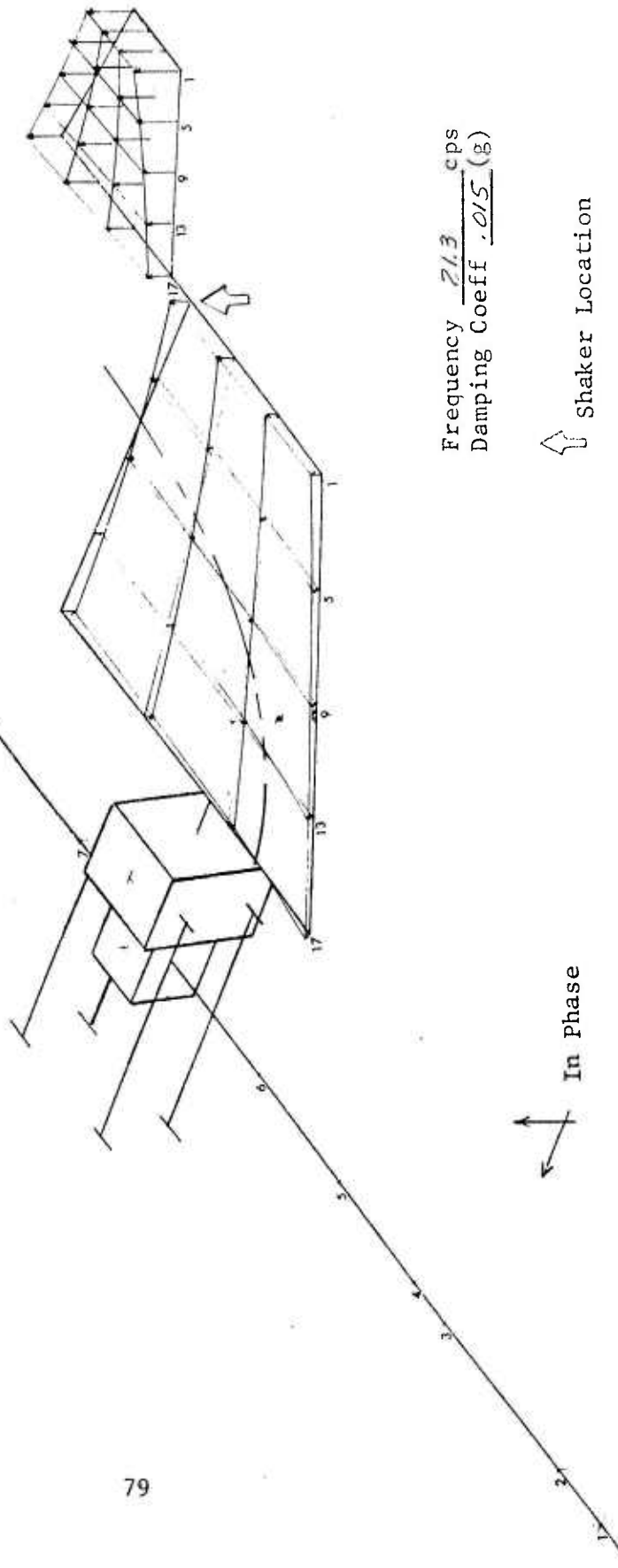


Figure 40
 TORSION FREE WING TREND FLUTTER MODEL
 MODE SHAPE PLOT
 SYMMETRIC BOUNDARY CONDITION

Root Thick	.052
Trim Surf. Pos.	A
Trim Surf. Pitch Stiff.	H
Boom Stiff.	H
Fus. Stiff.	H
Trim Surf. Size	B

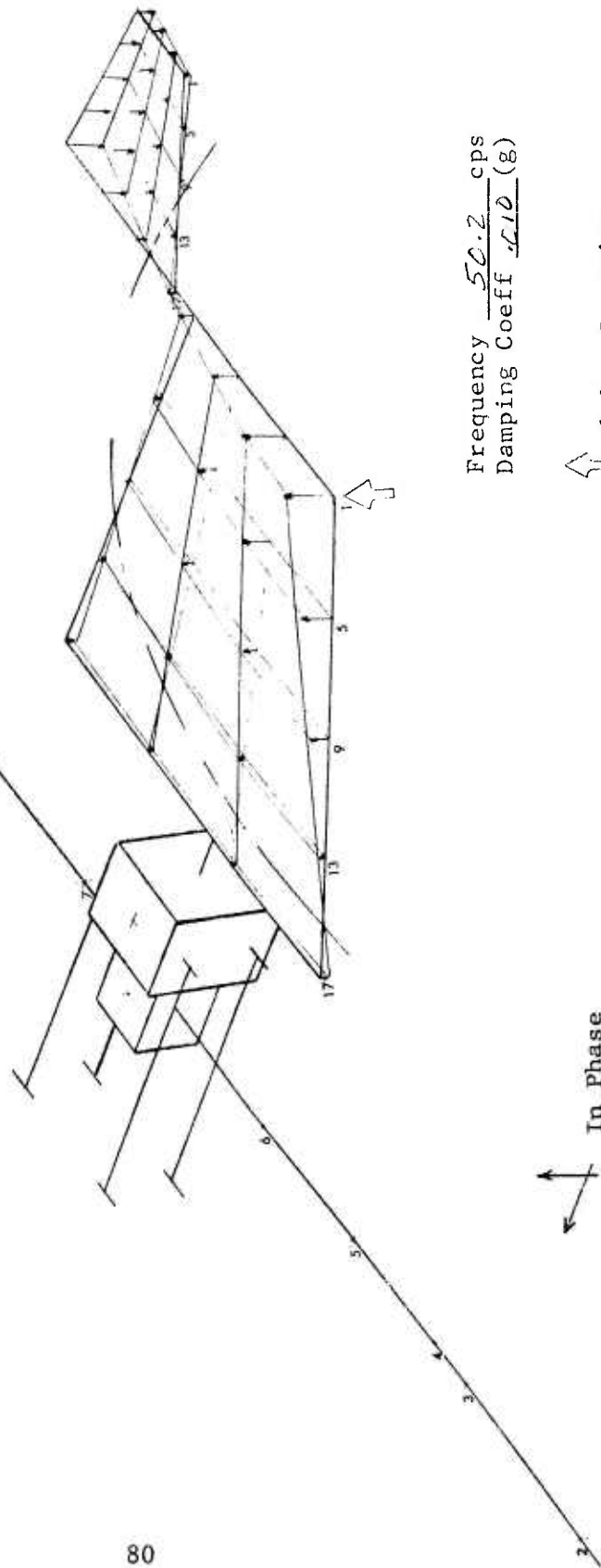


Frequency 213 cps
 Damping Coeff .015 (g)

↑ Shaker Location

Figure 41
 TORSION FREE WING TREND FLUTTER MODEL
 MODE SHAPE PLOT
 SYMMETRIC BOUNDARY CONDITION

Root Thick	.252
Trim Surf. Pos.	A
Trim Surf. Pitch Stiff.	H
Boom Stiff.	H
Fus. Stiff.	F
Trim Surf. Size	t



Frequency $\frac{50.2}{\text{cps}}$
 Damping Coeff $\frac{.170}{(g)}$

↑ Shaker Location

Figure 42
 TORSION FREE WING TREND FLUTTER MODEL
 MODE SHAPE PLOT
 SYMMETRIC BOUNDARY CONDITION

Root Thick .052
 Trim Surf. Pos. A
 Trim Surf. Pitch Stiff. H
 Boom Stiff. H
 Fus. Stiff. H
 Trim Surf. Size B

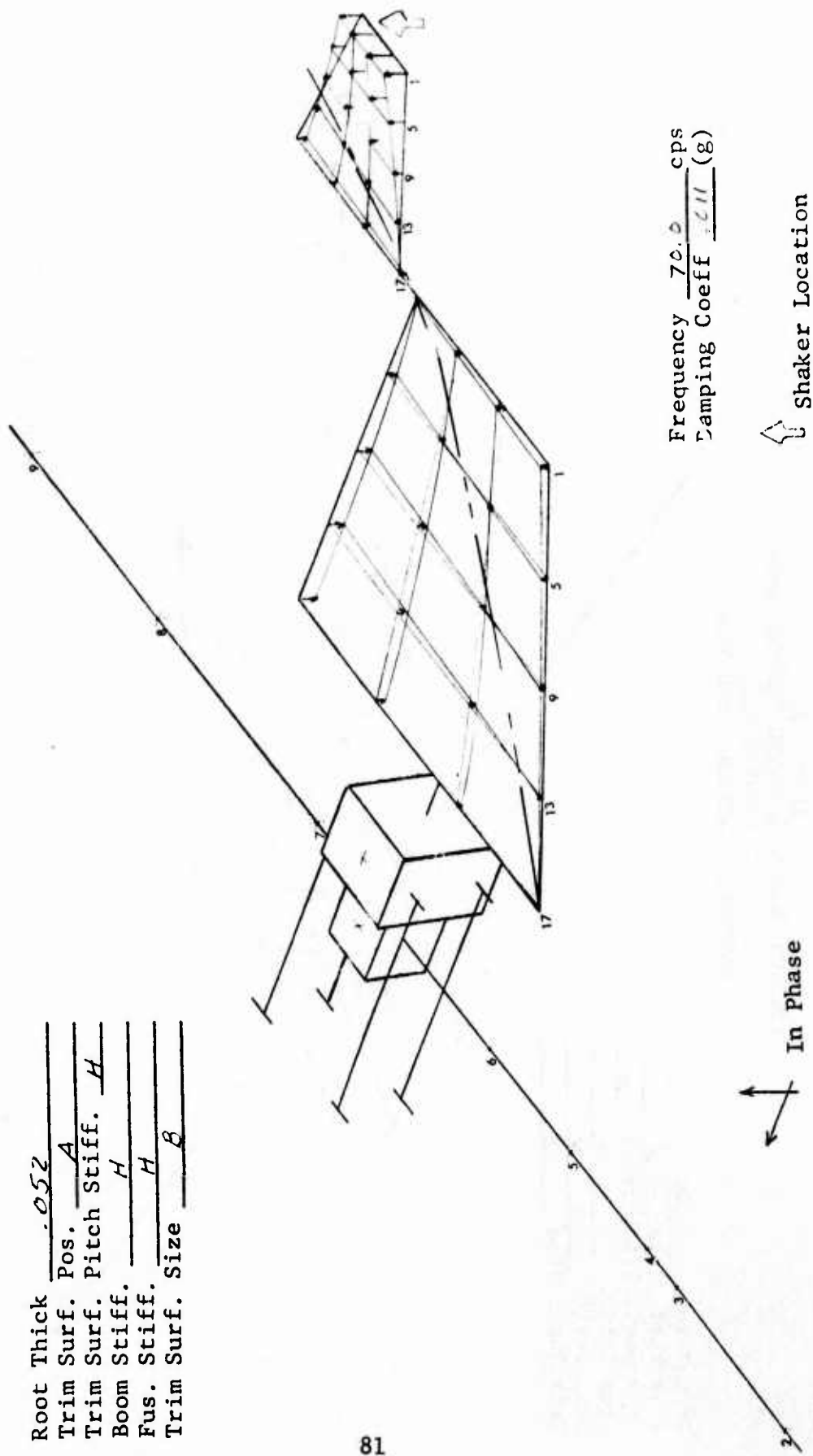


Figure 43
 TORSION FREE WING TREND FLUTTER MODEL
 MODE SHAPE PLOT
 SYMMETRIC BOUNDARY CONDITION

Root Thick .052
 Trim Surf. Pos. A
 Trim Surf. Pitch Stiff. H
 Boom Stiff. H
 Fus. Stiff. H
 Trim Surf. Size B

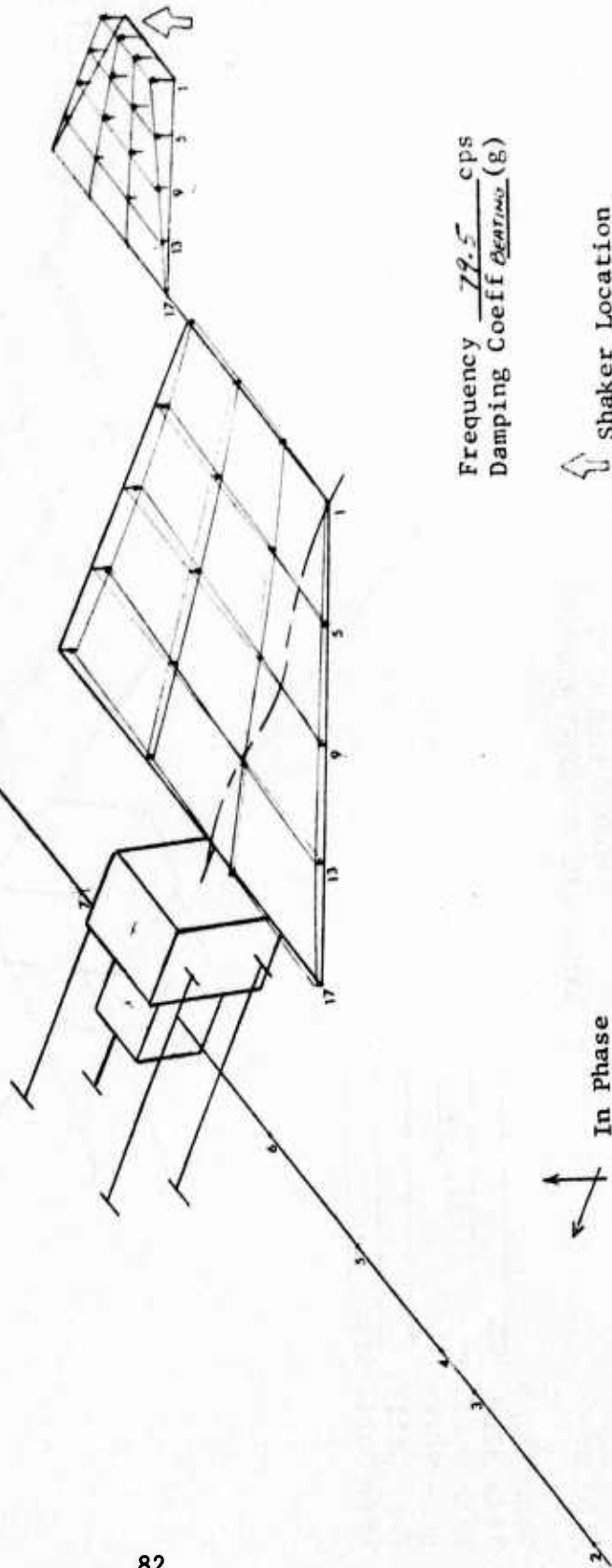


Figure 44
 TORSION FREE WING TREND FLUTTER MODEL
 MODE SHAPE PLOT
 SYMMETRIC BOUNDARY CONDITION

Root Thick 0.52
 Trim Surf. Pos. A
 Trim Surf. Pitch Stiff. H
 Boom Stiff. H
 Fus. Stiff. H
 Trim Surf. Size F

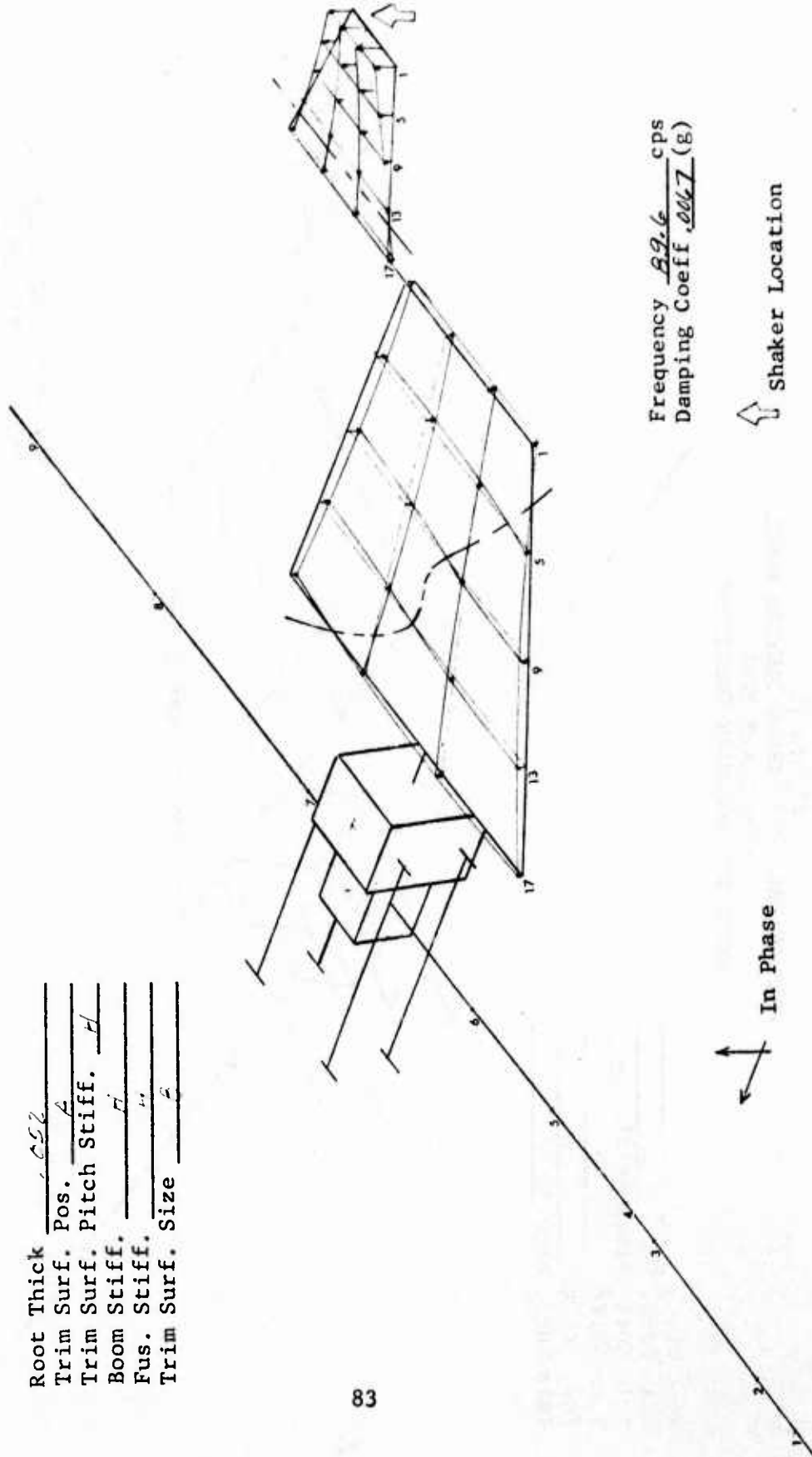


Figure 45
 TORSION FREE WING TREND FLUTTER MODEL
 MODE SHAPE PLOT
 SYMMETRIC BOUNDARY CONDITION

Root Thick .052
 Trim Surf. Pos. A
 Trim Surf. Pitch Stiff. H
 Boom Stiff. H
 Fus. Stiff. H
 Trim Surf. Size B

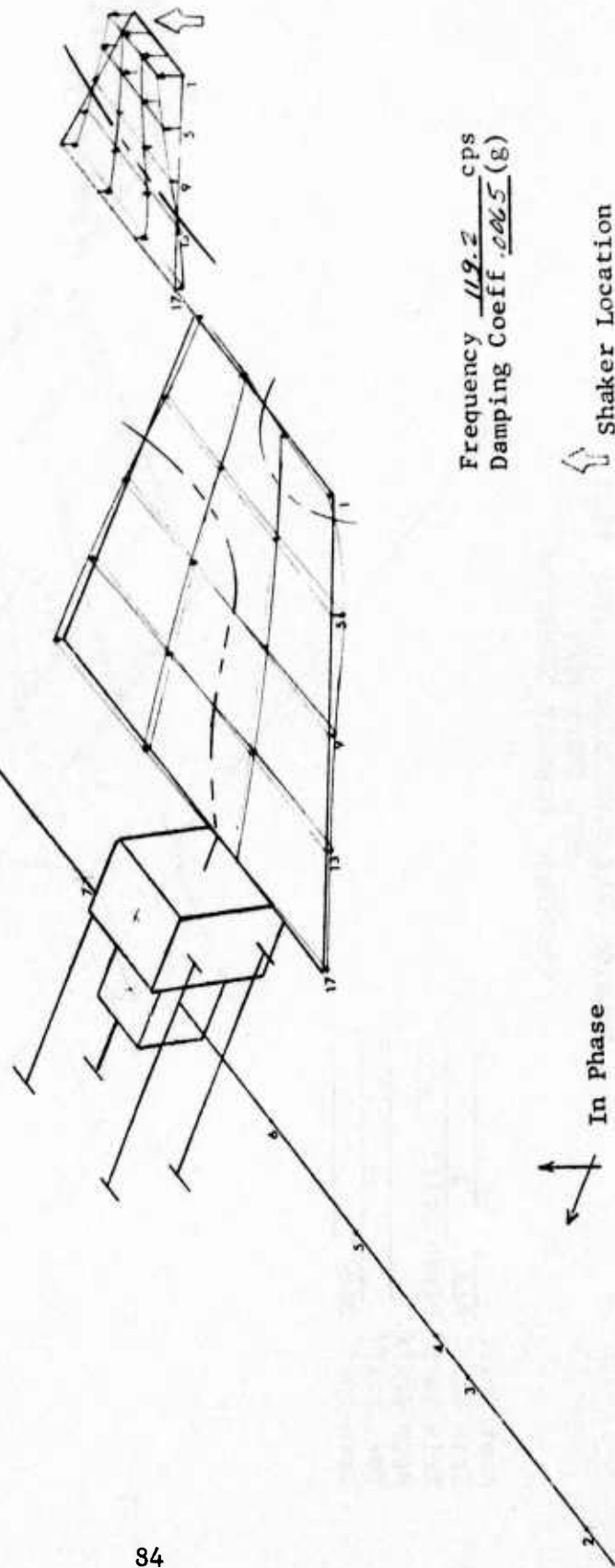
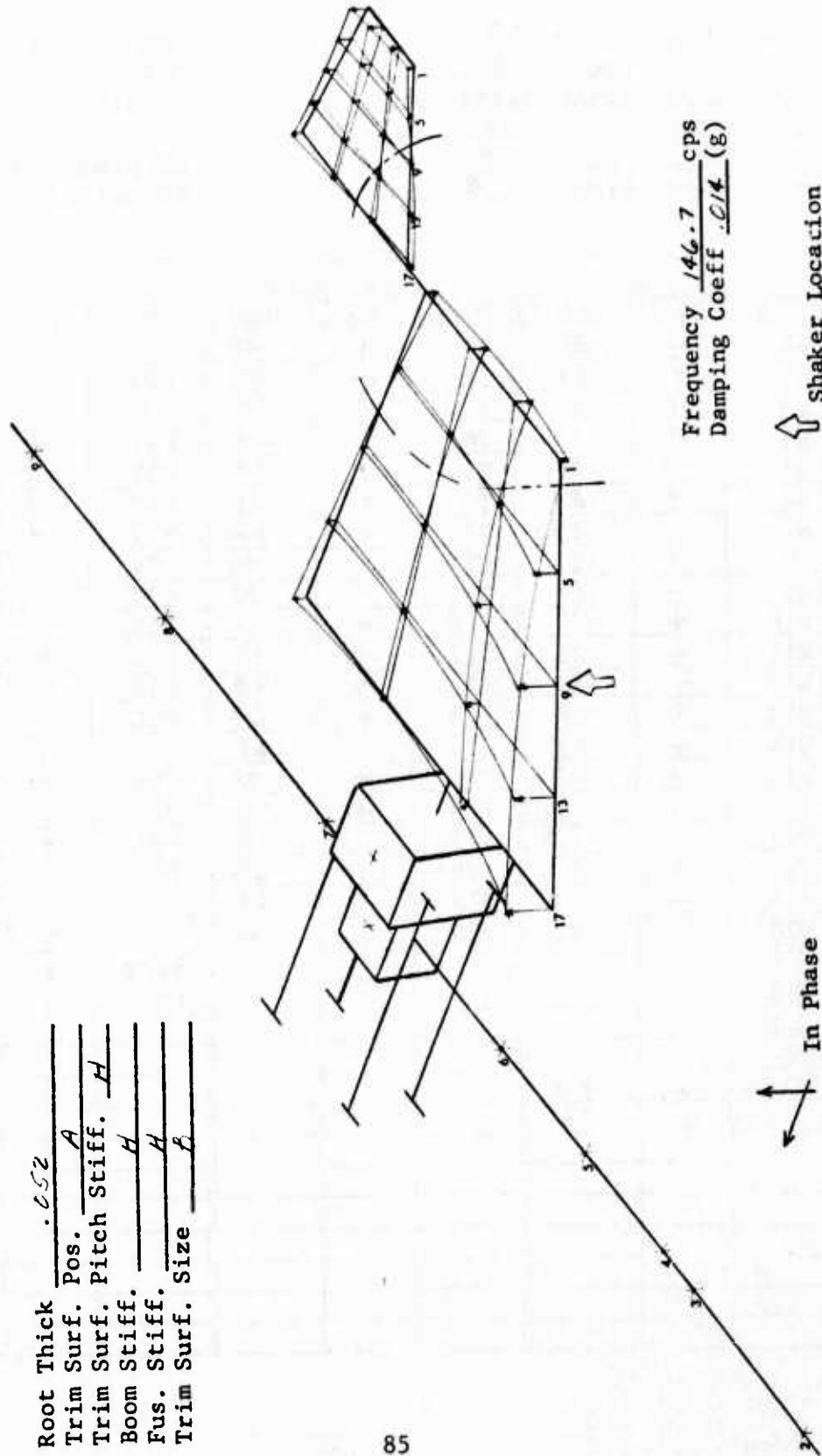


Figure 46
 TORSION FREE WING TREND FLUTTER MODEL
 MODE SHAPE PLOT
 SYMMETRIC BOUNDARY CONDITION

Root Thick .652
 Trim Surf. Pos. A
 Trim Surf. Pitch Stiff. H
 Boom Stiff. H
 Fus. Stiff. A
 Trim Surf. Size B



Frequency 146.7 cps
 Damping Coeff .014 (g)

↑ Shaker Location

Figure 47
 TORSION FREE WING TEND FLUTTER MODELS
 Frequency Survey

Model Config. TORSION FREE WING
 Root Thick. .052 Boundary Cond. SYMM
 Piv. Shaft Pos. F Trim Surf. Pos. F
 Trim Surf. Pitch Stiff. H Boom Stiff. HH
 Fus. Stiff. H Trim Surf. Size S

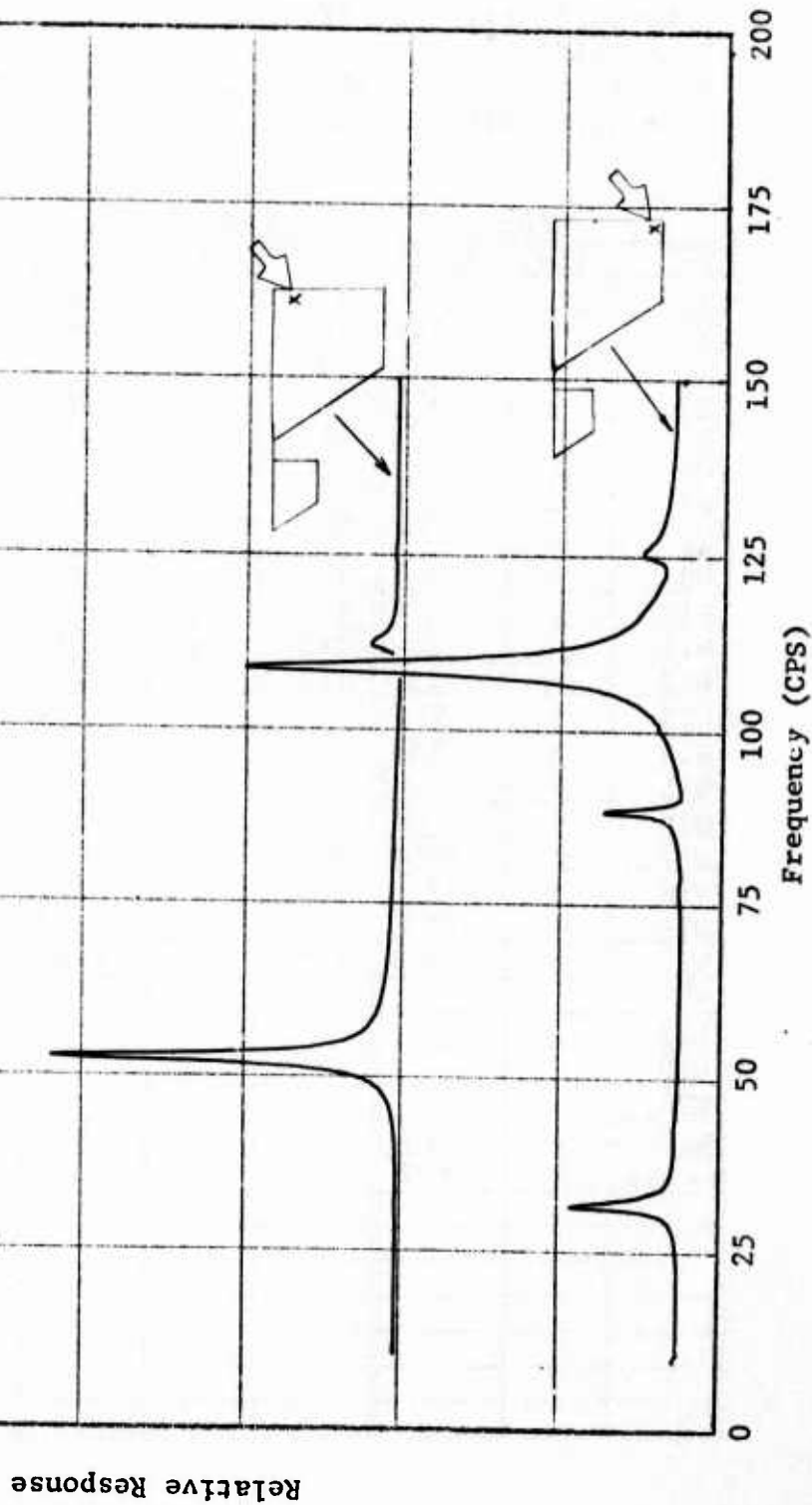
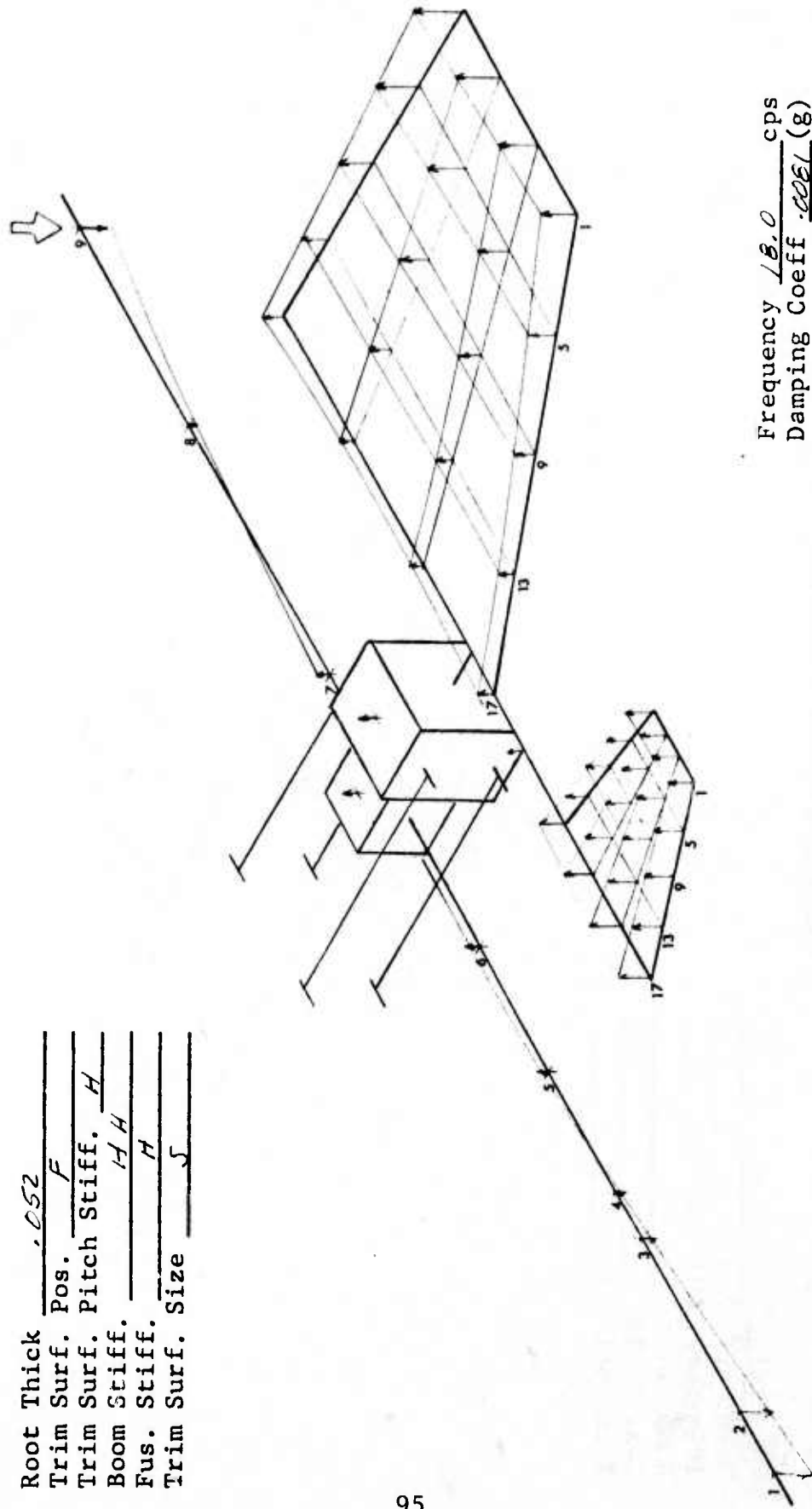


Figure 48
 TORSION FREE WING TREND FLUTTER MODEL
 MODE SHAPE PLOT
 SYMMETRIC BOUNDARY CONDITION

Root Thick	.052
Trim Surf. Pos.	F
Trim Surf. Pitch Stiff.	H
Boom Stiff.	H H
Fus. Stiff.	H
Trim Surf. Size	J



Frequency 18.0 cps
 Damping Coeff .0021 (g)

↑ Shaker Location

↔ In Phase

Figure 49
 TORSION FREE WING TREND FLUTTER MODEL
 MODE SHAPE PLOT
 SYMMETRIC BOUNDARY CONDITION

Root Thick .612
 Trim Surf. Pos. F
 Trim Surf. Pitch Stiff. 4
 Boom Stiff. 1
 Fus. Stiff. 1
 Trim Surf. Size 5

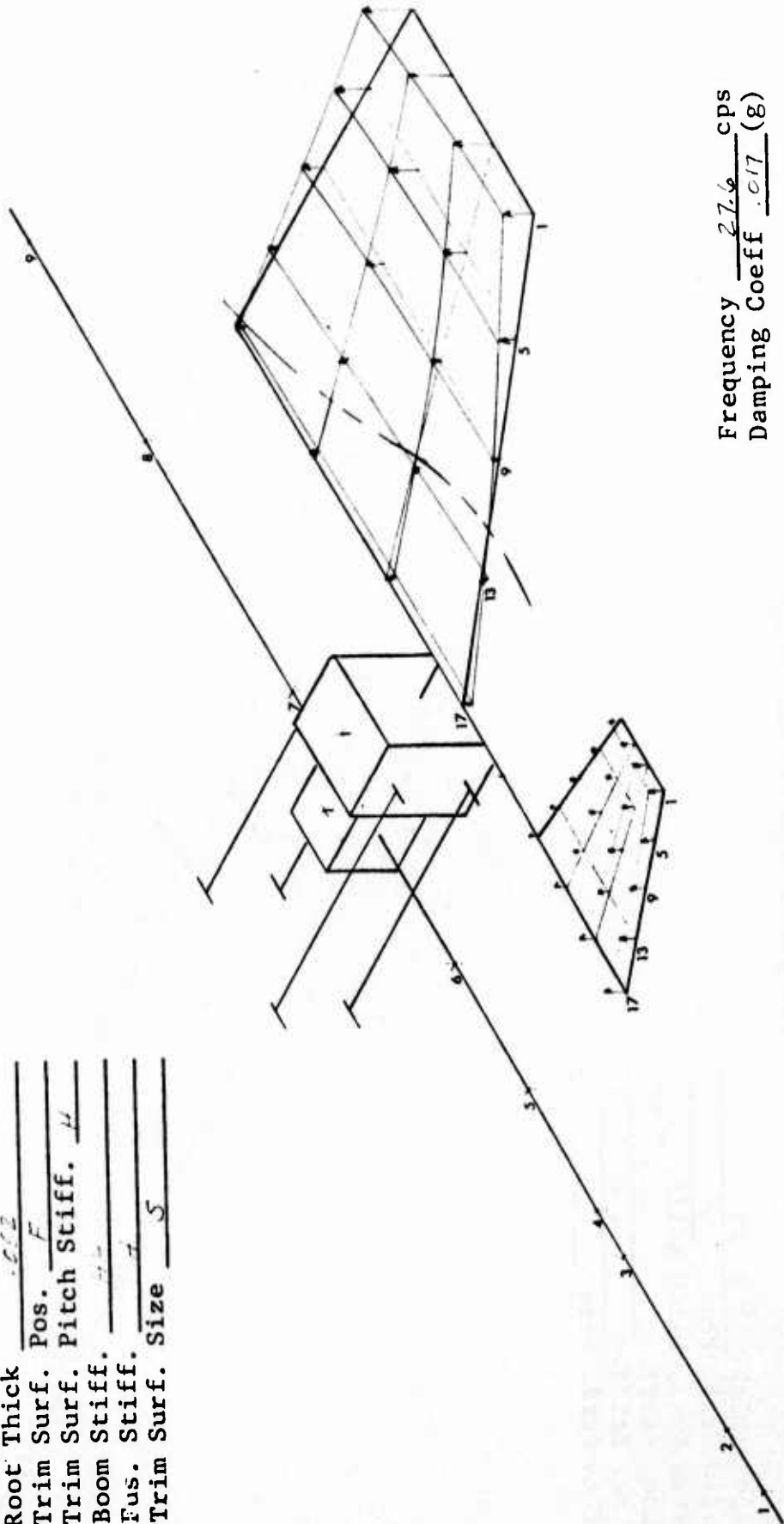


Figure 50
 TORSION FREE WING TREND FLUTTER MODEL
 MODE SHAPE PLOT
 SYMMETRIC BOUNDARY CONDITION

Root Thick 1.52
 Trim Surf. Pos. F
 Trim Surf. Pitch Stiff. 4
 Boom Stiff. 4
 Fus. Stiff. H
 Trim Surf. Size S

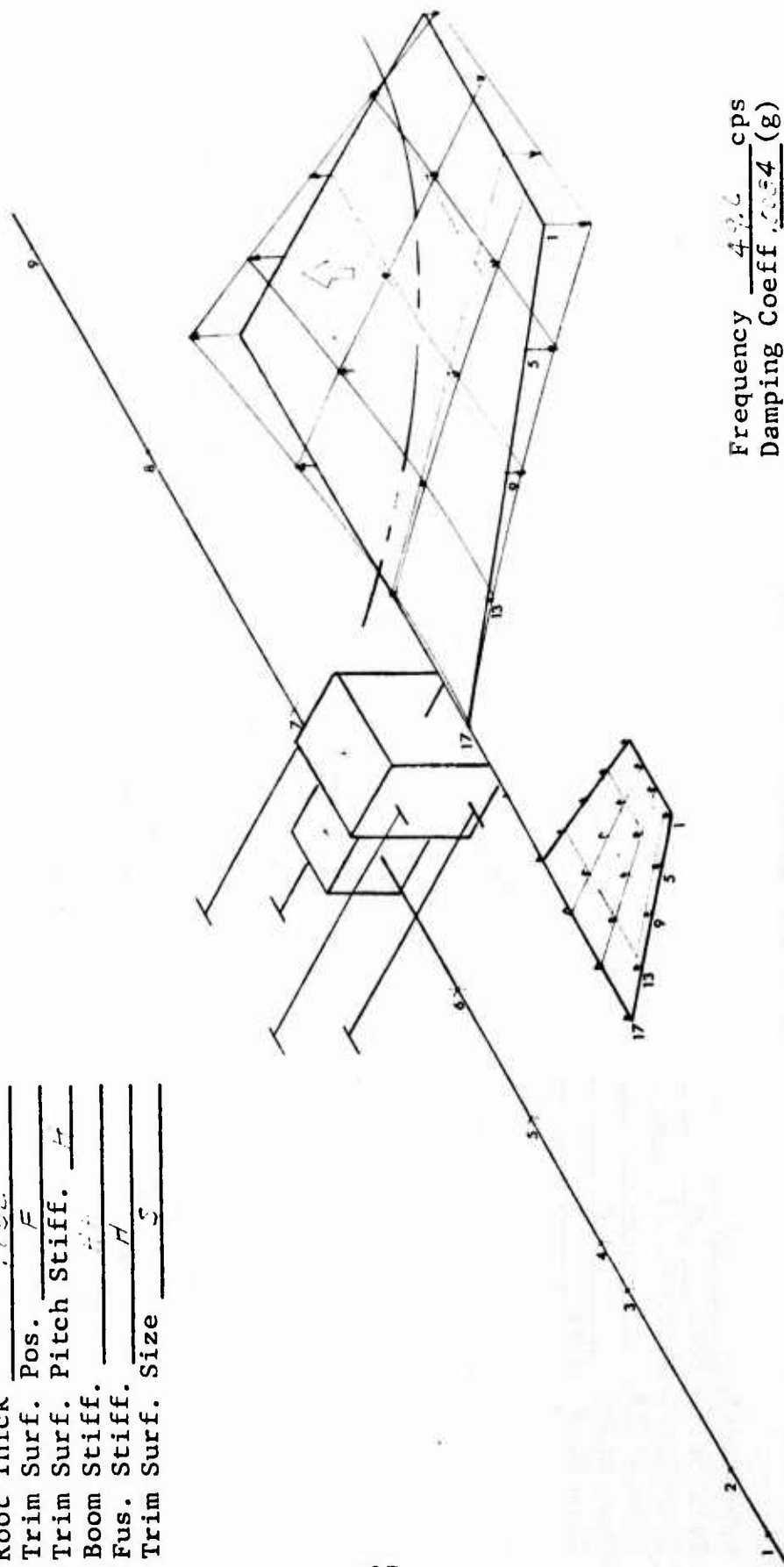
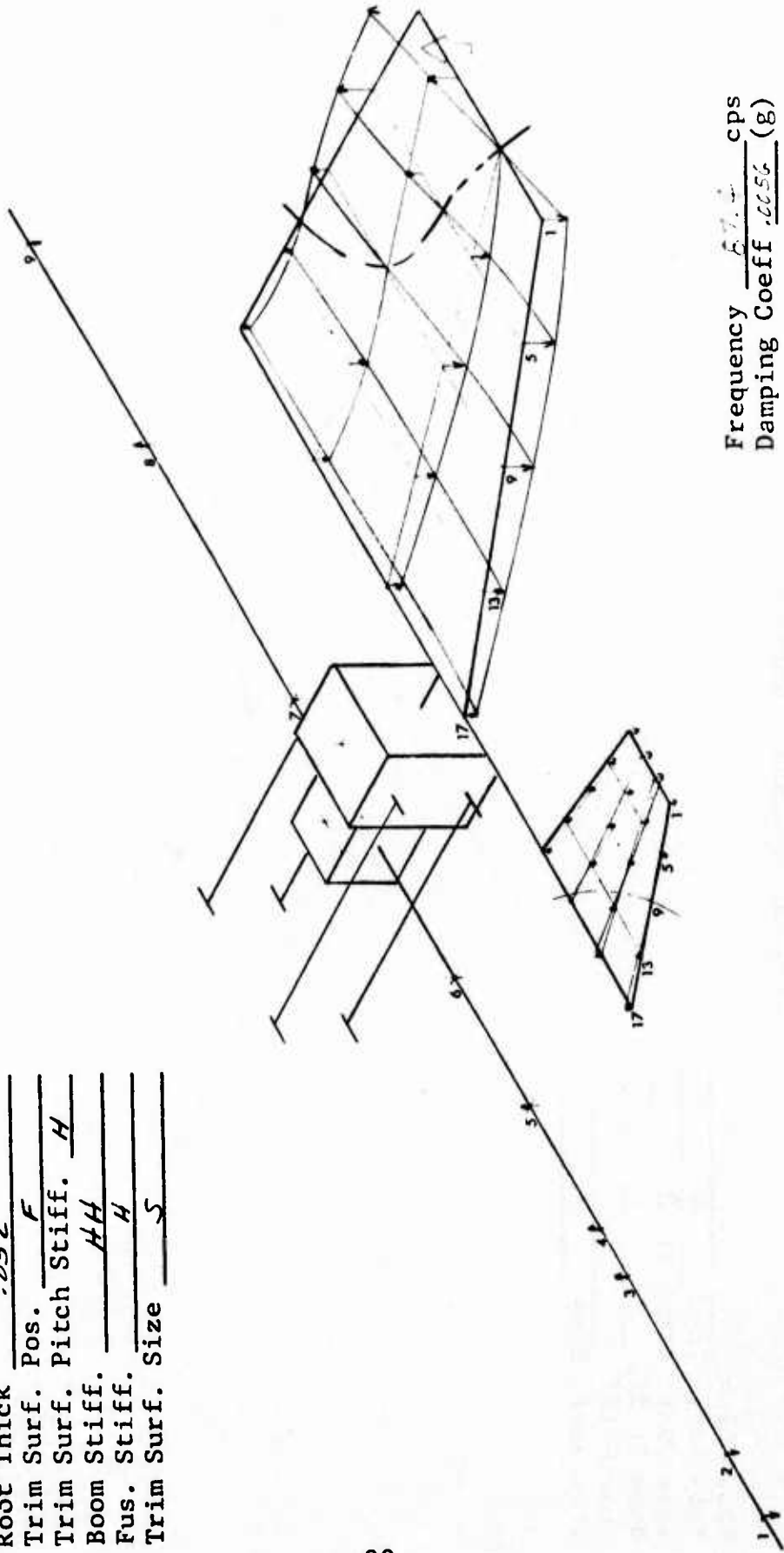


Figure 51
 TORSION FREE WING TREND FLUTTER MODEL
 MODE SHAPE PLOT
 SYMMETRIC BOUNDARY CONDITION

Root Thick 0.52
 Trim Surf. Pos. F
 Trim Surf. Pitch Stiff. H
 Boom Stiff. HH
 Fus. Stiff. H
 Trim Surf. Size S



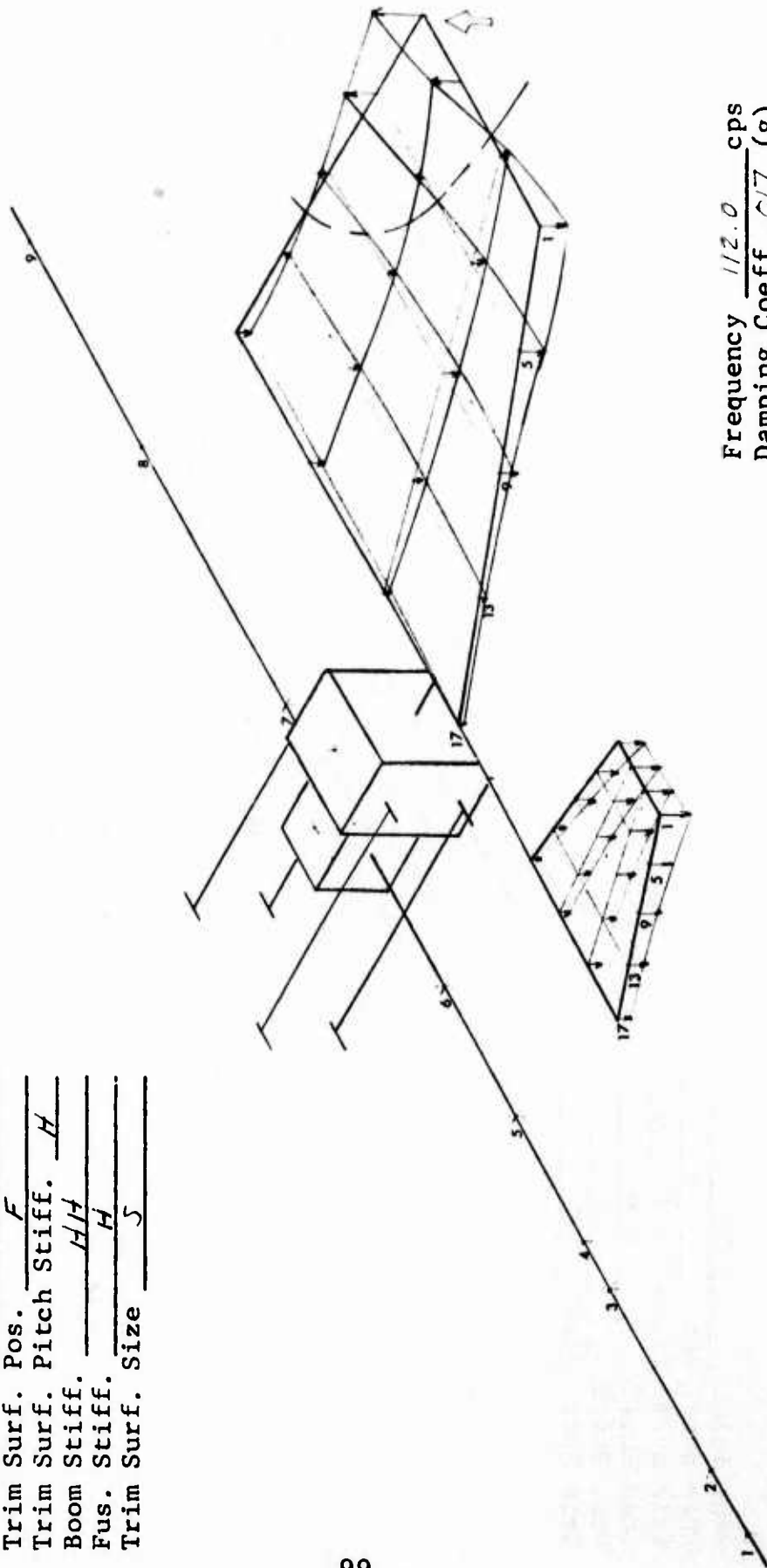
Frequency 87.4 cps
 Damping Coeff 0.056 (g)

↑ Shaker Location

↑ In Phase

Figure 52
 TORSION FREE WING TREND FLUTTER MODEL
 MODE SHAPE PLOT
 SYMMETRIC BOUNDARY CONDITION

Root Thick -.052
 Trim Surf. Pos. F
 Trim Surf. Pitch Stiff. H
 Boom Stiff. H/H
 Fus. Stiff. H
 Trim Surf. Size 5



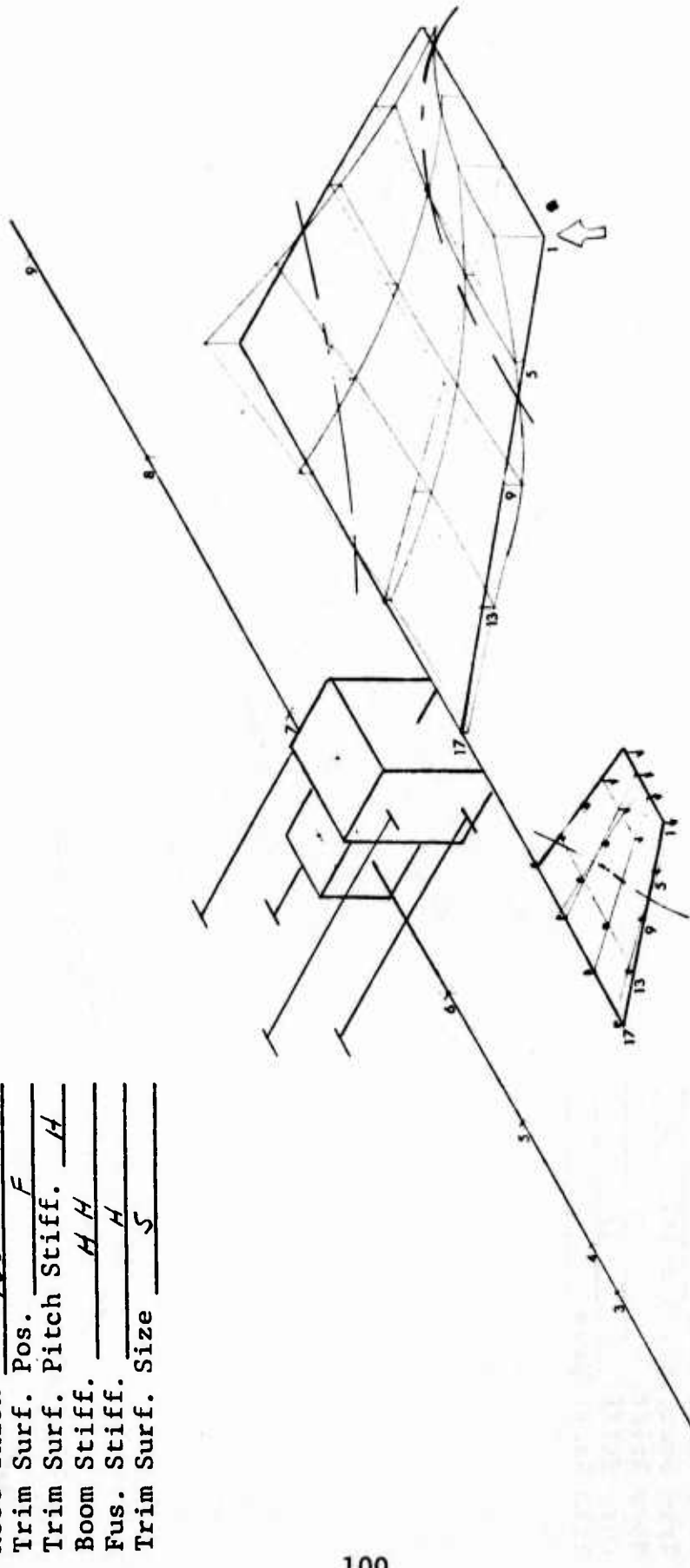
Frequency 112.0 cps
 Damping Coeff .017 (g)

↑ Shaker Location

↑ In Phase

Figure 53
 TORSION FREE WING TREND FLUTTER MODEL
 MODE SHAPE PLOT
 SYMMETRIC BOUNDARY CONDITION

Root Thick 052
 Trim Surf. Pos. F
 Trim Surf. Pitch Stiff. H
 Boom Stiff. HH
 Fus. Stiff. H
 Trim Surf. Size S



Frequency 123. cps
 Damping Coeff 0.0123 (g)

In Phase

Shaker Location

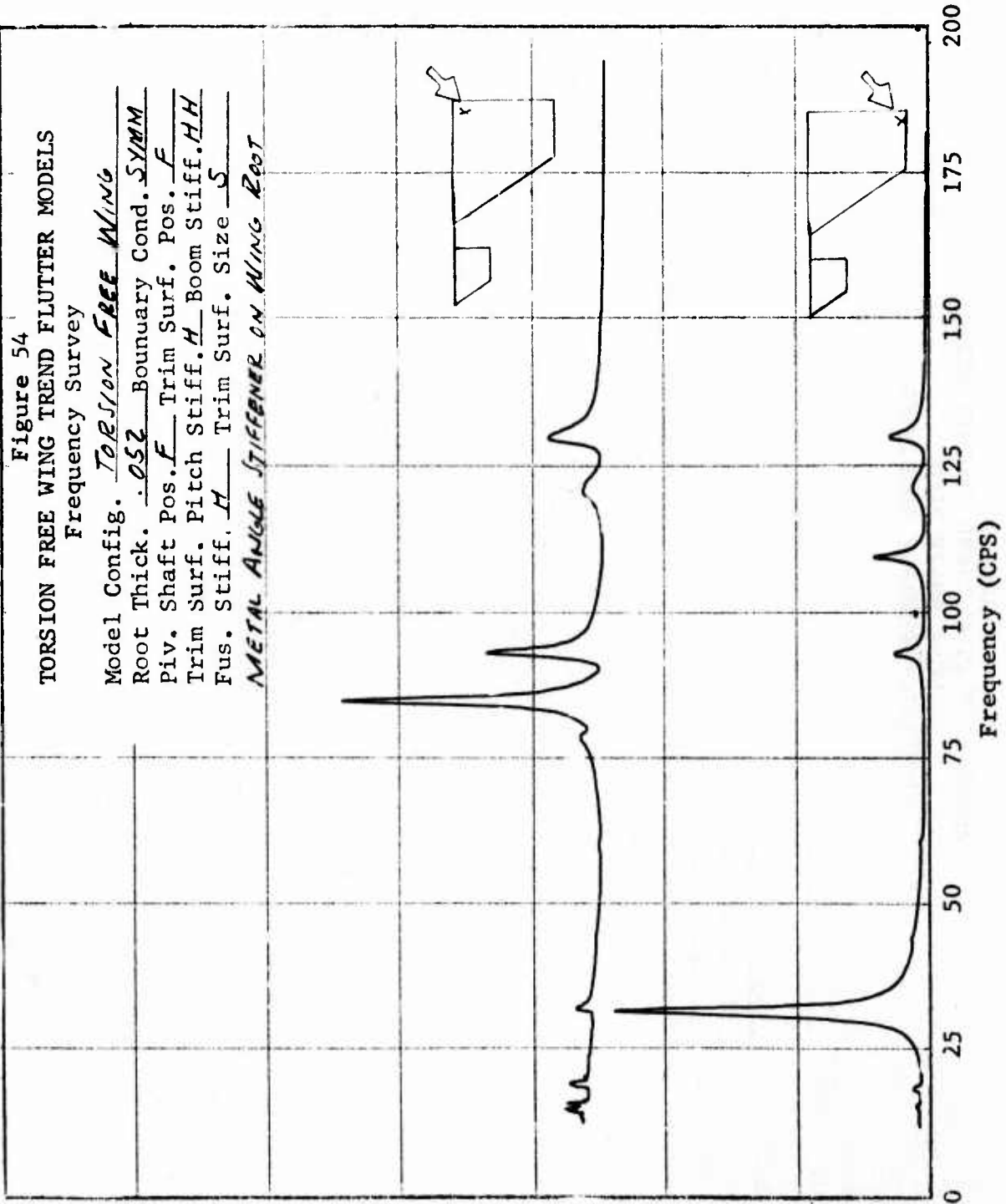
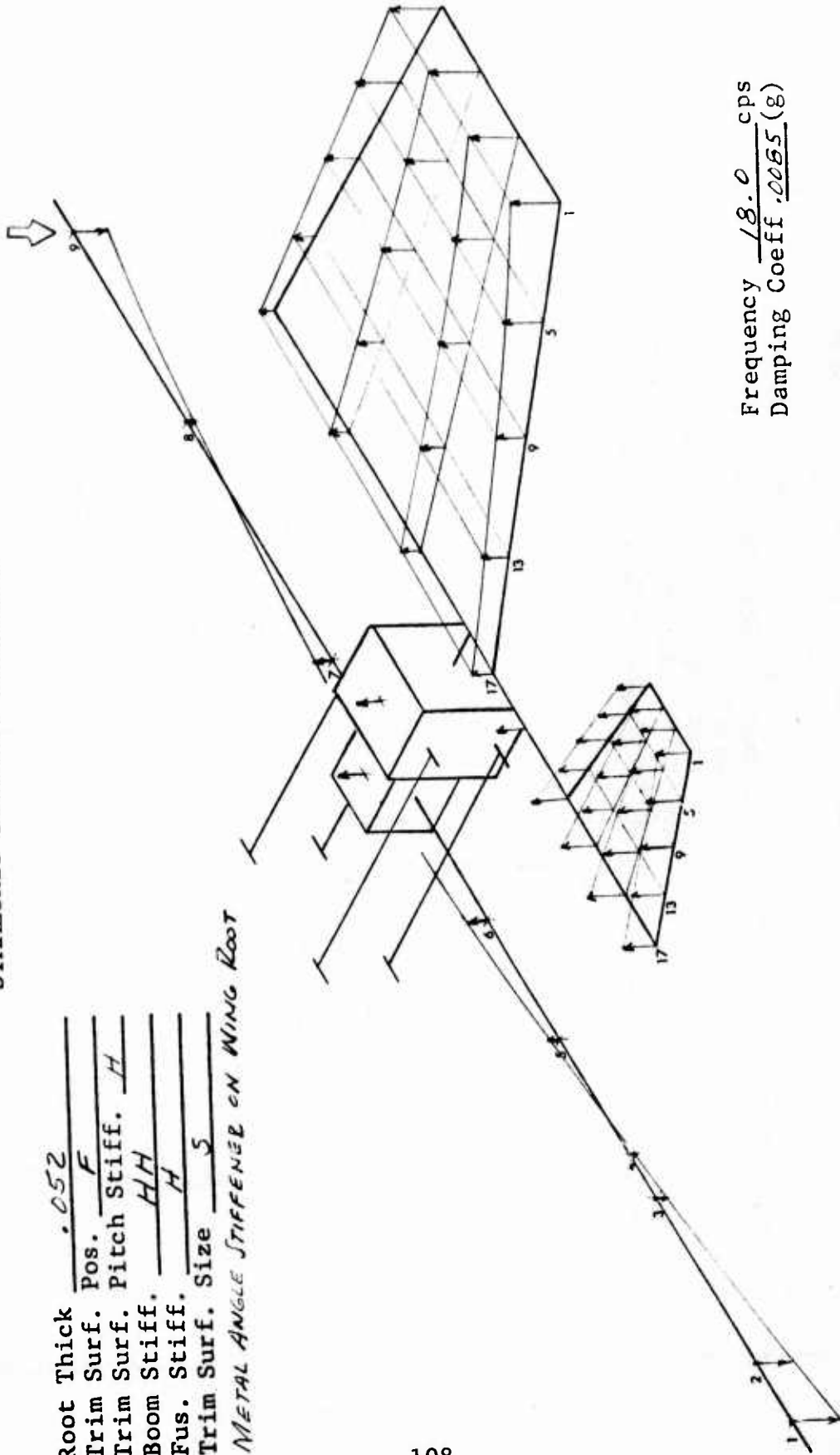


Figure 55
 TORSION FREE WING TREND FLUTTER MODEL
 MODE SHAPE PLOT
 SYMMETRIC BOUNDARY CONDITION

Root Thick .052
 Trim Surf. Pos. F
 Trim Surf. Pitch Stiff. H
 Boom Stiff. HH
 Fus. Stiff. H
 Trim Surf. Size S
 METAL ANGLE STIFFENER ON WING ROOT



In Phase

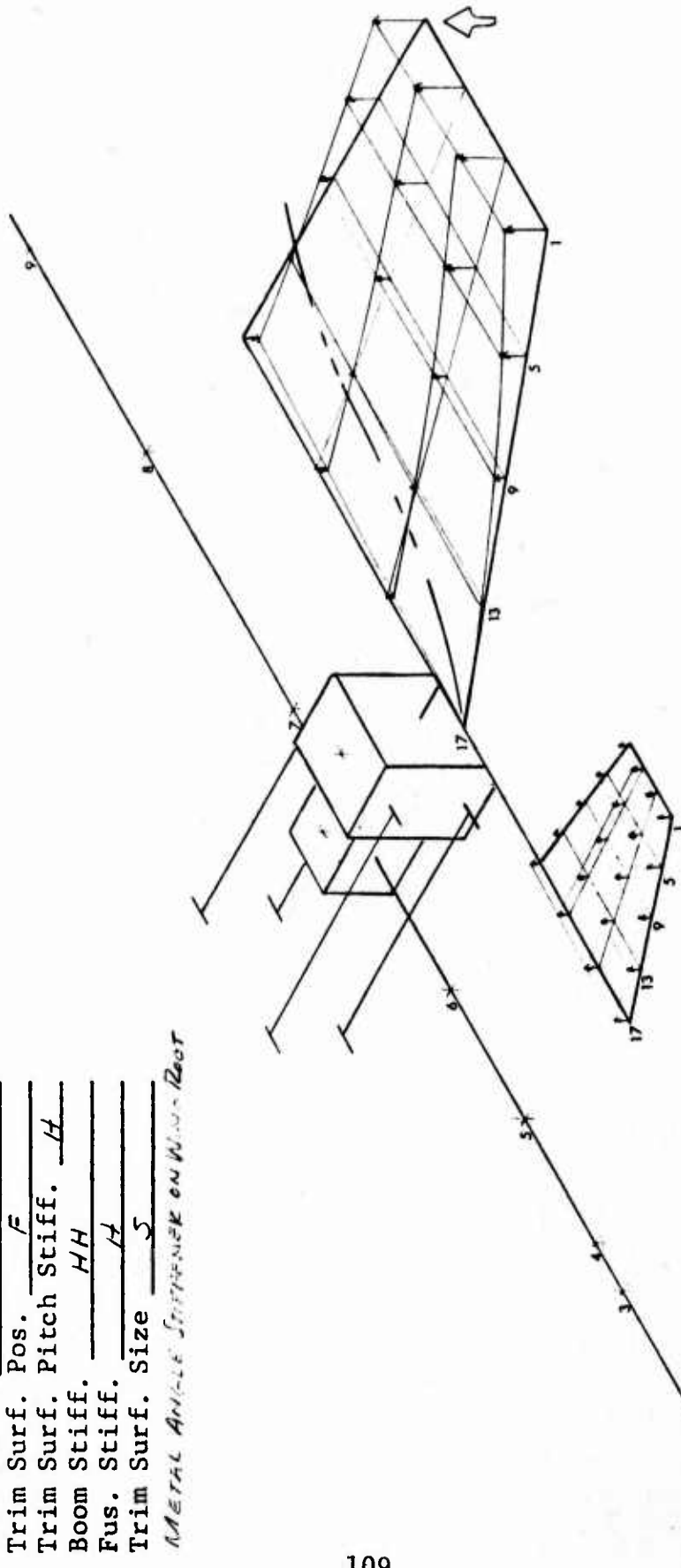
Frequency 18.0 cps
 Damping Coeff .0055 (g)

Shaker Location

Figure 56
 TORSION FREE WING TREND FLUTTER MODEL
 MODE SHAPE PLOT
 SYMMETRIC BOUNDARY CONDITION

Root Thick .652
 Trim Surf. Pos. F
 Trim Surf. Pitch Stiff. H
 Boom Stiff. HH
 Fus. Stiff. H
 Trim Surf. Size S

METAL ANGLE STIFFENER ON WING ROOT



Frequency 30.9 cps
 Damping Coeff .026 (g)

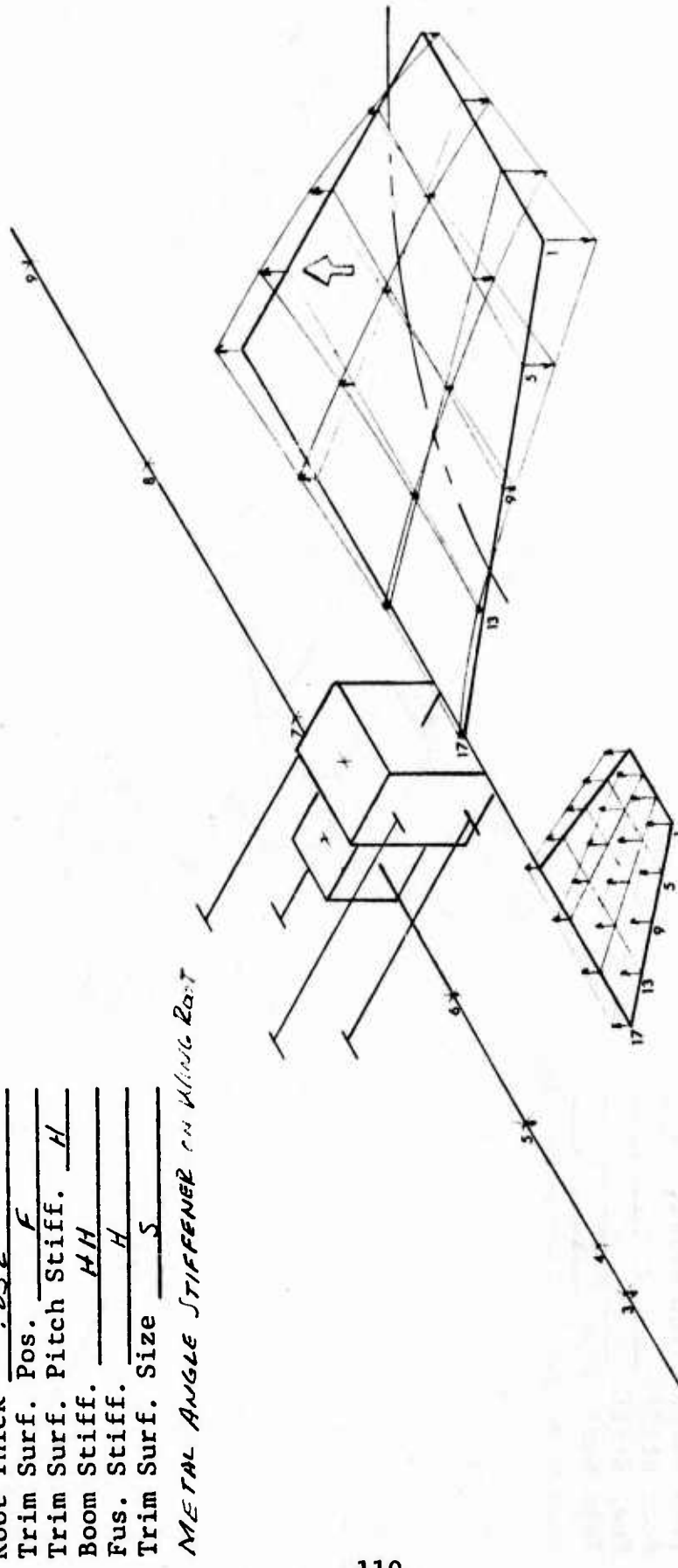
↑ Shaker Location

↑ In Phase

Figure 57
 TORSION FREE WING TREND FLUTTER MODEL
 MODE SHAPE PLOT
 SYMMETRIC BOUNDARY CONDITION

Root Thick .052
 Trim Surf. Pos. F
 Trim Surf. Pitch Stiff. H
 Boom Stiff. HH
 Fus. Stiff. H
 Trim Surf. Size S

METAL ANGLE STIFFENER ON WING ROOT



Frequency 77.9 cps
 Damping Coeff 0.027 (8)

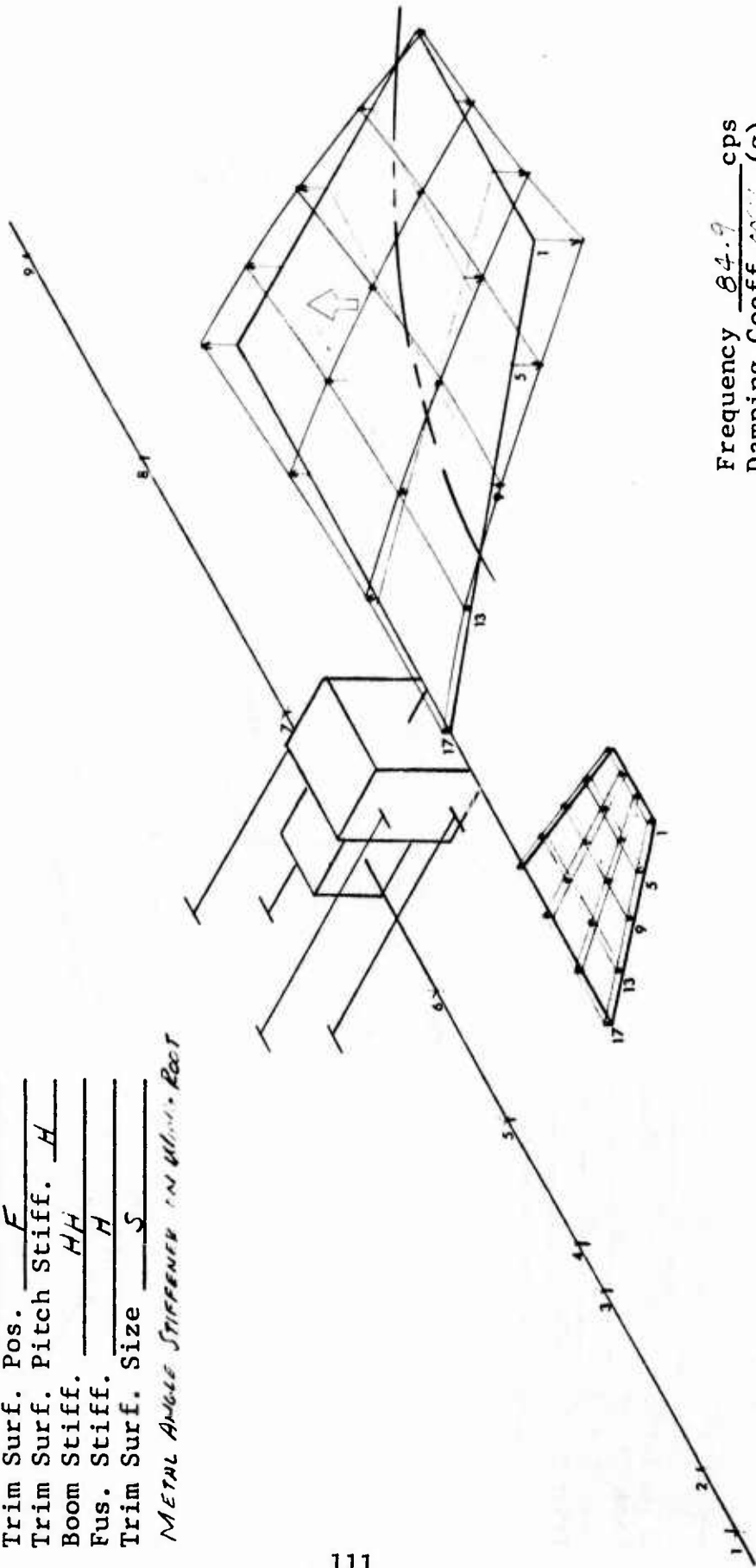
↑ Shaker Location

↑ In Phase

Figure 58
 TORSION FREE WING TREND FLUTTER MODEL
 MODE SHAPE PLOT
 SYMMETRIC BOUNDARY CONDITION

Root Thick .052
 Trim Surf. Pos. F
 Trim Surf. Pitch Stiff. H
 Boom Stiff. HH
 Fus. Stiff. H
 Trim Surf. Size S

METAL ANGLE STIFFENER IN WING ROOT



Frequency 84.9 cps
 Damping Coeff. 0.001 (g)

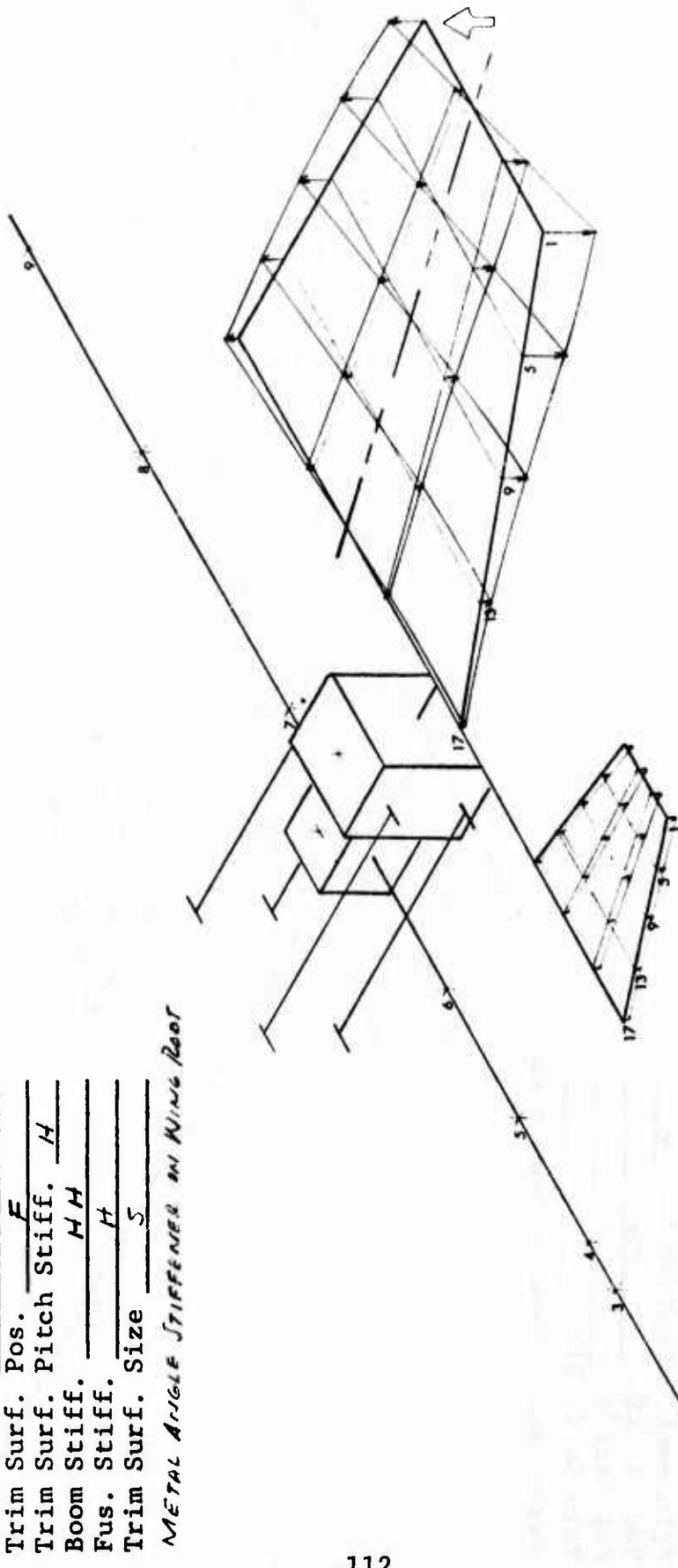
↑ Shaker Location

↗ In Phase

Figure 59
 TORSION FREE WING TREND FLUTTER MODEL
 MODE SHAPE PLOT
 SYMMETRIC BOUNDARY CONDITION

Root Thick	.052
Trim Surf. Pos.	F
Trim Surf. Pitch Stiff.	H
Boom Stiff.	HH
Fus. Stiff.	H
Trim Surf. Size	S

METAL ANGLE STIFFENER IN KING ROOT



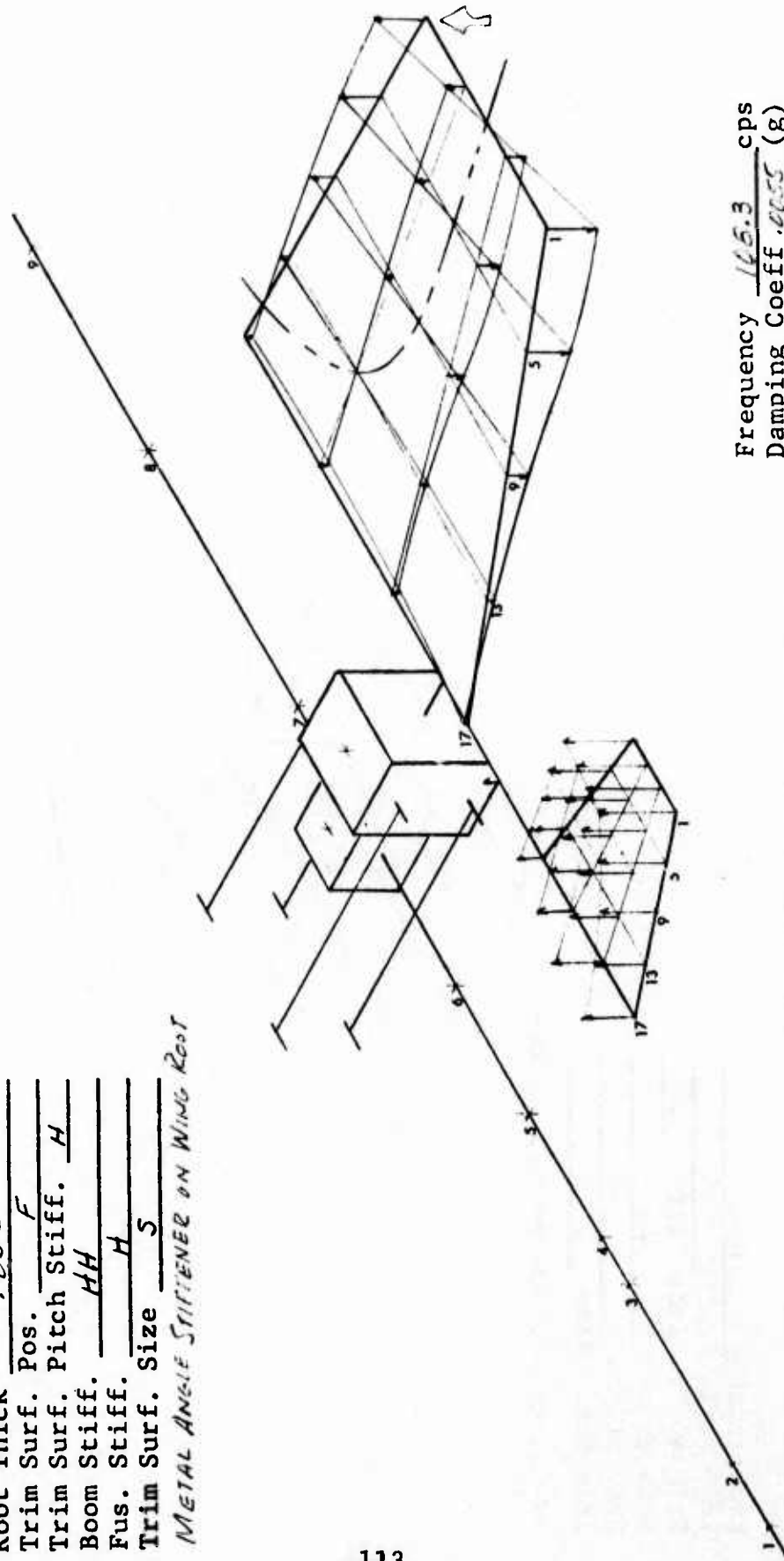
Frequency $\frac{94.5}{\text{cps}}$
 Damping Coeff. $\frac{.0051}{(g)}$

In Phase

Shaker Location

Figure 60
 TORSION FREE WING TREND FLUTTER MODEL
 MODE SHAPE PLOT
 SYMMETRIC BOUNDARY CONDITION

Root Thick .052
 Trim Surf. Pos. F
 Trim Surf. Pitch Stiff. H
 Boom Stiff. HH
 Fus. Stiff. H
 Trim Surf. Size S
 METAL ANGLE STIFFENER ON WING ROOT



Frequency 165.3 cps
 Damping Coeff. .055 (g)

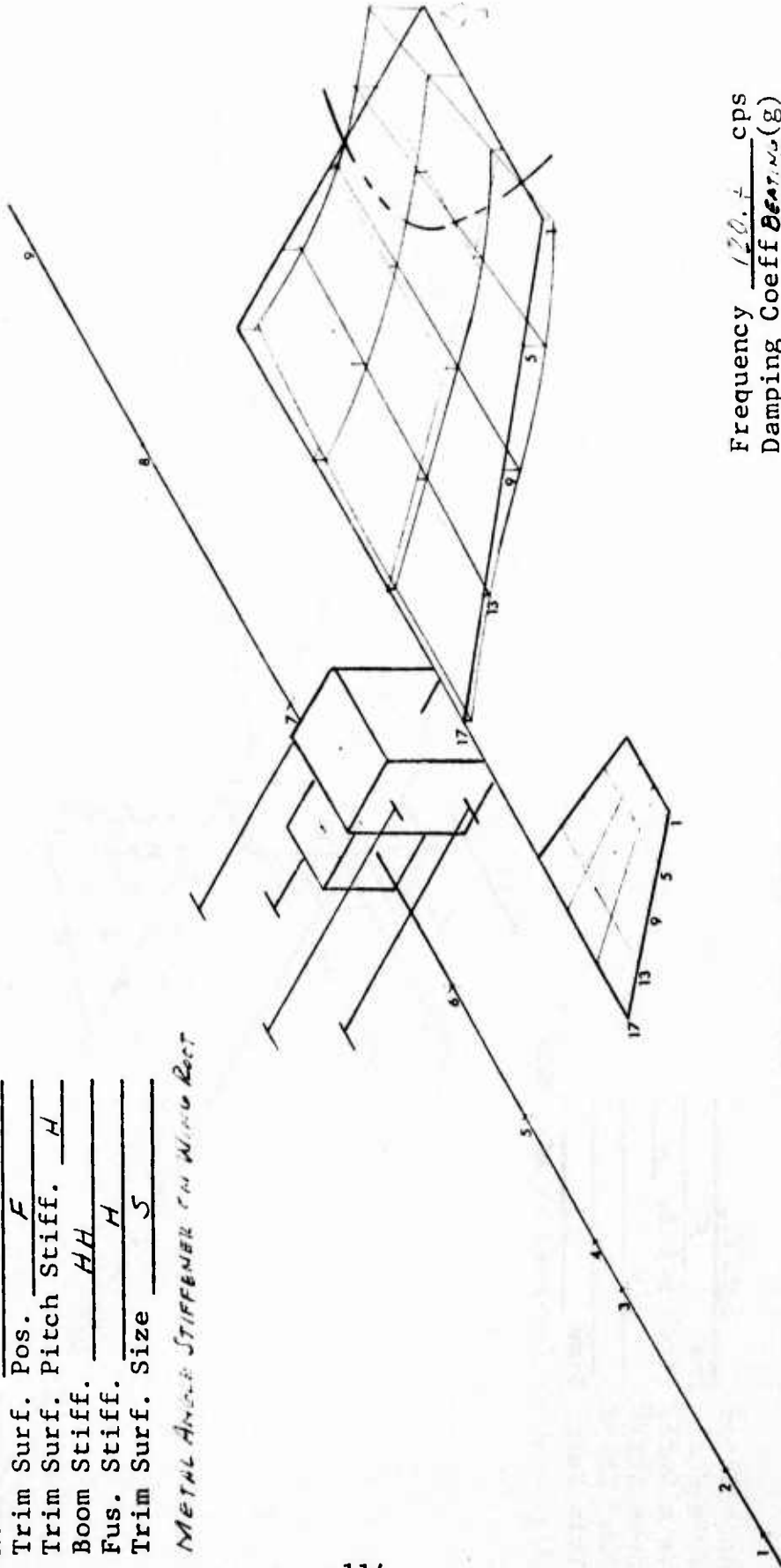
← Shaker Location

→ In Phase

Figure 61
 TORSION FREE WING TREND FLUTTER MODEL
 MODE SHAPE PLOT
 SYMMETRIC BOUNDARY CONDITION

Root Thick .052
 Trim Surf. Pos. F
 Trim Surf. Pitch Stiff. H
 Boom Stiff. HH
 Fus. Stiff. H
 Trim Surf. Size S

METAL ANGLE STIFFENER ON WING ROOT



In Phase

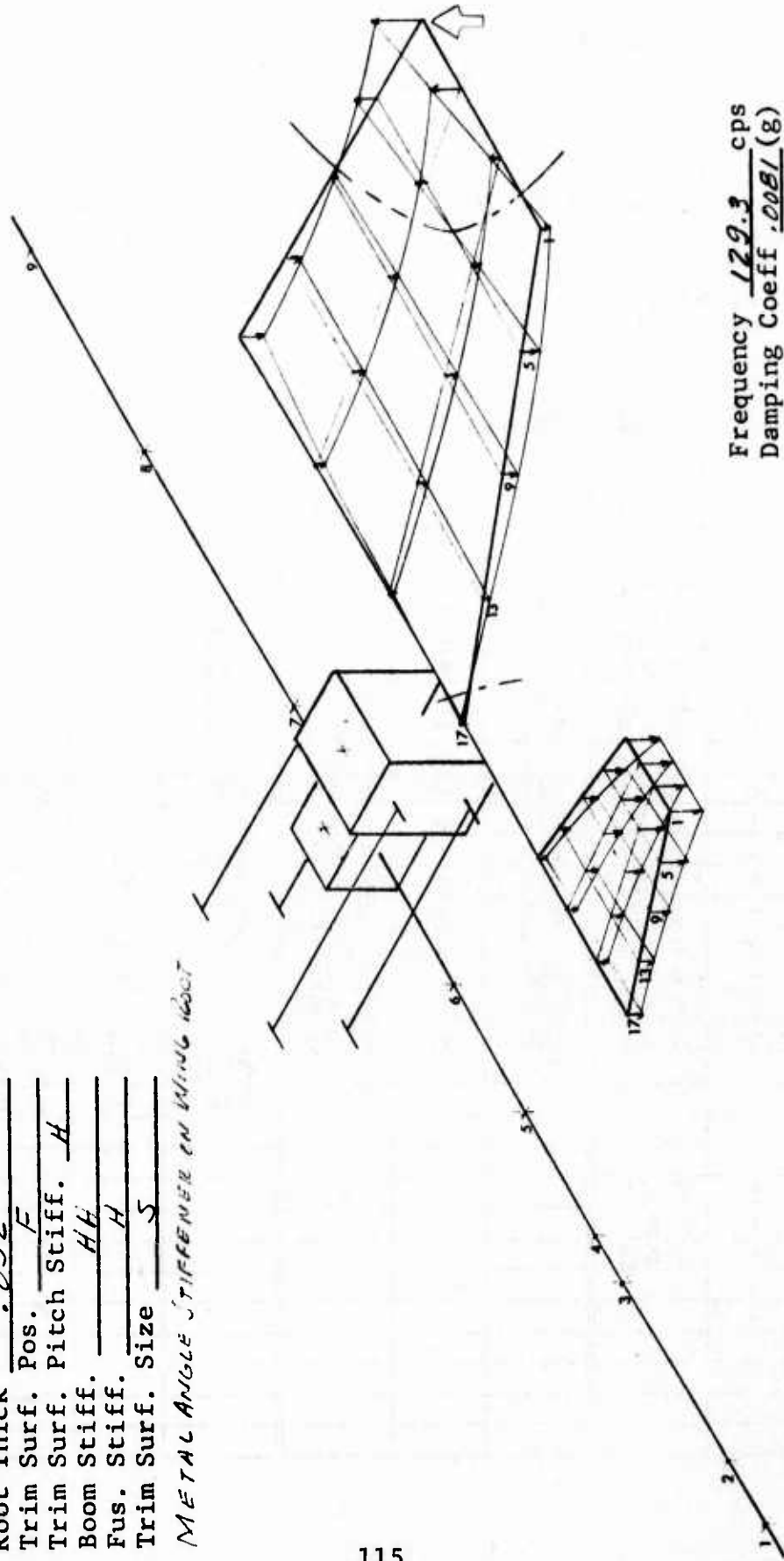
Frequency $\frac{120.7}{\text{cps}}$
 Damping Coeff $\frac{0.007}{(g)}$

Shaker Location

Figure 62
 TORSION FREE WING TREND FLUTTER MODEL
 MODE SHAPE PLOT
 SYMMETRIC BOUNDARY CONDITION

Root Thick .052
 Trim Surf. Pos. F
 Trim Surf. Pitch Stiff. H
 Boom Stiff. HH
 Fus. Stiff. H
 Trim Surf. Size S

METAL ANGLE STIFFENER ON WING ROOT



In Phase

Frequency 129.3 cps
 Damping Coeff .0081 (8)

Shaker Location

REFERENCES

1. Porter, R. and Brown, J., "The Gust Alleviation Characteristics and Handling Qualities of a Free-Wing Aircraft," AIAA Paper 70-947, AIAA Guidance, Control and Flight Mechanics Conference, August 17-19, 1970.
2. Wattman, W., et al., "Pivoting Wing Ride Smoothing/Flutter SAS Analyses," The Boeing Company, Wichita, Kansas, May 1971.
3. Harris, G., "Flutter Criteria for Preliminary Design," Navy, Bureau of Naval Weapons Final Engineering Report 2-53450/3R467, Prepared by LTV Aeronautics and Missile Division, September 1963.
4. Peloubet, R. P., "Finite Span Subsonic Flutter Analysis Method Utilizing M.I.T. Series Method for Computing Pressure Distributions," General Dynamics Memorandum Report SDGM-80, August 1958.
5. Hsu, P. T., "Flutter of Low Aspect Ratio Wings, Part I, Calculation of Pressure Distributions for Oscillating Wings of Arbitrary Planform in Subsonic Flow by the Kernel-Function Method," Aeroelastic and Structures Research Lab. TR 64-1, MIT, Cambridge, Mass., October 1957.
6. Albano, E., Rodden, W. P., "A Doublet Lattice Method for Calculating Lift Distribution on Oscillating Surfaces in Subsonic Flows," AIAA Paper No. 68-73, AIAA 6th Aerospace Sciences Meeting, January 1968.
7. Albano, E., "Planar Doublet-Lattice Method for Aerodynamic Forces," Northrop Corporation, Norair Division Report NOR 68-147, October 1968.
8. Hedman, S. G., "Vortex Lattice Method for Calculation of Quasi-Steady-State Loading on Thin Elastic Wings," Aeronautical Research Institute of Sweden Report 105, October 1965.

9. Woodward, F. A., Hague, D. S., "A Computer Program for the Aerodynamic Analysis and Design of Wing-Body-Tail Combinations at Subsonic and Supersonic Speeds, Volume I: Theory and Program Utilization," General Dynamics' Fort Worth Division ERR-FW-867, February 1969.
10. Hosek, J. J., Peloubet, R. P., Lyons, P. F., "Development of Airframe Structural Design Loads for Flexible Military Aircraft, Volume I: Theoretical Development," AFFDL-TR-75-79, July 1975.
11. Hosek, J. J., Peloubet, R. P., Lyons, P. F., "Development of Airframe Structural Design Loads for Flexible Military Aircraft, Volume II: Computer Program," AFFDL-TR-75-79, July 1975.
12. Simodynes, E. E., "Flutter Characteristics of a Torsion Free Wing," General Dynamics' Fort Worth Division ERR-FW-1337, 31 November 1972.
13. Waner, P. G., "Torsion Free Wing Flutter and Gust Response Analysis," General Dynamics' Fort Worth Division ERR-FW-1585, 31 December 1974.
14. Bhateley, I. C., "An Investigation of the Interference Effects Between Fuselage and Wing at High Relative Incidence," General Dynamics' Fort Worth Division ERR-FW-1464, 31 December 1973.
15. Joyce, G. T., "The Stability and Control Characteristics of a Torsion Free Wing Advanced Tactical Fighter," General Dynamics' Fort Worth Division ERR-FW-1451, 31 December 1973.
16. Rankin, E. E., "Torsionally Free Wing Subscale Remotely Piloted Research Vehicle Design and Flight Test," General Dynamics' Fort Worth Division ERR-FW-1490, December 1973.
17. Moseley, W. M., Jr., Roland, H. L., "Stress and Weight Analysis of a Torsionally Free Wing System," General Dynamics' Fort Worth Division ERR-FW-1446, 15 July 1973.

18. Moran, W. J., "ATF/TFW Feasibility Study - Performance Analysis," General Dynamics' Fort Worth Division ERR-FW-1459, 31 December 1973.
19. Waner, P. G., "Torsion Free Wing Gust Response Analysis," General Dynamics' Fort Worth Division ERR-FW-1525, 31 December 1973.
20. Haller, R. L., "Torsion Free Wing Studies," General Dynamics' Fort Worth Division ERR-FW-1493, 31 December 1973.